From Pete Bracken

log book

written by J. Scanlin
when she left

Pioneer F/G Data Processing

1) Bufop Tapes - Essentially Truck look data. Use file PGBuf on 360/91, Time H02H01. See documentation in Notebook (yellow pg.) for any changes to set up, or see Charlie.

2) Edr Tapes - Experiment Data Record - covers all data from satellite. Tape contains 4 files: 1) logistics; 2) Command; 3) Attitude; 4) actual experiment data. Process all Edr tapes through PIODRP to create time ordered and quality assessed PHA and Rates tapes. The following tapes are assigned for these purposes:

9 track	E00400 - E00487	PHA tapes, Pioneer F
9 track	E00493 - E00500	Primary + Backup Catalogs, Pioneer F
7 track	E00501 - E00599	Rates tapes, Pioneer F
9 track	E00 E00280	Backup PHA Tapes, Pioneer F
7 track	E00301 - E00399	Backup Rates tapes, Pioneer F
9 track	EC2301 - EC2392	PHA tapes, Pioneer G
9 track	EC2393 - EC2400	Primary + Backup Catalogs, Pioneer G
7 track	EC2401 - EC2499	Rates tapes, Pioneer G
9 track	EC2500 - EC2599	Backup PHA Tapes, Pioneer G
7 track	EC2600 - EC2699	Backup Rates Tapes, Pioneer G

Any tapes (Edr) rejected by PIODRP, run through The

Edr list program to determine if tape is OK. If Edr tapes are found to be bad, ask Ames to generate a new one (Arvid Naturch, Code 244-8, NASA, Moffett Field, California 94035).

3) The PHA tapes produced by PIODRP are processed through the PHA Summarize Program to create Daily Summaries on a standard basis. You will also need to run various time periods as requested, + they will be run either as special runs, or merged runs. The following tapes are used for the PHA Summarizer:

9 track E01001 → E01099 Pioneer F

9 track E01101 → E01199 Pioneer G

4) The PHA Summary tapes ~~produced~~ by the PHA Summarizer are read by the PHA Summary Plot program to produce matrices and/or histograms of the PHA data. 4 day plots (starting from launch) are produced on a standard basis for 9 plot types. Try to get 2 paper output for these, since you need to send 1 set to Dr. Webber at the University of New Hampshire. It is easier to plot 4 daily summaries on the same grid than to create 4 day summaries. One set of 4 day plots are separated and filed in the data room. [illegible] on a requested

basis, and the output given to the requestor.

5) The rates tapes produced by PIODEP are processed through the Rate Summary Program. The interval for standard processing is 1 hour & is the default interval of the program. To merge data into the rate summary tape, create a spread tape & then run the merge segment. The tapes allotted for Rate Summary tapes are: E00282 → E00291, and E00488 → E00491. I use them interchangeably between the 2 satellites. The current tape for Pioneer F is E00490, and the current tape for Pioneer G is E00286. (Pioneer G has 2 8/19 ~~files~~ files)

6) E00281 is my vbe backup tape file 1 is 75, file 2 is 91.

7) The rate summary tape is run through the rate summary plot program to produce 4060 plots for 12 standard rates & for any requested rate. The program also lists requested rates & counts & manually run list and plot separately as it takes too much time to run them all in the same job and it is not often that you would need both listings & plots for the same rates. The 12 standard rates are sent to Webber the following:

Rate Summary Plot / List

The following sets of 12 rates are standard for all Data to be processed through the 4060 plot. One copy goes to Bonnard, 1 copy filed in Data Room, 1 copy goes to Dr. Webber at U of New Hampshire, 1 copy to Dr. McDonald

R7b, R11a, R14a
SR2a(9), R13a, R15a
SR2e(9), R6a, R6b
R11b, R13b, R3b

```
00002300   R7B,R11A,R14A
00002400   SR2A(9),R13A,R15A
00002500   SR2E(9),R6A,R6B
00002600   R11B,R13B,R3B
```

Standard Listings are generated for daily avg (24 hr. invl) & given to Bonnard (it may be wise to keep one in the data room also)

S R2a, R3a (Sum of 2a + 3a)

R7b, R8a, R8b
R11a, R13a,

```
R11A,R13A,R8B
R6A,R6B,R7A
S R2A,R3A
```

We handplot histograms for most of these

Send to Dr. Webber (hourly avg. all data) Listing

Ratio

R R11a, R11b
R R12a, R12b
R R13a, R13b
R R7b, R3b
R R8a, R4a
R R8b, R5a

```
00002300  R R11A,R11B
00002400  R R12A,R12B
00002500  R R13A,R13B
00002600  R R7B,R3B
00002700  R R8A,R4A
00002800  R R8B,R5A
```

Process 2 - Order redo Edr tapes from Asrid Network ...

VHA Summarizer

Standard processing is for daily intervals. We used to process 4 days/period through the Merged Summary program but since the VHA Summary Plot program was corrected, we don't need to continue that.

VHA Summary Plot program

The following set of plots is generated for 4 day periods for both 1 + 2. We generate 2 copies; one is filed in the data room, the other is sent to Mrs. Webber at U. of New Hampshire

00000600	TDIDII	1			T		F
00000650	TDIDII	2			T		F
00000700	TDIE	1	4095		T		T
00000750	TDIE	4	4095		T		T
00000800	TAB	1			T		F
00000850	TAB	4			T		F
00000900	TACI+CII	1	4095	1	T		T
00000950	TACI+CII	4	4095	1	T		T
00001000	TBCIII	1	4095		T		F

Rate Summary

The standard interval for the rate summary is 1 hour, and the tape produced is used as input to the rate summary plot/list pgm.

TABLE 1H

Event Type	Particle	Event $I2=2^1$	Code $I1=2^0$	Relative Priority (1=highest) S1=S2=0	S1=1,S2=0	S1=0,S2=1	S1=S2=1
$A_1BK_2\overline{CIII}$	Stopping particles $Z\geq 2$	1	1	1*	2	2	2
$(A_2K_1 + A_1CI)\ B\overline{CIII}$	Stopping e^-, or stopping $p+$ and heavier	1	0	2	1	3	3*
A_2B CIII	Penetrating particles $Z\geq 2$	0	1	3	3	1	4*
$A_1\overline{A_2}$ B CIII	Penetrating e^-	0	0	4*	4*	4*	1

* Each event is analyzed as often as it occurs unless marked with *,

in which case that event type is analyzed only once per readout.

SPECIFICATIONS FOR PIONEER PHA DEAD TIME CORRECTION

The purpose of PHA dead time corrections is to derive a 'true' rate of occurrence of PHA events based on the actual measured rate of occurrence in the data. Clearly there will be some cases (e.g. very low bit rate periods or periods of very high counting rates such as during solar flares when nearly every PHA is non-zero) in which such a correction is not possible.

HET

The following notation will be used for event types and priorities:

EVENT TYPE	LOGIC CONDITION
0	$A_1\overline{A_2}BCIII$
1	A_2BCIII
2	$(A_2K_1 + A_1CI)\overline{BCIII}$
3	$A_1BK_2\overline{CIII}$

The priority orderings will be designated as follows:

PRIORITY NO.	3	2	1	0
EVENT TYPE	3	2	1	0
ORDERING	2	3	3	3
	1	1	2	2
	0	0	0	1

The relationship between the priority no and the value of the non-sectored subcom word occurring in the middle of priority sequence is

PRIORITY No.	SUBCOM WORD (E1-30)
3	0
2	2
1	4
0	6

In the following it will be assumed that in the program all variables will be subscripted according to bit rate. This subscript, however, will not be written down in the following. For all variables that are doubly subscripted (again neglecting the implied bit rate subscript) the first index will represent the event type and the second will be the priority. We define the following quantities:

N_{ij} $\equiv$ no. of i^{th} event types occurring during j^{th} priority

M_j $\equiv$ total no. of readouts (including both null and non-null events of all types) occurring in j^{th} priority

R'_{ij} $\equiv$ measured rate of occurrence of i^{th} event type during j^{th} priority

τ $\equiv$ readout time for PHA events (note that this will vary inversely as the bit rate)

Then the measured rate of occurrence in the data of PHA event types is:

$$R'_{ij} = \frac{N_{ij}}{M_j \tau}$$

We define the quantity α_{ijk} as follows:

For $i \neq j$ $\quad \alpha_{ijk} = 1$ if $k > i$ or if $k = j$
$= 0$ otherwise

For $i = j$ $\quad \alpha_{ijk} = 1$ if $k = j$
$= 0$ otherwise

As we have defined it, $\alpha_{ijk} = 1$ for all event types k whose priority is higher than the i^{th} event type when the j^{th} priority ordering is in effect. Some examples of the use of α_{ijk} are as follows"

$$\sum_{k=0}^{3} \alpha_{03k} R'_{k3} = R'_{13} + R'_{23} + R'_{33}$$

$$\sum_{k=0}^{3} \alpha_{12k} R'_{k2} = R'_{22} + R'_{32}$$

$$\sum_{k=0}^{3} \alpha_{30k} R'_{k0} = R'_{00}$$

Using the previously defined notation the true rate of occurrence of PHA events R_{ij} is given by:

$$R_{ij} = -\frac{1}{\tau}\left[\ln\left(1 - \frac{R'_{ij}\tau}{1-\sum_{k=0}^{3} \alpha_{ijk} R'_{kj}\tau}\right)\right] \qquad (1)$$

In the PHA summary plot program for each bit rate present during the summary interval there shall be displayed three 4x4 matrices. These shall be respectively the N_{ij}, R'_{ij}, and R_{ij} arrays. For a particular bit rate the display shall look as follows:

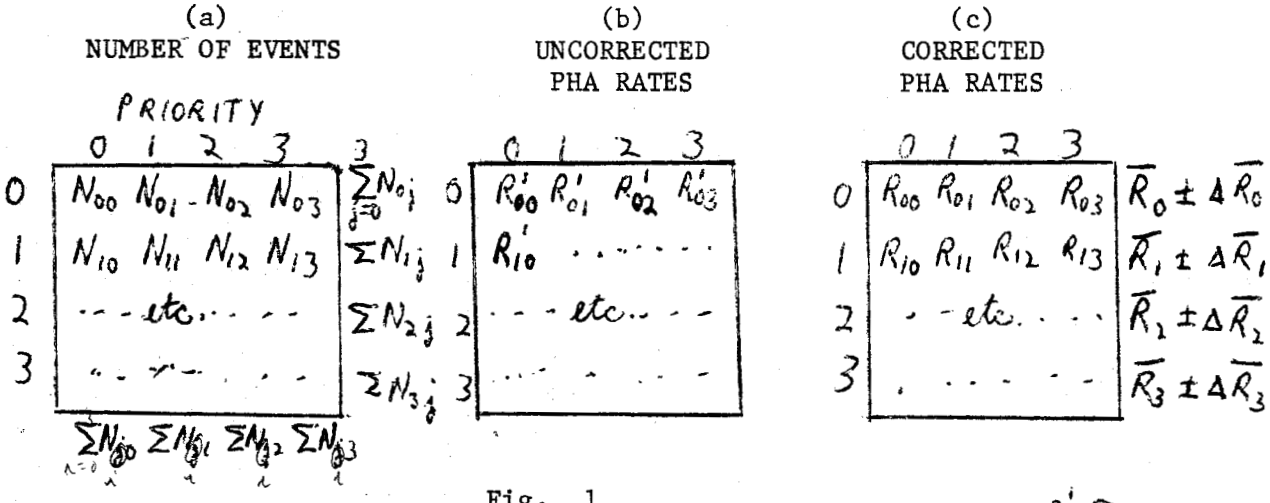

Fig. 1

Referring to equation (1) we see that if the quantity $X_{ij} = \dfrac{R'_{ij}\tau}{1 - \sum_{k=0}^{3} \alpha_{ijk} R'_{kj}\tau}$ is ≥ 1 then R_{ij} is not defined. Note that if $S'_{ij}\tau \equiv \sum_{k=0}^{3} \alpha_{ijk} R'_{kj}\tau = 1$ the quantity X_{ij} is infinite. The program shall check to see if $S'_{ij}\tau = 1$. If the equality holds then R_{ij} shall be set equal to -1. The quantity X_{ij} shall then be checked to see if its value exceeds 0.75. If this is true then R_{ij} shall also be set equal to -1.

The values of M_j for $j = 0,3$ shall be displayed for each bit rate

and shall be labelled "TOTAL READOUTS".

The error in each of the dead time corrected rates is given by:

$$\Delta R_{ij} = \left[\frac{R'_{ij}}{M_j \tau (1-S'_{ij}\tau)[1-(R'_{ij}+S'_{ij})\tau]} \right]^{1/2}$$

where $S'_{ij} = \sum_{k=0}^{3} \alpha_{ijk} R'_{kj}$

The average rate (over priorities) for the i^{th} event type is given by:

$$\overline{R}_i = \frac{\sum_{j=0}^{3} R_{ij}/(\Delta R_{ij})^2}{\sum_{j=0}^{3} (1/\Delta R_{ij}^2)}$$

where where those j values for which $R_{ij} = -1$ are excluded from the sum.

The error in the average rate is given by

$$\Delta \overline{R}_i = \left[\frac{1}{\sum_{j=0}^{3} 1/\Delta R_{ij}^2} \right]^{1/2}$$

In addition to the arrays for each of the bit rates a summary over all bit rates in the format shown in Fig. 1 shall also be displayed. For the array in Fig. 1(a) a simple sum will be displayed over all bit rates present during the summary interval. For Fig. 1(b) an average over bit rate (denoted by $\langle R'_{ij} \rangle_{br} = \frac{\sum_{br} R'_{ij} M_j}{\sum_{br} M_j}$

where $\sum_{br}$ denotes summation over all bit rates.

For Fig. 1(c) the average will be taken as follows:

$$\langle R_{ij} \rangle_{br} = \frac{\sum_{br} R_{ij} M_j}{\sum_{br} M_j}$$

$$\langle \Delta R_{ij} \rangle_{br} = \left[\frac{1}{\sum_{br} 1/\Delta R_{ij}^2} \right]^{1/2}$$

$$\text{and} \quad \langle \bar{R}_i \rangle_{bn} = \frac{\sum_{bn} \bar{R}_i / \overline{\Delta R_i}^2}{\sum_{bn} 1 / \overline{\Delta R_i}^2}$$

$$\langle \overline{\Delta R_i} \rangle_{bn} = \left[\frac{1}{\sum_{bn} 1 / \Delta \bar{R}_i^2} \right]^{1/2}$$

where again those bit rates for which a particular $R_{ij} = -1$ are eliminated from the sum for that particular i, j value.

LET-I

Exactly the same procedures and calculations shall be done for LET-I as have been done for HET. The only difference is that there are only two event types and priorities rather than four as in the case of the HET. The priority orderings are as follows:

PRIORITY No.	1	0
EVENT TYPE	1	0
ORDERING	0	1

The relationship between priority no. and the non-sectored rate ID in E1-30 is as follows:

PRIORITY No.	E1-30
1	0, 4
0	2, 6

DERIVATION OF PIONEER PHA DEAD TIME CORRECTION

Let R'_{ij} be the measured rate of i^{th} event types during the j^{th} priority, and let R_{ij} be the "true" rate. Then:

$$R'_{ij} = \frac{N_{ij}}{M_j \tau}$$

where N_{ij} = total number of i^{th} event types read out during j^{th} priority
M_j = " " " readouts in j^{th} priority
τ = readout time

Let P_1 be the probability of at least one event type i occuring during the time τ and let P_2 be the probability that an event of higher priority occurred in τ. Then the probability of reading out an i-type event is given by

$$P_{R/O} = P_1 (1 - P_2). \qquad (a)$$

The read-out probabity is $P_{R/O} = R'_{ij} \tau$ ✓ ≤ 1 (b)

and $P_1 = 1 - e^{-R_{ij}\tau}$ (c)

$$P_2 = \sum_{\text{higher priority}} R'_{kj} \tau = \sum_{k=0}^{3} \alpha_{ijk} R'_{kj} \tau \qquad (d)$$

(see specs for definition of α_{ijk})

Substituting (b), (c), and (d) into eqn. (a), we have

$$R'_{ij}\tau = \left(1 - e^{-R_{ij}\tau}\right)\left[1 - \sum_{k=0}^{3} \alpha_{ijk} R'_{kj}\tau\right]$$

Solving for R_{ij} gives:

$$R_{ij} = -\frac{1}{\tau} \ln\left[1 - \frac{R'_{ij}\tau}{1 - \sum_{k=0}^{3} \alpha_{ijk} R'_{kj}\tau}\right] \qquad (1)$$

$$= -\frac{1}{\tau} \ln\left[1 - \frac{R'_{ij}\tau}{1 - S'_{ij}\tau}\right]$$

where $S'_{ij} = \sum_{k=0}^{3} \alpha_{ijk} R'_{kj}$

~~The~~ Eqn (1) then gives the true rate of the i^{th} event type during the j^{th} priority calculated using only PHA data occurring in the j^{th} priority.

CALCULATION OF ERRORS

Assume that n trials are made with possible outcomes a, b, c, d ——, each having a ~~prob~~ probability P_a, P_b, P_c —— of occurring. The multinomial distribution gives the probability of the set of numbers of ~~occurrences~~ outcomes (n_a, n_b, n_c ——) as follows:

$$P(n_a, n_b, n_c, \ldots) = \frac{n!}{n_a! n_b! n_c! \ldots} p_a^{n_a} p_b^{n_b} p_c^{n_c} \ldots \quad (2)$$

The average values are given by

$$\bar{n}_a = n p_a \quad (3)$$
$$\bar{n}_b = n p_b$$
$$\text{etc.}$$

The standard deviations are

$$\overline{\Delta n_a^2} = \overline{(n_a - \bar{n}_a)^2} = n p_a (1 - p_a) \quad (4)$$

etc.

and the covariances are:

$$\overline{\Delta n_a \Delta n_b} = n p_a p_b \quad (5)$$

etc.

Suppose that we have some function of n_a and n_b, $f(n_a, n_b)$, for which we want to find the standard deviation. Expanding in a Taylor series and keeping only first order terms gives:

$$\Delta f(n_a, n_b) = \frac{\partial f}{\partial n_a} \Delta n_a + \frac{\partial f}{\partial n_b} \Delta n_b$$

Then $$\overline{\Delta f^2} = \left(\frac{\partial f}{\partial n_a}\right)^2 \overline{\Delta n_a^2} + \left(\frac{\partial f}{\partial n_b}\right)^2 \overline{\Delta n_b^2} + 2\frac{\partial f}{\partial n_a}\frac{\partial f}{\partial n_b}\overline{\Delta n_a \Delta n_b} \qquad (6)$$

We now make the following identifications:

$$n_a = R'_{ij}\tau M_j \qquad p_a = R_{ij}\tau$$
$$n_b = S'_{ij}\tau M_j \qquad p_b = S_{ij}\tau$$
$$n = M_j$$
and $$f(n_a, n_b) = R_{ij}$$

The ~~derivatives of the~~ 1st term on the l.h.s. of eqn. (1) is then

$$\left(\frac{\partial R_{ij}}{\partial R'_{ij}}\right)^2 \overline{\Delta R'^2_{ij}} = \left(\frac{\partial R_{ij}}{\partial R'_{ij}}\right)^2 \frac{R'_{ij}}{M_j\tau}(1 - R'_{ij}\tau) \qquad (7)$$

$$= \frac{1}{\left[1-(S'_{ij}+R'_{ij})\tau\right]^2}\frac{R'_{ij}}{M_j\tau}(1-R'_{ij}\tau)$$

The 2nd term is:

$$\overline{\Delta S'^2_{ij}}\left(\frac{\partial R_{ij}}{\partial S'_{ij}}\right)^2 = \left(\frac{\partial R_{ij}}{\partial S'_{ij}}\right)^2 \frac{S'_{ij}}{M_j\tau}(1-S'_{ij}\tau) \qquad (8)$$

$$= \left[\frac{R'_{ij}\tau}{1-S'_{ij}\tau}\frac{1}{1-(R'_{ij}+S'_{ij})\tau}\right]^2 \frac{S'_{ij}}{M_j\tau}(1-S'_{ij}\tau)$$

$$= \left[\frac{R'_{ij}\tau}{1-(R'_{ij}+S'_{ij})\tau}\right]^2 \frac{S'_{ij}\tau}{M_j\tau(1-S'_{ij}\tau)}$$

and the third term is:

$$2\,\frac{\partial R_{ij}}{\partial R'_{ij}}\,\frac{\partial R_{ij}}{\partial S'_{ij}}\,\overline{\Delta R'_{ij}\,\Delta S'_{ij}} = 2\,\frac{\partial R_{ij}}{\partial R'_{ij}}\,\frac{\partial R_{ij}}{\partial S'_{ij}}\,\frac{R'_{ij}\,S'_{ij}}{M_j} \qquad (9)$$

$$= -2\,\frac{R'_{ij}\,\tau}{(1-S'_{ij}\tau)}\,\frac{1}{\left[1-(R'_{ij}+S'_{ij})\tau\right]^2}\,\frac{R'_{ij}\,S'_{ij}}{M_j}$$

Combining eqns. (7), (8), and (9) gives:

$$\overline{\Delta R_{ij}^2} = \frac{R'_{ij}}{M_j\tau\,(1-S'_{ij}\tau)\left[1-(R'_{ij}+S'_{ij})\tau\right]} \qquad (10)$$

Then defining (awkwardly) $\Delta R_{ij} = \left(\overline{\Delta R_{ij}^2}\right)^{1/2}$

we have $$\Delta R_{ij} = \left[\frac{R'_{ij}}{M_j\tau\,(1-S'_{ij}\tau)\left[1-(R'_{ij}+S'_{ij})\tau\right]}\right]^{1/2} \qquad (11)$$

We consider a few special cases:

1. $\underline{S'_{ij}\tau \ll 1}$

$$\Delta R_{ij} \cong \left[\frac{R'_{ij}}{M_j\tau\,(1-R'_{ij}\tau)}\right]^{1/2} = \Delta R'_{ij} \quad \text{as expected}$$

2. $\underline{R'_{ij}\tau \ll 1}$

$$\Delta R_{ij} \cong \left(\frac{R'_{ij}}{M_j\tau}\right)^{1/2} \frac{1}{1-S'_{ij}\tau}$$

$$= \frac{(\Delta R'_{ij})_0}{1-S'_{ij}\tau}$$

3. $\underline{R'_{ij}\tau = S'_{ij}\tau = 1/4}$

$$\Delta R_{ij} = \left(\frac{R'_{ij}}{M_j\tau}\right)^{1/2} \left[\frac{1}{(1-1/4)(1-1/2)}\right]^{1/2}$$

$$= \sqrt{8/3}\ (\Delta R'_{ij})_0$$

$$= 1.63\,(\Delta R'_{ij})_0$$

where $(\Delta R'_{ij})_0$ = error in R'_{ij} if there were no priority system and no dead time correction necessary.

Stattlemyer / Broomhall / Lal

Pioneer 10 and 11
Goddard/U. New Hampshire Cosmic Ray Experiment
Jupiter and Saturn Encounter Data

Instrumentation

This experiment consists of a set of three solid-state telescopes, each designed to complement the others and to cover a broad range in energy, intensity and charge spectra. The three telescopes are shown schematically in the attached figure; they are the high-energy telescope (HET) and two low-energy telescopes (LET-I and LET-II). The HET and LET-I are designed primarily for measuring the relatively low fluxes of cosmic rays in interplanetary space. As such, their geometry factors are relatively large, and they cannot tolerate fluxes $\geq 2 \times 10^4/cm^2$ s sr. Their usefulness is, therefore, limited to the outer regions of the Jovian magnetosphere (≥ 20 R_J). They are, however, high-resolution double dE/dX vs. E instruments that provide unambiguous particle identification and precise energy spectra, so that their contribution to the overall body of data is quite significant.

The LET-II telescope was designed to measure low-energy solar flare particles in interplanetary space and trapped particles in the Jovian magnetosphere. It has a relatively small geometry factor (1.5×10^{-2} cm^2 sr) and can readily measure fluxes up to $\sim 5 \times 10^5/cm^2$ s sr. It is surrounded by a colimator and shield which will stop electrons up to ~ 4.5 MeV and protons up to ~ 40 MeV. The telescope employs a two-parameter analysis technique to separate electrons and protons. The front element SI has an electronic threshold that is set so that any electron penetrating to SII is below threshold and any proton penetrating to SII is above threshold. Selected counting rates in all three telescopes are divided into eight angular sectors to measure particle anisotropies.

A major effort has been devoted to understanding the response of all detector systems in the presence of intense particle fluxes. The onset of saturation in the LET and HET systems is abrupt and well defined. Negligible corrections are necessary prior to this saturation point.

There is significant overlap in the response functions of the three telecopes, and it was of great value to observe the consistency between flux measurements made with completely different detector systems. For example, the LET-I and LET-II proton data in the 0.5- to 2-MeV region are in excellent agreement. This finding is especially helpful in the outer Jovian magnetosphere where the nuclear component is small (1-10%) in comparison with electrons of the same energy. A complete description of this instrument has been published in the IEEE Transactions on Nuclear Science (Stilwell et al., 1975). The energy and charge ranges of each telescope are summarized in Table 1.

Since the Goddard/University of New Hampshire experiment was primarily designed as an interplanetary experiment, its telemetry assignment was minimal during the Jupiter and Saturn encounters. Consequently, individual pulse heights were sampled infrequently, and most of the results have to be based on rate data. This leaves some ambiguity about the type of particles responsible for the counts. This problem arises primarily in identifying protons vs. alpha particles and heavier ions. LET-I and LET-II respond differently because of the aluminized mylar foil in front of the LET-I detector. On this basis, it has been concluded (McDonald et al., 1979) that the nominal "proton channels" respond primarily to protons at Jupiter; however, some admixture of heavier ions is clearly present and the amount is time dependent. It is hoped that further analysis can narrow down the uncertainty.

Data have been included only for periods when the detectors operated in this design range. This excludes the inner magnetosphere. At Jupiter, the detectors were heavily saturated in this region, while at Saturn a very penetrating radiation prevented a clear identification of the type and energy of the particles responsible for our counts. Some of the published results from this experiment required extensive corrections for deadtime, accidental coincidences and anticoincidences (Trainor et al., 1974; McDonald and Trainor, 1976; McDonald et al., 1980). These corrections can be applied only on a case-by-case basis after careful study of the environment and many self-consistency checks. They cannot be applied on a systematic basis and we have no computer programs to do so. A special problem arose during the Pioneer 10 out pass from Jupiter. Radiation damage to the digital logics decreased the margins in these circuits. Although most of the data is good, certain bits failed to reset every now and then. For 15-minute averages, this effect can generally be ignored; but the user should be aware that a few points are off due to this problem. If a user is interested in data not included in this submission or has special questions, the experimenters will be glad to consider requests if the desired information can be extracted from the data.

Description of the Data

In the following rate definitions, individual detectors are identified by the same symbols as in the attched figure. Any subscripts refer to different trigger thresholds on that deector (SIIA is an annular guard detector in LET-II which is not labeled in the figure). Several detectors defining a rate are in coincidence unless a bar over the symbol indicates that the detector is in anticoincidence.

(1) A_2 Rate (Saturn only) gives the counting rate in a 2.5-mm thick Si detector with an area of 3.0 cm^2. Since the threshold is set at 2.01 MeV, it responds primarily to energetic electrons; however, the effective solid angle and detection efficiency are not well known. This rate is given for Saturn because the more desirable coincidence rates suffered from excessive accidentals (note A_2 is identified as A2 on tape).

(2) $A_1 \overline{A_2}$ B $\overline{CI}$ Rate (Jupiter only) gives the flux of electrons with a range between 2.5 and 5.0 mm of Si which deposit less than 2 MeV in the front detector. The electron energy falls into the range of about 1.8 to 3.2 MeV (on the tape this rate is identified as A1.¬A2.B.¬C1).

(3) $A_1 \overline{A_2}$ B CI $\overline{CII}$ Rate (Jupiter only) gives the electron flux with a range of 5 to 10 mm Si; the approximate energy range of 3.2 to 5.1 MeV (the rate ID is A1.¬A2.B.C1.¬C2).

(4) $A_1 \overline{A_2}$ B CI CII $\overline{CIII}$ Rate (Jupiter only) gives the electron flux with a range of 10 to 15 mm Si; the approximate electron energies are 5.1 to 8 MeV (the rate ID is A1.¬A2.B.C1.C2.¬C3).

(5) $\overline{SI}$ SII_5 $\overline{SIIA}$ $\overline{SIII}$ Rate gives the flux of electrons in LET-II which do not trigger the 0.145 MeV threshold in the 50 γ front detector and trigger the 50 keV threshold in the 2.5-mm thick second detector. The anticoincidence requirement with the annular guard counter SIIA and rear detector SIII insures that the electrons stop in SII. Our calibrations show that the 50% efficiency points occur at 0.16 and 2.0 MeV. If the electron spectrum is hard, this rate will also respond to bremsstrahlung and electrons penetrating the collimator. The latter effect made the

dominant contribution in the inner Saturnian magnetosphere; otherwise, it is believed to be small but is difficult to evaluate (the rate ID is ¬S1.S2(5).¬S2(A).¬S3).

(6) $\overline{SI}\ SII_6\ \overline{SIIA}\ \overline{SIII}$ Rate is equivalent to rate (5) but with a 0.35-MeV threshold in SII, corresponding to electron energies from 0.43 to 2.0 MeV (the rate ID is ¬S1.S2(6).¬S2(A).¬S3).

(7) $\overline{SI}\ SII_7\ \overline{SIIA}\ \overline{SIII}$ Rate is equivalent to rate (5) but with a 0.7 MeV threshold in SII corresponding to electron energies from 0.8 to 2.0 MeV (the rate ID is ¬S1.S2(7).¬S2(A).¬S3).

(8) $\overline{SI}\ SII_8\ \overline{SIIA}\ \overline{SIII}$ Rate is equivalent to rate (5) but with a 1.0-MeV threshold in SII corresponding to electron energies from 1.1 to 2.0 MeV (the rate ID is ¬S1.S2(8).¬S2(A).¬S3).

(9) DI_4 Rate gives the flux of protons and ions which penetrate a 0.53-mg/cm^2 aluminized mylar foil and deposits at least 0.60 (P-10) or 0.63 (P-11) MeV in detector DI of LET-I. (This rate is not given for the Saturn encounter because of substantial electron contamination.) For protons, this corresponds to energies from 0.84 to 15.1 MeV.

(10) DI_5 Rate is eqivalent to rate (9), but with a threshold in DI of 0.95 MeV corresponding to proton energies between 1.11 and 8.1 MeV.

(11) DI_6 Rate is equivalent to rate (9), but with a threshold in DI of 1.45 MeV corresponding to proton energies from 1.6 to 5.1 MeV.

(12) DI_7 Rate is equivalent to rate (9), but with a threshold energy in DI of 2.20 (P-10) or 2.05 (P-11) MeV corresponding to proton energies from 2.3 to 3.6 MeV and 2.1 to 3.8 MeV, respectively, for P-10 and P-11.

(13) DI DII $E_2\ \overline{F}$ Rate from LET-I gives the proton flux between 10.3 and 21 MeV for P-10 and between 11 and 21 MeV for P-11. A small correction has

been made for the contribution from alphas and heavier nuclei in the same energy/nucleus range (the rate ID is D1.D2.E2.¬F - D1.D2.$\sum$ D.E4.¬F).

(14) $SI_1 \neg \overline{SII} \neg \overline{SIIA} \neg \overline{SIII}$ Rate gives the flux of protons and heavier ions which stop in the 50γ-thick Si detector SI and deposits an energy between 0.16 and 2.6 MeV. This corresponds to proton energies between 0.20 and 2.15 MeV (P-10) or 2.17 MeV (P-11). Detector SI is shielded by only 0.12 mg/cm^2 of Al and is, therefore, relatively sensitive to low-energy ions. At Saturn, the ion contribution is negligible; however, it may be significant at Jupiter (the rate ID is S1(1).¬S2.¬S2)A).¬S3 - S1(4).¬S2.¬S2(A).¬S3).

(15) SI_6 $\overline{SII}$ $\overline{SIIA}$ $\overline{SIII}$ Rate is equivalent to rate (14) except that the threshold in SI is 0.47 (P-10) or 0.5 (P-11) MeV, this corresponds to proton energies of 0.50 to 2.15 and 0.53-2.17 MeV for P-10 and P-11, respectively (the rate ID is S1(6).¬S2.¬S2(A).¬S3 - S1(4).¬S2.¬S2(A).¬S3).

(16) SI_2 $\overline{SII}$ $\overline{SIIA}$ $\overline{SIII}$ Rate is equivalent to rate (14) except that the threshold is 0.74 (P-10) an 0.72 (P-11), this corresponds to proton energies of 0.76-2.15 MeV (P-10) and 0.74-2.17 MeV (P-11) (the rate ID is S1(2).¬S2.¬S2(A).¬S3 - S1(4).¬S2.¬S2(A).¬S3).

(17) SI_3 $\overline{SII}$ $\overline{SIIA}$ $\overline{SIII}$ Rate is equivalent to rate (14) except that the threshold is 1.2 MeV, corresponding to proton energies of 1.24 to 2.15 MeV (1.24-2.17, P-11) (the rate ID is S1(3).¬S2.¬S2(A).¬S3 - S1(4).¬S2.¬S2(A).¬S3).

(18) SI SII_1 $\overline{SIIA}$ $\overline{SIII}$ Rate gives the flux of protons between 3.13 and 14.8 MeV for Pioneer 10 (3.19-14.9 MeV, P-11) (the rate ID is S1.S2(1).¬S2(A).¬S3 - S1.S2(3).¬S2(A).¬S3).

(19) SI SII_2 $\overline{SIIA}$ $\overline{SIII}$ Rate is equivalent to rate (18) except for a higher threshold and covers protons from 5.65 to 14.8 MeV for P-10 (5.68 to 14.9 MeV for P-11) (The rate ID is S1.S2(2).¬S2(A).¬S3 - S1.S2(3).¬S2(A).¬S3).

Data Format

Time history of Pioneer Cosmic Ray Telescope data described above is being submitted on 9-track tapes recorded at 1600 BPI. Tape marked PIOJUF contains Pioneer-10 data, the one marked PIOJUG contains Pioneer-11 data for Jupiter encounter and tape marked PIOSAG contains Pioneer-11 data for the Saturn encounter. Averaging interval for all data is fifteen minutes.

PIOJUF and PIOJUG each have five files and PIOSAG has four files. Contents of PIOJUF, PIOJUG and PIOSAG are described in Tables 2 to 4, respectively. Each file consists of a number of Flux Time History (FTH) records. An FTH record contains a count of the number of data items (NBIN) whose time-history is included in the record, a count of the number of averaging intervals (NINT) included in the record and definitions of data items included and time-history data. Table 5 defines the structure of an FTH record in detail. These tapes were generated on an IBM System 360 computer; thus, a word consists of 32 bits, half-word 1 is the high order 16-bit field of the word and half-word 2 the low order half (bits 16-31, with the left-most or MSB numbered 0). Characters are represented in 8-bit EBCDIC bytes, real numbers are represented in the IBM single precision floating point format. Length (in words) of an FTH record is given by:

$$200 + (3 + 2 * NBIN) * NINT.$$

REFERENCES

McDonald, F.B., and J.H. Trainor, Observations of Energetic Jovian Electrons and Protons," in Jupiter, ed. T. Gehrels, Univ. Ariz. Press, 961, 1976.

McDonald, F.B., A.W. Schardt and J.H. Trainor, "Energetic Protons in the Jovian Magnetosphere," J. Geophys. Res. 84, 2579, 1979.

McDonald, F.B., A.W. Schardt and J.H. Trainor, "If You've Seen One Magnetosphere, You Haven't Seen Them All: Energetic Particle Observations in the Saturn Magnetosphere," J. Geophys. Res. 85, 5813, 1980.

Stilwell, D.E., R.M. Joyce, J.H. Trainor, H.P. White, G. Streeter and J. Bernstein, "Pioneer 10/11 and Helios A/B Cosmic Ray Instruments," IEEE Trans. Nucl. Sci. 22, 570, 1975.

Trainor, J.H., F.B. McDonald, B.J. Teegarden, W.R. Webber and E.C. Roelof, "Energetic Particles in the Jovian Magnetosphere," J. Geophys. Res. 79, 3600, 1974.

TABLE 1: Pioneer 10 and 11 Detectors Used during Planetary Encounters

Detector	Shielding	Energy Range (MeV)	Geometric Factor (cm^2 sr)	Comments
PROTONS:				
o LET I	0.53 mg/cm^2 Mylar			Several channels of protons and ions that exceed threshold in DI. The proton flux from rate agrees with pulse-height analyzed data.
DI only		0.84-15.1	1.13	
DI DII E_2 $\overline{F}$		10.3 -21 (P10) 11.0 -21 (P11)	0.155	
o LET II	0.120 Mg/cm^2 Al			
SI $\overline{SII}$ $\overline{SIIA}$ $\overline{SIII}$		0.2 - 2.15 (P10) 0.2 - 2.17 (P11)	0.015	Several channels of protons and some heavier ion contributions.
SI SII $\overline{SIIA}$ $\overline{SIII}$		3.2 -14.8		Protons.
ELECTRONS:				
o HET				
A_1 $\overline{A_2}$ B $\overline{CI}$	2.5- 5 mm Si	1.8 - 3.2	0.22	Coincidence rates with good background rejection, but accidental coincidence problems at high counting rate.
A_1 $\overline{A_2}$ B CI $\overline{CII}$	5.0-10 mm Si	3.2 - 5.1		
A_1 $\overline{A_2}$ B CI CII $\overline{CIII}$	10 -15 mm Si	5.1 - 8		
o LET II				
SI SII $\overline{SIIA}$ $\overline{SIII}$		0.16- 2	0.015	Several electron channels. Some contamination from collimator penetration and bremsstrahlung.

Table 2. Contents of PIOJUF

FILE	RATES	TIME PERIOD		
1	$A_1\ \overline{A_2}$ B $\overline{CI}$	11/26/73	00:00:00-12/01/73	18:00:00
			AND	
	$A_1\ \overline{A_2}$ B CI $\overline{CII}$	12/04/73	22:00:00-12/16/73	00:00:00
	$A_1\ \overline{A_2}$ B CI CII $\overline{CIII}$			
2	$\overline{SI}$ SII_5 $\overline{SIIA}$ $\overline{SIII}$	11/26/73	00:00:00-12/03/73	08:00:00
			AND	
	$\overline{SI}$ SII_6 $\overline{SIIA}$ $\overline{SIII}$	12/04/73	15:00:00-12/16/73	00:00:00
	$\overline{SI}$ SII_7 $\overline{SIIA}$ $\overline{SIII}$			
	$\overline{SI}$ SII_8 $\overline{SIIA}$ $\overline{SIII}$			
3	DI_4	12/26/73	00:00:00-12/03/73	08:00:00
			AND	
	DI_5	12/04/73	22:00:00-12/16/73	00:00:00
	DI_6			
	DI_7			
	DI DII E_2 $\overline{F}$			
4	SI_1 $\overline{SII}$ $\overline{SIIA}$ $\overline{SIII}$	11/26/73	00:00:00-12/03/73	08:00:00
			AND	
	SI_6 $\overline{SII}$ $\overline{SIIA}$ $\overline{SIII}$	12/04/73	15:00:00-12/16/73	00:00:00
	SI_2 $\overline{SII}$ $\overline{SIIA}$ $\overline{SIII}$			
5	SI_3 $\overline{SII}$ $\overline{SIIA}$ $\overline{SIII}$	11/26/73	00:00:00-12/03/73	08:00:00
			AND	
	SI SII_1 $\overline{SIIA}$ $\overline{SIII}$	12/04/73	15:00:00-12/16/73	00:00:00
	SI SII_2 $\overline{SIIA}$ $\overline{SIII}$			

Table 3. Contents of PIOJUG

FILE	RATES	TIME PERIOD
1	$A_1\ \overline{A_2}$ B $\overline{CI}$	11/26/74 00:00:00-12/02/74 16:00:00
		AND
	$A_1\ \overline{A_2}$ B CI $\overline{CII}$	12/04/74 22:00:00-12/10/74 00:00:00
	$A_1\ \overline{A_2}$ B CI CII $\overline{CIII}$	
2	$\overline{SI}\ SII_5\ \overline{SIIA}\ \overline{SIII}$	11/26/74 00:00:00-12/02/74 18:00:00
		AND
	$\overline{SI}\ SII_6\ \overline{SIIA}\ \overline{SIII}$	12/03/74 09:00:00-12/10/74 00:00:00
	$\overline{SI}\ SII_7\ \overline{SIIA}\ \overline{SIII}$	
	$\overline{SI}\ SII_8\ \overline{SIIA}\ \overline{SIII}$	
3	DI_4	11/26/74 00:00:00-12/02/74 16:00:00
		AND
	DI_5	12/03/74 08:00:00-12/10/74 00:00:00
	DI_6	
	DI_7	
	DI DII $E_2\ \overline{F}$	
4	$SI_1\ \overline{SII}\ \overline{SIIA}\ \overline{SIII}$	11/26/74 00:00:00-12/02/74 18:00:00
		AND
	$SI_6\ \overline{SII}\ \overline{SIIA}\ \overline{SIII}$	12/03/74 08:00:00-12/10/74 00:00:00
	$SI_2\ \overline{SII}\ \overline{SIIA}\ \overline{SIII}$	
5	$SI_3\ \overline{SII}\ \overline{SIIA}\ \overline{SIII}$	11/26/74 00:00:00-12/02/74 18:00:00
		AND
	$SI\ SII_1\ \overline{SIIA}\ \overline{SIII}$	12/03/74 08:00:00-12/10/74 00:00:00
	$SI\ SII_2\ \overline{SIIA}\ \overline{SIII}$	

Table 4. Contents of PIOSAG

FILE	RATES	TIME PERIOD		
1	A_2	8/31/79	00:00:00-9/01/79	13:30:00
			AND	
	$\overline{SI}\ SII_5\ \overline{SIIA}\ \overline{SIII}$	9/01/70	19:00:00-9/04/79	12:00:00
	$\overline{SI}\ SII_6\ \overline{SIIA}\ \overline{SIII}$			
	$\overline{SI}\ SII_7\ \overline{SIIA}\ \overline{SIII}$			
	$\overline{SI}\ SII_8\ \overline{SIIA}\ \overline{SIII}$			
2	DI_5	8/31/79	00:00:00-9/01/79	13:30:00
			AND	
	DI_6	9/01/70	19:00:00-9/04/79	12:00:00
	DI_7			
	$DI\ DII\ E_2\ \overline{F}$			
3	$SI_1\ \overline{SII}\ \overline{SIIA}\ \overline{SIII}$	8/31/79	00:00:00-9/01/79	13:30:00
			AND	
	$SI_6\ \overline{SII}\ \overline{SIIA}\ \overline{SIII}$	9/01/79	19:00:00-9/04/79	12:00:00
	$SI_2\ \overline{SII}\ \overline{SIIA}\ \overline{SIII}$			
4	$SI_3\ \overline{SII}\ \overline{SIIA}\ \overline{SIII}$	8/31/79	00:00:00-9/01/79	13:30:00
			AND	
	$SI\ SII_1\ \overline{SIIA}\ \overline{SIII}$	9/01/79	19:00:00-9/04/79	12:00:00
	$SI\ SII_2\ \overline{SIIA}\ \overline{SIII}$			

Table 5. STRUCTURE OF FLUX TIME-HISTORY RECORD

WORD	HALFWORD	TYPE	DESCRIPTION
1	1	Integer	Number of data items contained in the record (NBIN).
2	2	Integer	Number of averaging intervals (NINT) contained in the record.
3-35		character	132-character title identifies satellite and gives the start time of first averaging interval and last averaging interval in the record.
36-68		character	132-character description of first data item.
69-101		character	132-character description of second data item, if NBIN $\geq$ 2. Otherwise, not used.
102-134		character	132-character description of third data item, if NBIN $\geq$ 3. Otherwise, not used.
135-167		character	132-character description of fourth data item, if NBIN $\geq$ 4. Otherwise, not used.
168-200		character	132-character description of fifth data item, if NBIN $\geq$ 5. Otherwise, not used.
		NBIN $\leq$ 5	
201-			NINT Averaging Interval Entries (AIE). The structure of an AIE is shown in Table 5.
		NBIN = 6	
201-233		character	132-character description of sixth data item.
234-			NINT Averaging Interval Entries.

Table 6. STRUCTURE OF AVERAGING INTERVAL ENTRY

WORD	HALFWORD	TYPE	DESCRIPTION	
1	1	Integer	2-digit year	
	2	Integer	month of year	
2	1	Integer	day of month	Start time of averaging interval
	2	Integer	hour of day	
3	1	Integer	minute of hour	
	2	Integer	second of minute	
4-(3+2*NBIN)		Real	NBIN FLUX entries. Each FLUX entry is two words long. If the second word of the entry is -1.0, data for this item is not available; otherwise the first word is the value of flux and the second word contains the associated statistical error.	

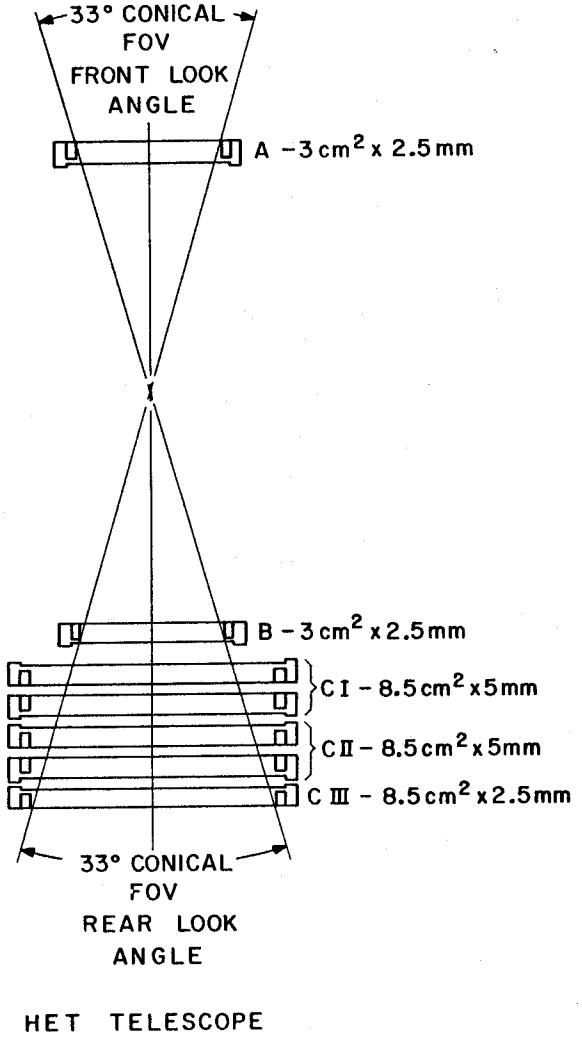

HET TELESCOPE

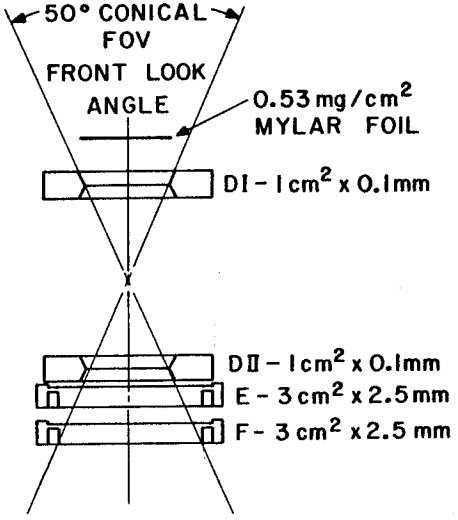

LET-I TELESCOPE

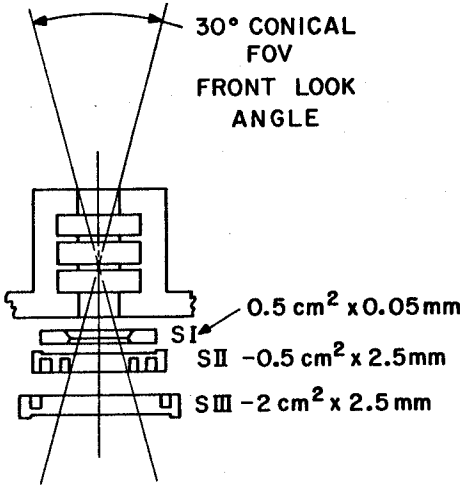

LET-II TELESCOPE

PIONEER F & G DETECTOR COMPLEMENT
COSMIC RAY ENERGY SPECTRA

telemetry notes

The GSFC experiment on the Pioneer spacecraft consists of the "Cosmic Ray Telescopes" and their associated electronics.

1. High Energy Telescope (HET)
2. Low Energy Telescope 1 (LET-1)
3. Low Energy Telescope 2 (LET-2)

The data derived from these telescopes are of two basic forms:

1. Pulse Height Analysis (PHA)
2. Events per second (rates)

The solid state detectors comprising each of the three telescopes are shown in table 1.

HET	LET-1	LET-2
A	DI	SI
B	DII	SII
CI	E	SIIa
CII	F	SIII
CIII		

Table #1 Solid State Detectors Names

The charge liberated, in the detector, by the passage of particle is summed in a charge sensative preamplifier which produces an output voltage pulse whose height is linearly related to the incident particle energy loss in the detector.

The output of the preamplifier is then passed through a post amp where it is given the optimum realizable shape for discrimination and analysis while preserving the amplitude-energy relationship.

The pulses out of the amplifier are fed to their associated linear electronics card where they are differentially buffered and applied to a host of amplitude discriminators. The nominal detection threshold for each of the discriminators is shown in Table 2.

HET		LET-1		LET-2	
Discrim.	Threshold (MeV)	Discrim.	Threshold	Discrim.	Threshold
A1	0.2	DI	.2	SI	.15
A2	2.0	DI_1	.2 .3 .43 .64	SI_1	.15 .7 1.2 2.5
		•		•	
		•	.94	•	.05
		•	1.4	•	.5
		•	2.0	•	1.0
B	0.2	DI_8	3.0	SI_8	1.5
CI	1.0	DII	.2	SII	.06
CII	1.0	ΣD	54.	SII_1	2.0 5.0 15 2.5
				•	
				•	35 .05
				•	.70
CIII	0.2	E1	2.0	SII_8	1.0
*K1	13.6<T<36	E2	9.0	SIIa	.2

Table 2 (cont.)

HET		LET-1		LET-2	
Discrim.	Threshold (MeV)	Discrim.	Threshold	Discrim.	Threshold
*K2	57<T<150	E3	9.0	SIII	.1
		E4	40.0		
		F	.2		

*K = A+B+1.8 (CI+CII)

It can be seen that A1, A2, E1 ....E4 are separate and simultaneous discriminations while DI1...DI8, SI_1....SI8, and SII_1...SI8 are programmable discriminators. These programmable discriminators are slaved either to the telemetry frame rate or to the spacecraft roll rate.

In order to examine as large a portion of the Cosmic Ray Spectrum as possible, and to distinguish between the various species therein, the experiment has built in an elaborate scheme to share it's 32 available rate counting channels and six PHA channels. This is done by imposing coincidence/anti-coincidence requirements upon the pulses appearing in any telescope. These requirements are now discussed on an individual telescope basis.

HET SYSTEM

PHA Data

There are four separate coincidence conditions which will initiate a pulse height analysis. They are:

1) $(A_2K_1$ or $A_1CI)$ $B\overline{CIII}$

2) A_1BK_2 $C\overline{III}$

3) $A_1\overline{A}_2$ BCIII

4) A_2 BCIII

Since there are five detectors to be analyzed and the experiment has only three channels, call them A, B, and C, the available channels are shared as follows: If either of the first two coincidence conditions cause the analysis, CIII has no pulse, therefore; channel A contains the analysis of detector A's pulse, channel B the analysis of detector B's pulse, while channel C contains the analysis of the sum of the pulses appearing in detectors CI and CII ~~two~~. If either of the last two coincidence conditions which causes the analysis, CIII has a pulse Channel A is switched to analyze this CIII pulse. The other channels produce the same analysis.

The PHA's are of the linear, capacitive discharge type, using a gated delay line oscillator to produce a string of pulses whose frequency is 666 KHz and length (Channel #) is related to incident particle energy as follows:

A'	0.2 MeV/Channel
B	0.2 MeV/Channel
CI & CII	1.0 MeV/Channel
CIII	0.2 MeV/Channel

In order to enhance the number of rare particles analyzed, a priority system is built into the HET system. The priority assigned to the four event types is a function of the telemetry frame and is changed every 64 frames as shown in Table 1H.

SEQUENCE ID BITS		EXTERNAL ID BITS		INTERNAL ID BIT	REMARKS
S_1	S_2	I_1	I_2	I_3	
0	0	0	0	0	SYSTEM WILL ACCEPT $A_1\overline{A_2}BC\overline{III}$ FOR ANALYSIS.
0	0	0	0	1	ACCEPT $A_2BC\overline{III}$
0	0	1	0	1	ACCEPT $A_2BC\overline{III}$ AS MANY TIMES AS IT APPEARS OR $(A_2K_1+A_1C_1)BC\overline{III}$
0	0	0	1	1	ACCEPT $(A_2K_1+A_1C_1)BC\overline{III}$ AS MANY TIMES AS IT APPEARS OR $A_1BK_2C\overline{III}$
0	0	1	1	1	I.B. BITS INDICATE $A_1BK_2C\overline{III}$ WAS ACCEPTED FOR ANALYSIS BUT NO MORE OF THESE EVENTS WILL BE ACCEPTED. PHA'S REMAIN INACTIVE UNTIL COMPLETION OF THE NEXT READ-OUT.
1	0	0	0	0	ACCEPT $A_1\overline{A_2}BC\overline{III}$
1	0	0	0	1	ACCEPT $A_2BC\overline{III}$
1	0	1	0	1	ACCEPT $A_2BC\overline{III}$ AS MANY TIMES AS IT APPEARS OR $A_1BK_2C\overline{III}$
1	0	1	1	1	ACCEPT $A_1BK_2C\overline{III}$ AS MANY TIMES AS IT APPEARS OR $(A_2K_1+A_1C_1)BC\overline{III}$
1	0	0	1	1	ACCEPT $(A_2K_1+A_1C_1)BC\overline{III}$ AS MANY TIMES AS IT APPEARS.
0	1	0	0	0	ACCEPT $A_1\overline{A_2}BC\overline{III}$
0	1	0	0	1	ACCEPT $(A_2K_1+A_1C_1)BC\overline{III}$
0	1	0	1	1	ACCEPT $(A_2K_1+A_1C_1)BC\overline{III}$ AS MANY TIMES AS IT APPEARS OR $A_1BK_2C\overline{III}$
0	1	1	1	1	ACCEPT $A_1BK_2C\overline{III}$ AS MANY TIMES AS IT APPEARS OR $A_2BC\overline{III}$
0	1	1	0	1	ACCEPT $A_2BC\overline{III}$ AS MANY TIMES AS IT APPEARS
1	1	0	0	0	ACCEPT $A_2BC\overline{III}$
1	1	1	0	1	ACCEPT $(A_2K_1+A_1CI)BC\overline{III}$
1	1	0	1	1	ACCEPT $A_1BK_2C\overline{III}$
1	1	1	1	1	ACCEPT $A_1BK_2C\overline{III}$ AS MANY TIMES AS IT APPEARS OR $A_1\overline{A_2}BC\overline{III}$
1	1	0	0	1	ACCEPT $A_1\overline{A_2}BC\overline{III}$ AS MANY TIMES AS IT APPEARS

TABLE 1H

Event Type	Particle	Event Code I2=2^1	I1=2^0	Relative Priority (1=highest) S1=S2=0	S1=1,S2=0	S1=0,S2=1	S1=S2=1
$A_1BK_2\overline{CIII}$	Stopping particles Z≥2	1	1	1*	2	2	2
$(A_2K_1 + A_1CI)\ B\overline{CIII}$	Stopping e^-, or stopping p+ and heavier	1	0	2	1	3	3*
A_2B CIII	Penetrating particles Z≥2	0	1	3	3	1	4*
$A_1\overline{A_2}$ B CIII	Penetrating e^-	0	0	4*	4*	4*	1

* Each event is analyzed as often as it occurs unless marked with *,

in which case that event type is analyzed only once per readout.

To uniquely "tag" a PHA event it is necessary to readout the "Seq. I.D." and "External I.D. bits" shown in table 1H. "Internal ID bits" is not read out but this does not produce an ambiquity. Referring to table 1H for S1=S2=0: If I_1=1 and I_2=0 (lowest Priority) the event is the last A2BCIII event encountered (note that the system will continue to accept new A2BCIII events without shanging ID bits). If I_1=0, I_1=1 the event is the last (A_1BK_2CI) BCIII event encountered. If I_1=I2=1, (highest priority) the PHA's contain the first A_1BK2CIII event encountered. Table 1H may be read in similar fashion for the other three combination of S1 and S2 where, it is seen, the priorities are reorder for each combination.

As a further aid in determining the species of particle analyzed the HET electronic produces a 1 bit of the CII threshold has been exceeded which is also read out in the associated tag word.

To meet the scientific objective of the CRT some indication of the direction of the incoming particle is also necessary. Therefore, for each PHA event an indication of the orientation of the spacecraft (one of eight possible sectors is also placed in the tag word of PHA event.

Rate Data

The HET system has assigned to it, 9 accumulators (R_1-R_9) exculsively and shares 8 accumulators (SR1) on a fifty-fifty basis with the LET-1 system. (See Table 2H.

Table 2H.

NAME OF OUTPUT	RATE EQUATION	A1 / B	S1	S2	SS1	SS2	SS3
R1	$(\bar{A}_2 K_1 + A_1 C_I) B \bar{C}_{III}$	1					
R2A	$\bar{A}_2 A_1 B C_{III}$	0					
" B	$A_1 B K_2 \bar{C}_{III}$	1					
R3A	$A_2 B C_{III}$	0					
" B	$A_2 B K_2 \bar{C}_I$	1					
R4A	$A_2 B K_2 C_I \bar{C}_{II}$	0					
" B	A_1	1					
R5A	$A_2 B K_2 C_I C_{II} \bar{C}_{III}$	0					
" B	A_2	1					
R6A	$A_1 \bar{A}_2 B \bar{C}_I$	0					
" B	$A_1 \bar{A}_2 B C_I \bar{C}_{II}$	1					
R7A	$A_1 \bar{A}_2 B C_I C_{II} \bar{C}_{III}$	0					
" B	$A_2 B K_1 \bar{C}_I$	1					
R8A	$A_2 B K_1 C_I \bar{C}_{II}$	0					
" B	$A_2 B K_1 C_I C_{II} \bar{C}_{III}$	1					
R9A	B	0	0				
" B	C_I	1	0				
" C	C_{II}	0	1				
" D	C_{III}	1	1				
SR11	$A_1 \bar{A}_2 B C_I \bar{C}_{II}$				0	0	
" C	$A_2 B K_1 \bar{C}_{III}$				1	0	

Table 2H - HET Rates

Referring to Table 2H it is seen that: only rate 1 is not commutated, rate 9 is commutated between four rate equations by the bit labeled A/B, and SR1 is commutated between two rate equations by the bits SS1 and SS2. All other rates are toggled equally between the two rate equations shown in Table 2H by bit A/B except rate SR1 which is controlled by bits SS1 and SS2.

Bits A/B, S1, and S2 are derived in the experiment data system and their periods are bit rate and format dependent i.e. A/B changes every 32 S/C frames in format A, every 64 frames in format B and A/D, and every 128 S/C frame in format B/D. S1 changes every other A/B and S2 every other S1. (Standard binary ripple through counter)

Bits SS1, SS2, and SS3 also come from the data system but in normal operation are simultaneously bit rate, format, and S/C spin rate dependent.

See data system section for operation of Sector Synchronizer. For the present only note that in normal operation the SS1, SS2, and SS3 bits may only change after an integral number of S/C revolutions. Again SS1, SS2, and SS3 are generated in a binary ripple counter.

LET-1 SYSTEM

PHA Data

There are two separate coincidence conditions which will initiate a pulse height analysis. They are:

1) DI DII $\overline{F}$
2) DI DII ΣD $\overline{F}$

In LET-1 there are four detectors. Since only three channels (again A, B, and C) are available they are assigned to detectors DI, DII, and E respectively. Since the above PHA equations require detector F to have no pulse nothing is lost. The LET-1 PHA's, like the HET PHA's are the linear, capacitive descharge type using the fated delay line oscillator to produce 66 KHz channel address advance pulses. The channel number is related to incident particle energy loss in each detector as follows:

DI - 0.1 MeV/Channel
DII - 0.1 MeV/Channel
E - 1.0 MeV/Channel

The LET-1 PHA system is, like the HET system, priority oriented. The LET-1 system operates in response to the S1 bit as follows:

S1=0 Analyze either type of event as often as they occur.
S1=1 Analyze DI DII $\overline{F}$ type events as often as they occur until a DI DII ΣD event occurs, then analyze only the ΣD events until data is readout.

The S1 bit is the same bit that was applied to the HET linear electronics and hence, changes every 64 S/C frames.

Rate Data

The LET-1 system is assigned four rate accumulators exclusively and shares 8 accumulators with the HET system on a fifty-fifty basis and 1 accumulator is shared with the LET-2 system on an equal basis.

RATE OUTPUT	RATE EQUATION	P/B	S1	S2	S5, $S5_2$	
R14A	DI_1	0	0	0		
" B	DI_2	1	0	0		
" C	DI_3	0	1	0		
" D	DI_4	1	1	0		
" E	DI_5	0	0	1		
" F	DI_6	1	0	1		
" G	DI_7	0	1	1		
" H	DI_8	1	1	1		
R11A	$DI\ DII\ \bar{F}$	0				
" B	$DI\ DII \geq D\ \bar{F}$	1				
R12A	$DI\ DII\ E_1\ \bar{F}$	0				
" B	$DI\ DII \geq D E_3 \bar{F}$	1				
R13A	$DI\ DII\ E_2\ \bar{F}$	0				
" B	$DI\ DII \geq D E_1 \bar{F}$	1				
R14A	DI	0	0	0		
" B	DII	1	0	0		
" C	E_1	0	1	0		
" D	F	1	1	0		
R11	$DI\ DII\ \bar{F}$				0	1
"	$DI\ DII\ E_1\ \bar{F}$				1	1

Table 1L1

Table 1L1 shows that rate 10 is the accumulation of an integral analyzer which is commutated through eight levels by bits A/B, S1 and S2, 11, 12, and 13 are commutated two ways between the indicated rate equations by bit A/B. Rate 14 has 4 levels of communication in the LET-1 system and another four in the LET-2 system for a total of 8 levels of commutation controlled by bits A/B, S1, and S2. SR1 is commutated through the last two, of four levels, by bits SS1, and SS2. The other two comutator positions are assigned to the HET system.

LET-2 SYSTEM

PHA Data

There are no pulse height analyses associated with the LET-2 telescope.

Rate Data

Three rate accumulators are dedicated to LET-2 data while one accumulator is shared with the LET-1 system on a fifty-fifty basis. (See Table 1L2.)

Table 1L2 shows that R14 is assigned to LET-2 for the last four of it's eight levels of commutation. The commutation of R14 is controlled by bits A/B, S1, and S2 from the experiment data system.

R15 and R16 are commutated through four levels each, as shown in table 1L2, by bits A/B and S1.

The sectored accumulator SR2 is switched between eight rate equations by bits SS1, SS2, SS3, from the data system.

Sectored Rate Accumulators.

SR1 and SR2, in addition to being commutated through their respective energy levels, are directionally resolved into eight equal sectors of 45°. The sectors are generated as the spacecraft spins with the first beginning at the time fo the roll index pulse. Each sector is assigned a separate accumulator.

Table 1L2

NOTE OUTPUT	RATE EQUATION	A/B	S1	S2	SS1	SS2	SS3
R/S	S_I 5	0	0	1			
" F	S_{II} 6	1	0	1			
" G	S_{III} 7	0	1	1			
" H	S_{II_a} 8	1	1	1			
R/S	$S_I, \overline{S_{II}}, \overline{S_{II_a}}, \overline{S_{III}}$	0	0				
" B	$S_{I_2}, \overline{S_{II}}, \overline{S_{II_a}}, \overline{S_{III}}$	1	0				
" C	$S_{I_3}, \overline{S_{II}}, \overline{S_{II_a}}, \overline{S_{III}}$	0	1				
" D	$S_{I_4}, \overline{S_{II}}, \overline{S_{II_a}}, \overline{S_{III}}$	1	1				
R/S	$S_I, S_{II_1}, \overline{S_{II_a}}, \overline{S_{III}}$	0	0				
" B	$S_I, S_{II_2}, \overline{S_{II_a}}, \overline{S_{III}}$	1	0				
" C	$S_I, S_{II_3}, \overline{S_{II_a}}, \overline{S_{III}}$	0	1				
" D	$S_I, S_{II_4}, \overline{S_{II_a}}, \overline{S_{III}}$	1	1				
SR 2	$S_{I_5}, \overline{S_{II}}, \overline{S_{II_a}}, \overline{S_{III}}$				0	0	0
" B	$S_{I_6}, \overline{S_{II}}, \overline{S_{II_a}}, \overline{S_{III}}$				1	0	0
" C	$S_{I_7}, \overline{S_{II}}, \overline{S_{II_a}}, \overline{S_{III}}$				0	1	0
" D	$S_{I_8}, \overline{S_{II}}, \overline{S_{II_a}}, \overline{S_{III}}$				1	1	0
" E	$\overline{S_I}, S_{II_5}, \overline{S_{II_a}}, \overline{S_{III}}$				0	0	1
" F	$\overline{S_I}, S_{II_6}, \overline{S_{II_a}}, \overline{S_{III}}$				1	0	1
" G	$\overline{S_I}, S_{II_7}, \overline{S_{II_a}}, \overline{S_{III}}$				0	1	1
" H	$\overline{S_I}, S_{II_8}, \overline{S_{II}}, \overline{S_{III}}$				1	1	1

Data Format

The Pioneer spacecraft data formats for format A and format B are shown in Figs. D1 and D2.

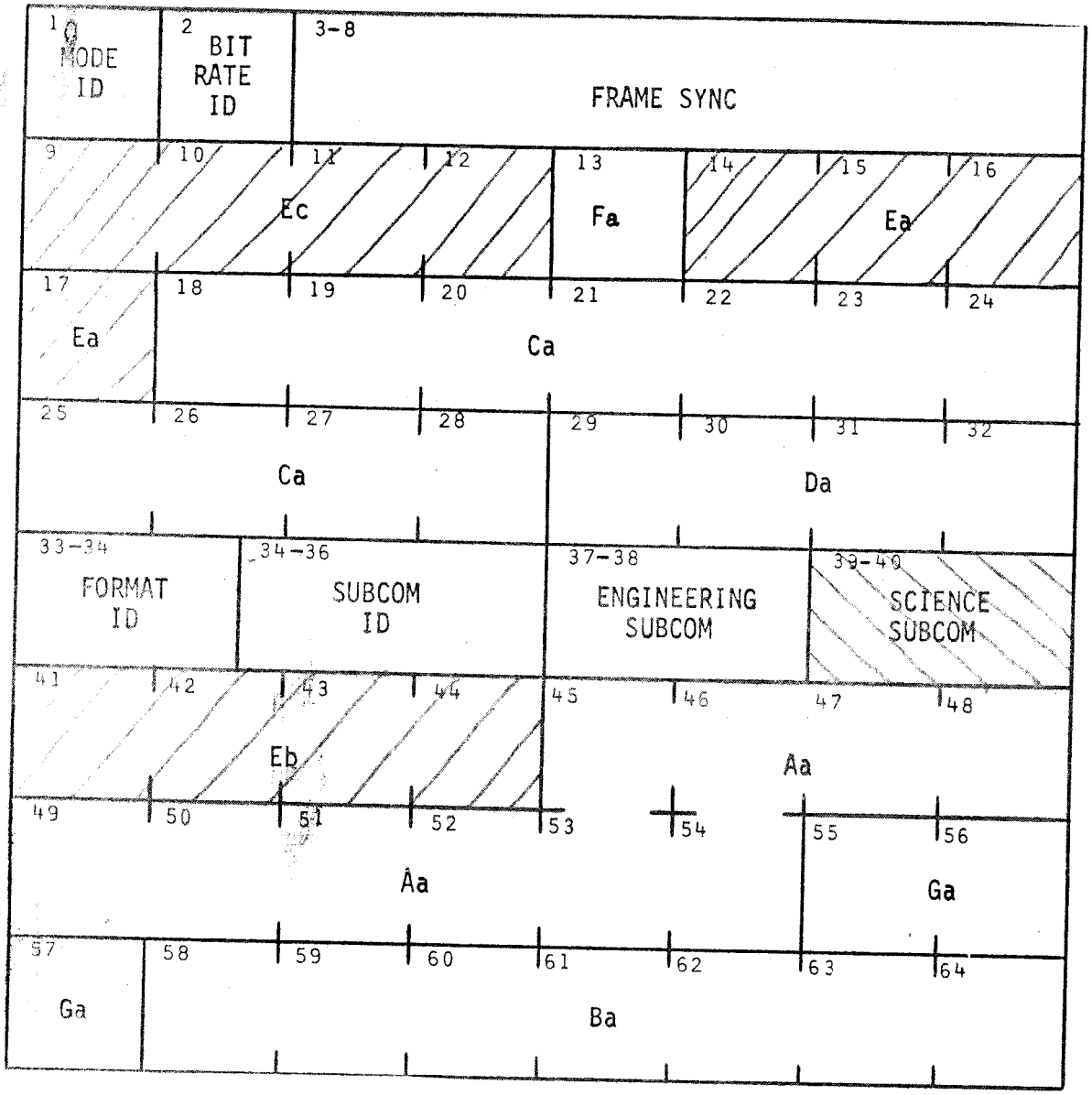

Fig. D1 S/C Mainframe format A

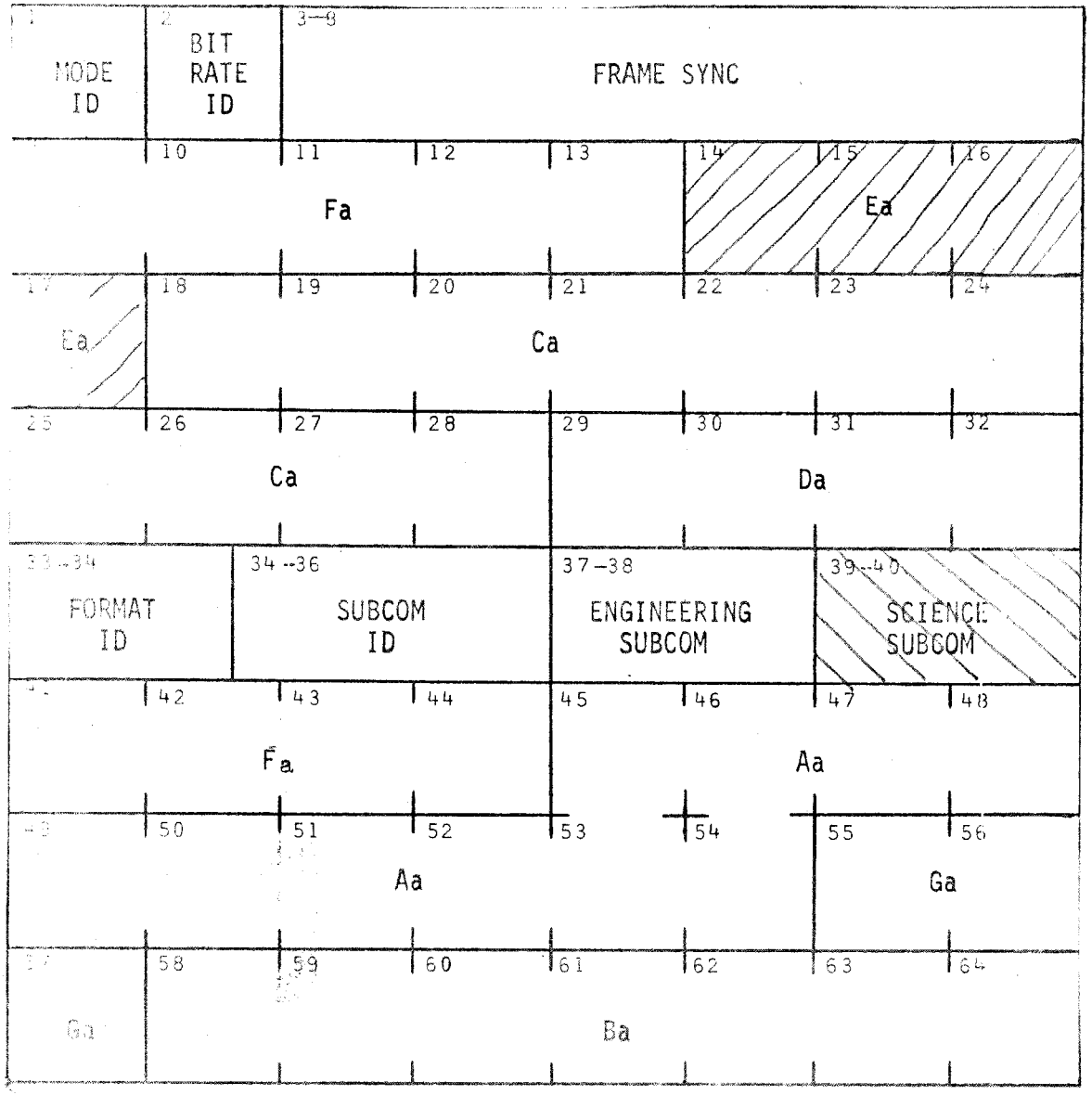

Formats A and B are only operating modes in which experiment data is outputed to the spacecraft. The words shown crosshatched are allotted to the GSFC experiment. It is seen that the CRT receives three M/F 12 bit words in format A and one S/SC 6 bit word. In format B there is one 12 bit M/F word and on S/SC 6 bit word the S/SC word is only present (to the CRT) in one of each 64 mainframes and will be used as a starting point and synchronization check in interpreting the output data.

Format A

As shown in Figure D3 below the experiment is assigned three M/F data words Ec, Eg, and Eb. Further, Fig. D3 shows how the data is assigned to these words within the instrument.

S SEQ ID = SECTORED RATE SEQUENCE ID
R SEC ID = UNSECTORED RATE SEQUENCE ID

□ RATE WORDS ARE 24 BIT LOG COMPRESSED TO 12 BITS.

* SEE FIGURE 3.1.1-2

URseq	S/C WORDS	MF, 9-12	MF, 14-17	MF, 41-44	E-1, 30	
	WEIGHTING	$2^{11}\,2^{10}-2^{1}\,2^{0}$	$2^{11}\,2^{10}-2^{1}\,2^{0}$	□	$2^2\ 2^1\ 2^0$	$2^2\ 2^1\ 2^0$
	TYPE DATA	PHA	PHA	RATE	RSEQ ID	S SEQ ID
8	n	LET-B	LET-C	R16	0 0 0	X X X
1	n+1	*HET-TAG	HET-A	S1		
	n+2	HET-B	HET-C	S1		
	n+3	*LET-TAG	LET-A	S1		
	n+4	LET-B	LET-C	S1		
	n+5	*HET-TAG	HET-A	S1		
	n+8	LET-B	LET-C	S1		
	n+9	*HET-TAG	HET-A	S2		
	n+10	HET-B	HET-C	S2		
	n+15	*LET-TAG	LET-A	S2		
	n+16	LET-B	LET-C	S2		
	n+17	*HET-TAG	HET-A	R1		
	n+31	*LET-TAG	LET-A	R15		
	n+32	LET-B	LET-C	R16		
	n+33	*HET-TAG	HET-A	S1		
	n+64	LET-B	LET-C	R16	0 1 0	X X X
	n+65	*HET-TAG	HET-A	S 1		
		LET-B	HET-C	R16	1 0 0	X X X

NUMBER

FRAME

Figure D3-Data to Word Assignments GSFC/CRT

If frame number N is arbitrarily assigned to the one frame in 64 which the C.T is assigned the SSC Wd (Wd 30 FMT E-1), we shall let the data frame begin with the next frame. i.e., N+1 in Fig. D3.

In Frame N+1, Fig. D3 shows that word Ec contains HET tag data, word Ea contains HET-A (A=DetA of Det CIII. See HET PHA section.) PHA data and word Eb contains sectored rate 1-sector 1 (SR1-1) data. In frame N+2 word Ec contains HET -B (Det B), word Ea contains HET-C (ΣDETCI+DETCII), and Eb contains SR1-2.

In frame N+3 LET-1 PHA tag data is read out in word Ec. Word Ea contains LET-A (Det DI), while word Eb continues the rate data: SR1-3. In frame N+4 LET-1 PHA data is continued in word Ec, LET-B (Det DII), and word Ea, LET-C (Det E), while word Eb has SR1-4.

In frame N+5 words Ec and Ea return to HET tags and HET-A and the frame sequence continues in the manner modulo four. Word Eb, however, continues to sequence through SR1 (-5, 6, 7, and 8), SR 2 (-1, 2, 3, 4, 5, 6, 7, 8) and unsectored rates 1, 2, 3, 4, 5, 6, 7, 8, 10, 11, 12, 13, 14, 15, 16. (See sections on HET and LET rates for the rate equation of these rates in terms of detector outputs). At frame N+33 word Eb reads out SR1-1 again and the rate data has come full cycle in 32 frames. At this time the A/B bit is changed and the unsectored rate accumulators step to count on the next, in its particular rate equation sequence. The cycle continues, this way for 31 more frames at which time (N+64) the S SC Wd is again applied to the CRT experiment and the complete data cycle is begun anew with the next (N+65) frame. In this new cycle (64 frames) the PHS priorities have been changed (See HET and LET PHA sections) and the rate accumulators are once again advanced to the next rate equation.

The experiment continues in this manner as long as the spacecraft is in format A.

A description of how to extract the exact rate equation for each word Eb readout and how to establish the exact source of the PHA readouts will be given following the Format B section.

Format B

Since the CRT experiment now receives only one M/F word and it was not desired to sacrifice one type of data for another it was necessary to readout both types of data in word Ea. This was accomplished by alternating the 32 rate readouts with 8 PHA event readouts. NOTE: 1 PHA event is readout in 4 words therefore 8 events take 32 frames.

Figure D4 shows the word assignments in Format B.

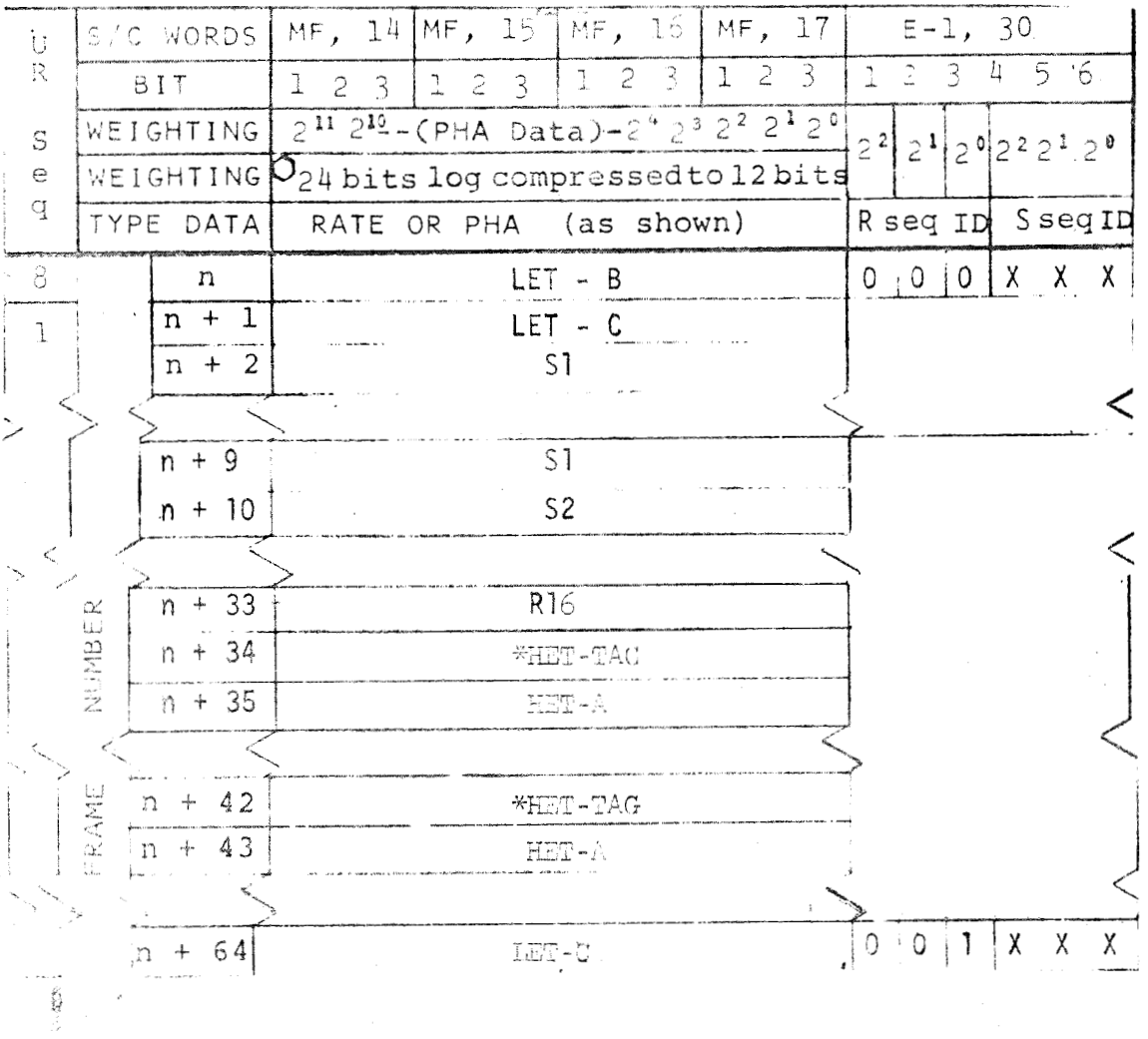

Figure D4 Data to Word Assignments Format B GSFC/CRT

The sequence of rate data readouts is chronologically the same as in format A, however, it should be noted that cycle begins one frame late with respect to the SSC Wd, i.e., SR1-1 now is read out in the second frame following the SSC Wd. (frame W+2). Following the rate data come 32 frames of PHA data, N+34 to N+65 and the SSC Wd is once again received from the S/C and the experiment begins into cycle once again with SR1-1.

Form A/D B/D:

Data Synchronization

As was seen in the HET and LET descriptions the bits which control rate equation a given rate readout was accumulated under is controlled by the bits A/B, S1, and S2 for unsectored rates and SS1, SS2, and SS3 for sectored rates. These bits are readout once each 64 frames by the SSC Wd (Wd 30, E-2) in the format shown below:

S2-S1-A/B-SS3-SS2-SS1

The unsectored rate counter is advanced each 32 frames on Format A and each 64 frames in format B. In addition, in format A the unsectored rate counter LSB is reset by the SSC Wd and will therefore be equal to zero at readout time. The number readout in bits (S2, S1, A/B) will always advance by two and be an even number (i.e., A/B≠1). In format B this flip-flop is not reset and will, therefore, advance by one each SSC Wd readout.

The bits SS1, SS2, and SS3, of the sectored rate counter are dependent upon the S/C spin rate and therefore may change asychronously with the S2, S1, A/B bits. Therefore in order to give a closer indication of when the counter was advanced the SS1 bit of the counter is readout as bit #7 (LSB+S) of the HET-tag word (See Figure D5). The criteria applied to determine which rate equation a read out sectored rate was accumulated under is dependent on whether or not the experiment has its sector synchronizer on or off. The status of the s.s. is found by examining bit 8 (LSB+4) of the HET-tag word.

Sector Sync Inhibited

The sectored rate data should be treated in the same manner as the unsectored rate data, i.e. the S seg ID readout in Wd 30 (SSC Wd) indicates the rate equation under which the following 16 sectored rate readouts were accumulated. E.G. If the S seg ID in Wd 30 were 3 this would indicate that the following sectored rate data were accumulated as follows:

Sectored Rate 1 = SID = DIDIIE $\overline{F}$

Sectored Rate 2 = S2D= SI_3 $\overline{SII}$ $\overline{SIIa}$ $\overline{SIII}$

The sectored SEQ counter is advanced every 32 frames, therefore, the next sectored rate data readout were accumulated under S SEQ ID-4. It is NOT possible to have redundant readouts with sector sync inhibited.

Sector Sync Not Inhibited

In this mode the internal sectored SEQ counter can only be updated at the time in the telemetry frame when unsectored rates are being readout and a prescribed number of S/C rolls have been completed.

To obtain sync with the sectored rate data one proceeds as follows: Note the reading of the SSEQ ID previously noted in Wd 30 (SSC Wd) if bit 7 does not change state the data in the following sectored rate readouts is redundant and should be discarded). Bit 7 of HET-tag Wd should be continuously monitored for state changes and S SEQ ID mentally increased by one for each change noted. A check may be had at each Wd 30 by comparing S SEQ's ID.

As an example suppose the S SEQ ID in Wd 30 were found to be 6 and during the next 32 frames examination of bit 7 of HET-tag Wd showed no state changes. The following data in the sectored rate words whould be rejected as redundant. SEQ. ID & Data. if in the next 32 frames bit 7 changes state, (change the mental S SEQ ID to 7) sectored rate data this following readout would be fresh data and it accumulated under S SEQ ID = 6.) Sectored rate - 1= S1C=DIDIIF sectored rate 2 = S2G=SI SII3 SIIa SIII. At the following word 30 (SSC Wd) the S SEQ ID should be verified: It should read 7.

In order to know the type of event (See HET and LET PHA sections) readout in the PHA words the event is modified by its accompanying tag word. Figure D5 shows the format meaning of both the HET and LET tag words.

BIT	1 2 3	4	5 6	7	8	9 10 11 12
WEIGHTING	2^2 2^1 2^0	2^0	2^1 2^0	2^0	2^0	2^3 2^2 2^1 2^0
HET-TAGS	SEC. ID	R	*□	S	SS	△ 0 0 0 0
WEIGHTING	2^2 2^1 2^0	2^0	2^0 2^0 2^0 2^0 2^0 2^0 2^0 2^0			
LET-TAGS	SEC. ID	ΣD	1 1 1 1 1 1 1 1			

NOTES:

A) * WHEN BIT = 0: HET-A = DETECTOR A
WHEN BIT = 1: HET-A = DETECTOR CIII

B) △ HIGH/LOW POWER 1 1 1 1 = ~~LOW POWER~~ High Power
0 0 0 0 = ~~HIGH POWER~~ Low Power

C) □ ANALYSIS CONDITION

D) R = RANGE (O/1) = ~~TBS~~ 0= CII threshold not exceeded
1: CII " is exceeded

E) S = LEAST SIGNIFICANT BIT OF SECTORED RATE SEQUENCE ID.

F) SS = SECTOR SYNC 1 = INHIBITED
0 = NOT INHIBITED

G) ΣD = 1 if event contains ID

Fig. D5 HET & LET Tag Words

The sector in which the event was encountered is found in bits 1, 2, and 3 of the tag words. For a LET event the type of event (ΣD of $\bar{\Sigma}$D) is revealed in bit 4 (the rest of the LET tag word is filled with ones). For a HET event an indication of the contribution of the CII detector to the channel number readout in the HET-C (ΣCI+CII) is found in bit 4 of the HET tag word. If the CII threshold (MeV) is exceeded the bits is 1 if not, a zero.

The type of event that triggered the HET analysis is contained in bits 5 and 6 of the HET tag word. If bit 5=1 the HET A detector CIII is output. If a zero' HET-A is related to detector A's output. Bits 4 and 5 provide more information as to the coincidence conditions resulting in the analysis when modified by the S1 bit readout in SSC Wd (see HET PHA section for priority description).

Bits 7-8-9 of the HET-tag contain information on whether the sector sync is on or off (bit 8), when the bit SS1 toggles (bit 7) and whther the experiment is in the high power mode or not. (bit 9=1 for high power) Bits 10-12 of HET tag word are unused.

ANALOG DATA SYSTEMS

The analog outputs of the CRT experiment together with the experiment connector (0854-J1) pin number are shown in Fig. AD1 below.

Pin Number	SC WORD (FMT. E-1)	Data
24	Wd 25	Power Supply Mon (Temp)
26	Wd 28	DET Temp (ARC-Therm)
27	Wd 26	Power Supply Mon. (Voltage)
28	Wd 27	Calib on/off
29	Wd 29	+RV Mon
30	Bit Wd 24	CRT Status

These analog output on pin 27 is an eight level commutation of seven voltage outputs of the experiment power supply and a ground position. The voltages in order of commutation are:

1) 0V
2) +12V
3) +7.75V
4) +6.25V
5) +4.6V
6) -2V
7) -6.25V
8) -12V

All voltages are converted to the range $0.0 \leq V \leq 3.0$ before they are sent to the spacecraft quantizer.

The out-put on pin 28 indicates whether the CRT is being stimulated by it's internal calibrator. (0V=NO; 3V=yes)

The output on pin 30 supplies confirmation of the format in which the CRT is operating and, of course, should agree with that of the S/C. Pin 30=0V for format A and +3V for format B.

The output on Pin 24 comes from a thermister mounted directly on the power supply-input regulator-series transistor and serves as an indication of the dissipation of that device.

The output on Pin 26 comes from the Project Office supplied thermister which is mounted directly to LET-1 telescope housing.

DATA SYSTEM

The data system of the CRT may be broken up into two major areas: The "COSMIC RAY INTEGRATED MOSFET PROCESSOR" (CRIMP) and the INTERFACE DATA SYSTEM (IDS)

Crimp

The Crimp system is a design using LSI MOS technology to produce a logical building block normally referred to as a "bug." Some of the "bugs" used in the Crimp are:

1. Universal 4 bit MOS commutator C-1074
2. 10 channels of switch C-1070
3. Tree Bug
4. Mars bug
5. ATX, most bug C-1276

The hearts of the Crimp system are the Mars bugs which each contain a 24 bit accumutator, a 24 bit to 12 bit logarithmic compressor, readout gates which with suitable control produce the 12 bit compressed word as 3 bytes of 4 bits each. The compressed word is generated on command by disconnecting the accumulator input, transferring the contents to a 25 bit shift registers, shifting right until a "1" is found in the MSB of the register or 31 shifts have been made; counting the number of shifts required in a 5 bit counter, reading out the counter as the first five bits (characteristic) and the 7 MSB's of the shift register (after discarding the "1" in the MSB) as the last seven bits (Mantissa). It is seen that if the numbers accumulated is greater than 255 there will be some uncertainty in the number due to truncation from the left. Appendix A contains a listing of all possible outputs of rate data together with the uncertainty in the number read out. Included are octal and decimal representations of the rate number read out - neglecting the fact that it is compressed.

The Crimp also contains 6 PHA data accumulators of 12 bits and associated with each accumulator are 12 bits of interim storage, 12 bits of read out storage and necessary gating to sequentially produce, on application of control signals, the 12 bit PHA word as 3 bytes of 4 bits each. The PHA data is straight binary number representing the number of pulses produced by the HET or LET pulse height analyzers. Each LET or HET event has also a "tag" word associated with it which is formed in the IDS and shifted into readout storage with the 3 PHA words it modifies.

The Crimp contains circuitry necessary to produce the data format of the CRT. In a 6 stage binary counter, which is reset to all "1's" the the SSCWd (Wd 30 E-1), the Crimp keeps track of which frame it is in and sets up linkage to; the proper words (format A), or word (fromat B) to be read out in that frame. In format A the CRT receives three 12 bit words per frame making it is

necessary to know where in the frame you are. For this purpose the Crimp has a sub counter (3 bit-set to all "1's" by the SSC Wd) which modifies the coarse address generated by the 6 bit counter reading out the 8 words of PHA data. Sectored rate (SR1 and SR2) accumulators are selected on the basis of 3 binary weighted lines from IDS which are decoded to one of eight lines by a "tree" bug in the Crimp. These lines in conjunction with a low "go" signal from IDS enable the Crimp to sequentially select the eight available accumulators are frozen.

INTERFACE DATA SYSTEM

The functions of the IDS are fourfold:

1. Provide specified impidence matching at the S/C-Experiment interface.
2. Provide interface between the MOS of the Crimp and the T^2L of the IDS.
3. Generate all necessary timing and control signals for operation of the experiment in gathering data.
4. Generate necessary timing signals to output data to the spacecraft date system.

S/C Experiment Interface

The IDS meets the required interface specification through the use of discrete amplifier on the input signals and discrete passive components output signals.

Crimp-IDS Interface

The IDS makes the voltage level shiftsnecessary between the MOS logic levels of the Crimp and its own transistor-transistor logic through discrete component inverting amplifier on all lines crossing the interface.

Timing and Control Signals

The IDS provides signals to both the linear system for PHA, control and rate commutation, and to the Crimp for accessing and fetching data for readout to the S/C.

The PHA's, their respective counters and tag registers in Crimp and IDS, and the control signals operate as shown the simplified block diagrams and timing diagram, figures IDS 1 and IDS 2.

Energy loss data from each PHA, only one of which is shown, consists of number N of logical pulses, (denoted GPT) which are counted in the 12 bit MOS counter. One additional dignal from each group of three PHA, designated' HET BUSY or LET BUSY is a pulse whose width is at least as long as the N pulses and therefore brackets all pulses to be counted. This signal indicates

when the analyzers are busy and is used to inhibit any other analysis from overlapping the one in process. The TE of BUSY also initiates the transfer and reset pulse which moves data from the counters to intermediate storage and prepares the counters and PHA's for future analysis. The identifying tag bits associated with each event are strobed into the tag bit register in IDS shortly after the LE of BUSY. Subsequent events may be analyzed and written into intermediate storage, erasing all previous data. This is controlled by the priority system discussed above.

Once each 4 frames in format A or each 8 frames in format B, immediately prior to a PHA event readout. The PHA's are inhibited so that no analysis can take place, and the STU 32 KHz colck (after being divided by 2 to produce 16 KHz) is used to serially shift all data for both HET and LET events into readout storage. This data is fetched by Crimp under control of IDS in exactly the same way as rate data, i.e. by addressing each register sequentially and causing its data to be gated onto the output data bus. This is discussed in more detail later.

IDS also contains two counters, each with a capacity of 3 bits, which control commutation or rate data within the linear system. This allows the 32 rate counters of Crimp to be used for counting many more discrete coincidence rates from the various detector systems. Since the rates are basically of two types, sectored rates and unsectored rates, these two counters are called the sectored rate sequence counter (SRS) and the unsectored rate sequence counter (URS). The commutatuion sequence of each has already been described above. Operation and timing of each is described here.

The unsectored rate sequence counter is advanced by one count at the end of each unsectored rate accumulation interval as defined by the telemetry format in use. In format A, this occurs once each 32 main frames on the LE of the first Main Frame Word 14-17 (Ea) following the occurance of the subcom word E1-30 (SSC Wd) and 32 frames thereafter. The advance pulse also initiates log conversion of all unsectored rate counters so that, on the TE of Ea, new rate data is converted and ready to be fetched for readout in MFWd 41-44 (Eb). The URS is always advanced every 32 frames in format A. In format B URS is advanced every 64 frames, also on the first main frame word Ea following the subcom word E1-30. The unsectored rate data is thus converted and ready to be fetched on the TE of Ea for readout. The rate data readout cannot commence on MFWd 41-44, as it did in format A, however, because Ea is the only word present. Thus, in format B readout of rate data commences on the second Ea after E1-30.

In contrast to the above, the sectored rate sequence counter (SRS) can advance on one of two signals, either synchronously with the URS as described above, or in accordance with the Roll Index Pulse (RIP). In the former case, advance of SRS is synchronize with telemetry and has been fully described above. In the latter case, advance is synchronized with the S/C spin. One of these two signals is specified by the sector synchronizer command flip-flop and is indicated in the HET-tag word.

When the sector synchronizer is enabled, the sectored counters are allowed to accumulate for an integral number of complete S/C revolutions. The number of rolls is dependent upon the bit rate in use and present into the roll counter at the beginning of each accumulate interval. The roll counter increments by one on each RIP until the specified number of rolls has been completed. On the last roll pulse of each accumulate interval, a flip flop is set which enables the next Main Frame Word Ea in frames 17 through 32 or 49 through 64 initiate sectored accumulator data transfer and log compression. The next accumulate interval begins on the first RIP following data transfer.

Data transfer is not allowed during frames 1-16 or 33-48 (Mode A) because sectored rate data in readout storage is being shifted out to the S/C. If transfer to readout storage was allowed during a sectored rate readout sequence. Two sources of error might arise. First, suppose the last RIP of an accumulate internal occured in frame 7. If transfer were allowed, the data transmitted to the ground in frames 1-7 would correspond to a different accumulate interval than that readout in frames 8-16. Recall that the sectored accumulators are commutated between several different rates, hence, adjacent accumulate intervals do not correspond to the same rate inputs. Allowing transfer as supposed above would intermaingle two intirely different coincidence rates in the data.

Secondly, if transfer were allowed during sectored rate readout, if if possible that a complete set of 16 readouts would be interrupted if the last RIP occured during the first readout of the sectored data. This can happen if the prescribed number of rolls for a high bit rate (size 1024 or 2048 bps, in which case m=31 is preset into the rolls counter, and the S/C is subsequently commanded into a lower bit rate in which the readout sequence is very long compared to one roll period.

Format B, shows sectored data trnsfer is also inhibited furing those frames in shich rate data is being readout to telemetry. The frame numbers when transfer is inhibited are m to m+32, which is different than in format A.

One last feature should be noted. It is very likely, indeed it is desired, that the accumulate interval for sectored rate data will be longer than the readout interval, hence data for a given intervals will be repeated in the telemetry. This redundant data may be used for bit error checks in the processing system, but cannot be included in the rate averages. It is easy to identify which data is a repeat of old data and which is new data by use of the LSB of the sectored rate sequence counter (SRS) which is readout every four frames in HET-tag. This bit will change state every time SRS is incremented.

The contents of the two 3-bit counters, are readout fully in the subcom word E1-30. On the leading edge of E1-30, the state of each bit is stribed into a six bit shift register and immediately readout by the S/C. Advance of either counter must be at the time of Main Frame Word Ea, hence, no error due to strobing during counter transition is possible. (See Data Format Section for information on how to obtain data synchronization.)

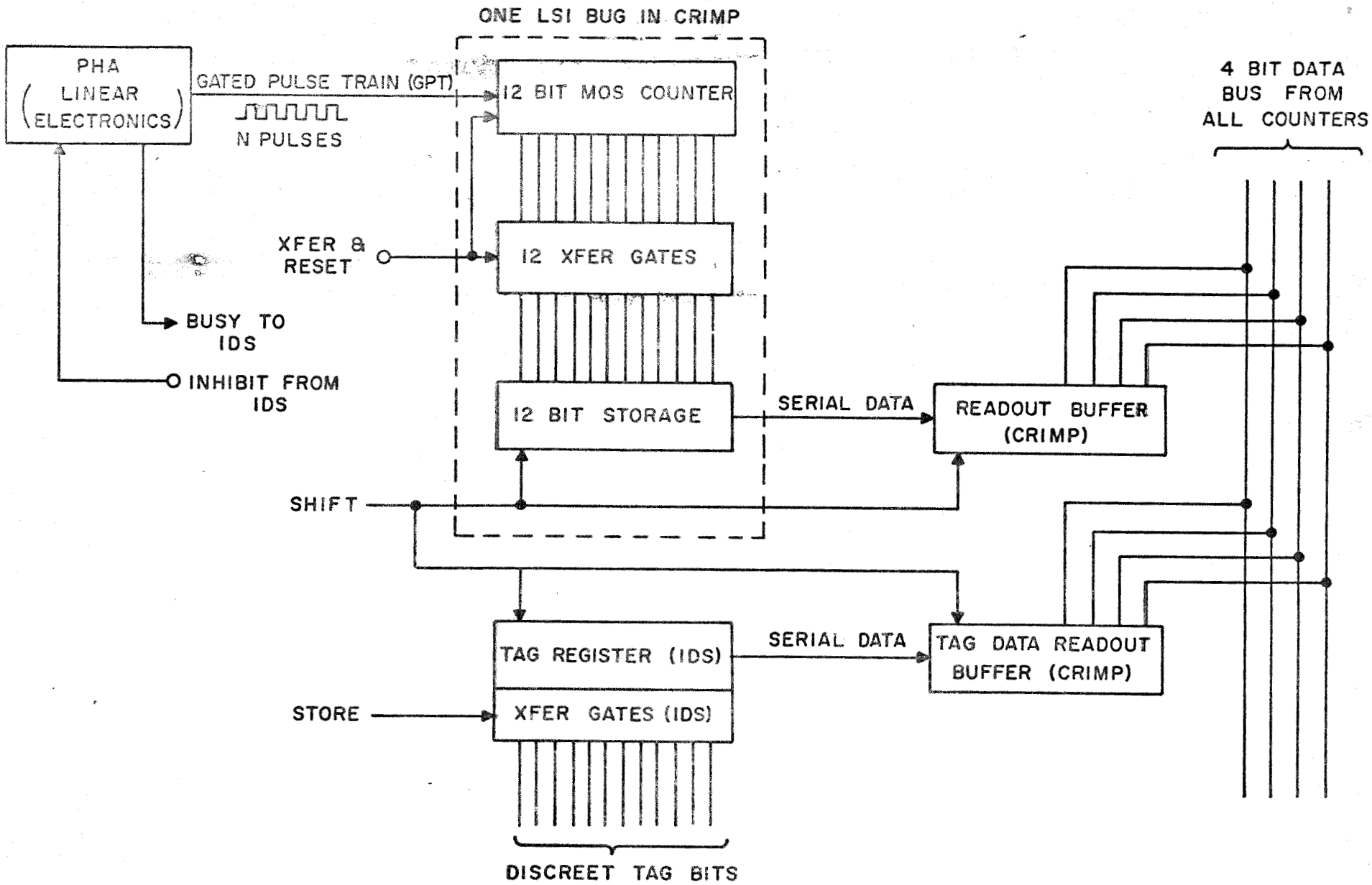
ONE LSI BUG IN CRIMP
PHA
LINEAR
ELECTRONICS
GATED PULSE TRAIN (GPT)
N PULSES
12 BIT MOS COUNTER
4 BIT DATA
BUS FROM
ALL COUNTERS
XFER &
RESET
12 XFER GATES
BUSY TO
IDS
INHIBIT FROM
IDS
12 BIT STORAGE
SERIAL DATA
READOUT BUFFER
(CRIMP)
SHIFT
TAG REGISTER (IDS)
SERIAL DATA
TAG DATA READOUT
BUFFER (CRIMP)
STORE
XFER GATES (IDS)
DISCREET TAG BITS

IDS 1

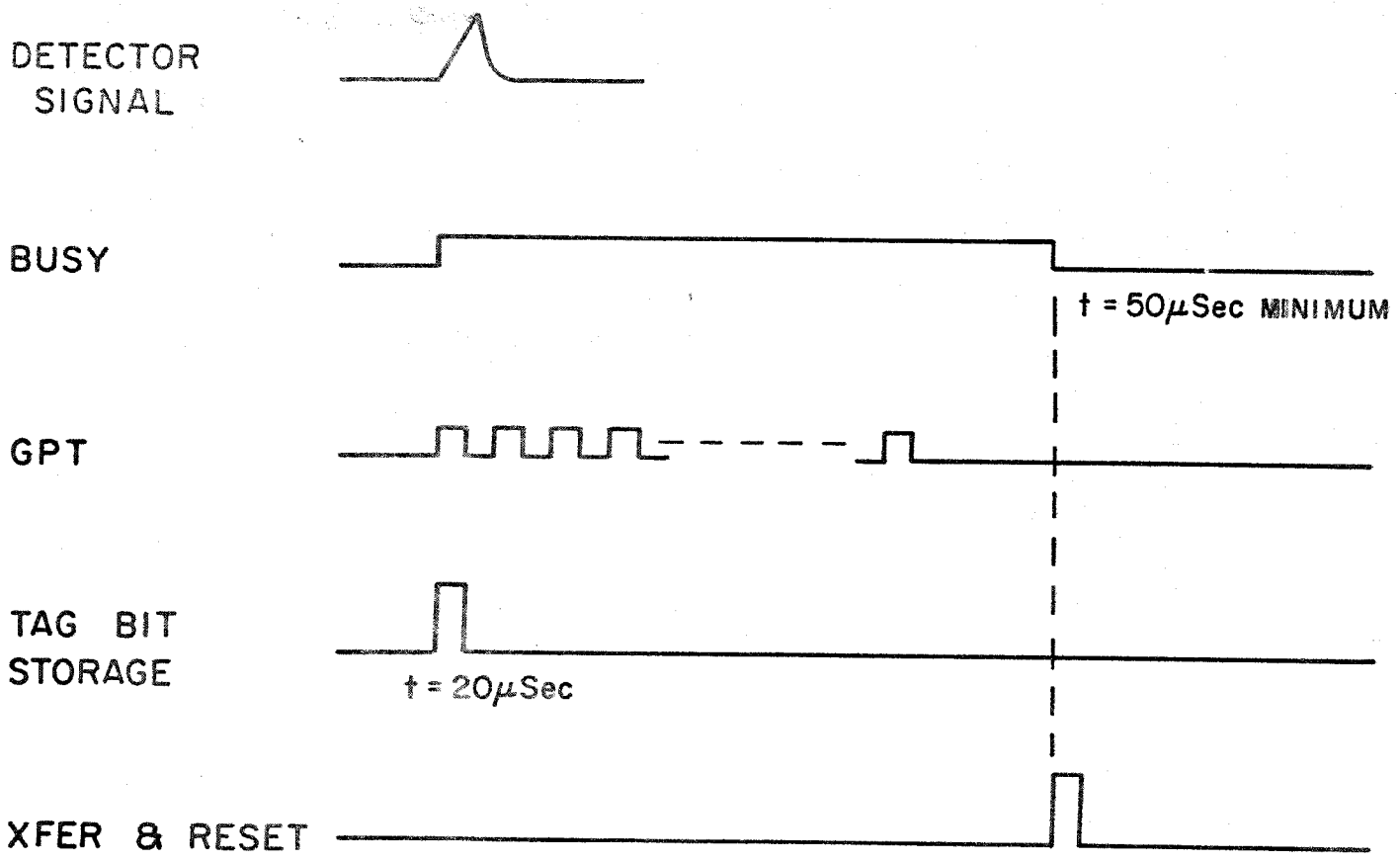
DETECTOR SIGNAL
BUSY
t = 50μSec MINIMUM
GPT
TAG BIT STORAGE
t = 20μSec
XFER & RESET

IDS 2

The Pioneer 10/11 Cosmic Ray Experiment of Goddard Space Flight Center/University of New Hampshire

The Goddard/University of New Hampshire cosmic-ray experiments on Pioneers 10 and 11 and the Goddard cosmic-ray experiment on Helios-1 and -2 are essentially identical. A schematic drawing of the detector systems is shown in Figure 1 and their parameters are summarized in Table 1. The High-energy Telescope (HET) is used to determine the helium energy spectrum between 20 and 500 MeV per nucleon and the proton spectrum between 20 and 56 MeV and 120 and 300 MeV. The particle trajectory for the HET is defined by the A and B detectors. Stopping particles in this telescope are identified by the additional requirement that there is no signal from the CIII detector. This stopping particle mode covers the range from 20 to 56 MeV per nucleon for both protons and α-particles. For penetrating α-particles and protons with energies greater than 56 MeV per nucleon, the HET becomes a triple dE/dx device. In this case, the energy is determined by the energy loss measured in the 1 cm CI + CII stack of solid-state detectors and the pulse-heights measured in B and CIII are both required to be in an interval that is consistent with a given particle of this energy. This threefold multiparameter analysis reduces the background level of spurious events to a negligible level. It is estimated that the absolute uncertainty in the α flux is ~ 12% at 400 MeV and ~ 7% at energies below 200 MeV. The operation of the LET-I telescope (Fig. 1) is similar to the stopping particle mode of the HET except that the thin 100 μm dE/dx devices (DI and DII; Fig. 1) permit multiparameter measurements to be made from 3.2 to 21.6 MeV per nucleon for protons and helium nuclei. The multiparameter measurements used in this study reduce to a negligible amount any corrections due to the presence of large quantities of radioactive material in the Pioneer 10 and 11 power supplies.

The total radiation damage produced by energetic electrons and protons incident on the Goddard/University of New Hampshire experiment during the passage of Pioneer 10 through the Jovian magnetosphere was sufficiently high that some four electronic failures were induced by radiation damage effects. The most serious of these was the loss of the E detector information from the LET-1 telescope. It was found that the complete 3-21 MeV per nucleon energy range of this detector could be obtained for stopping α-particles by using a two-parameter analysis of DI vs. DII with only a small increase in background ($\leq$ 7%). The other failures occurred at several points in the data system but in such a manner that either redundant information is available or--in one case--a correction factor (which generally was on the order of 3-5%) could be derived from the available data.

ELECTRONICS

Pulses from each detector are amplified and shaped in a preamp/post-amplifier, and applied to one or more pulse-height discriminators which produce logic pulses of uniform amplitude and width for each input pulse exceeding the threshold. These logical pulses are used to form the many coincidence-anticoincidence conditions corresponding to various particle energies and types. Both single detector rates and coincidence rates are counted in 24-bit binary counters. Sixty-one such rates are monitored in the Pioneer instrument and 83 rates are monitored in Helios. The Pioneer rates are shown in Table 2; Helios rate data includes additional LET-II rates and the 2-8-keV X-ray rates. Certain coincidence conditions may initiate pulse-height analysis of selected events. The pulse amplitudes of three selected detector outputs are digitized by three 10-bit analog-to-digital converters (ADC).

Linear Circuits

The pulse-height analyzer and coincidence system electronics for the Pioneer and Helios missions were accomplished using nearly identical designs. The same building blocks contained in Pioneer were used, with only slight modification, in the Helios systems. Each experiment contained three mechanically- and electrically-separate subsystems, one for each telescope. Since Helios contains two identical LET-II's, this subsystem is exactly double its Pioneer counterpart.

The preamps use an FET input in a conventional cascade configuration. After shaping with single integration and differentiation time constants of 0.6 μsec, the pulses are differentially coupled to noise-cancelling linear buffers to eliminate common mode noise pickup. CMRR was measured to be ~ 50 db at the frequencies of interest.

Each of the HET, LET-I and LET-II subsystems operates in a similar fashion. Figure 2 shows the HET system. Each noise-cancelling buffer is followed by another buffer to boost the incoming signal to a level suitable for pulse-height discrimination. The nominal low-level signal to be discriminated corresponds to Channel 1 of the PHA, or 5 millivolts. These low-level discriminators are stable with $\pm$ 0.5% total drift from -20°C to +40°C. A lower power version of discriminator is also used where $\pm$ 2% stability is tolerable. Three of eight discriminators in HET are of this variety.

Two linear summing amplifiers are used in HET. The first linearly adds the CI and CII buffered inputs. This sum is presented to the PHA for analysis under the proper conditions, and, hence, must exceed the linearity requirements of the PHA. The second summing amplifier adds the signals A and B with a weighted output from the first summing amplifier

(A + B + 1.8 [CI+CII]). This signal is fed into two discriminators for use in the coincidence logic to separate protons from electrons and to separate $Z \geq 2$ particles from protons.

In the HET system there are 15 basic coincidence equations, none of which has less than 5 terms. Six additional singles rates are produced. These are multiplexed into the 10 rate outputs. Four of the coincidence conditions are used in the PHA control logic. Inputs to these equations are both pulse and level. The pulse inputs are derived from the discriminators while the levels are derived from the data system to control commutation of the rates.

To insure that coincidence timing is not affected by "discriminator walk" when two pulse inputs are coincident, an active delay has been incorporated. Since the B input appears in all multi-pulse equations, it is delayed 1.5 microseconds using a monostable circuit. The remaining 7 discriminators are followed by 3.0 microsecond monostables. The delayed edge of the B monostable is fed to an edge-coupled high-speed gate, whose other "anding" inputs are 3.0 microsecond-wide pulses or levels. This method insures that if all inputs are coincident with 1.5 microseconds, the proper equation timing will be fulfilled.

The coincidence system also selects events for pulse-height analysis. There are four coincidence conditions which can initiate analysis; two contain the term CIII (penetrating particles) in which case BI, (CI+CII)and CIII are analyzed. The other two conditions contain $\overline{\text{CIII}}$ (stopping particles) for which A, B and (CI+CII) are analyzed. Priority selection of event types allows higher priority events to be analyzed and stored in place of lower priority events. The relative priority of the four event types is rotated so that each type has highest priority for one-fourth the time. This emphasizes the occurrence of relatively rare events in the data.

The PHA system contains four delay lines and linear gates, three height-to-time converters, a gated current source and a gated clock. When an acceptable event has occurred, "open" signals are sent to the proper linear gates (B, [CI+CII] and A or CIII). The input signals are delayed 3.5 microseconds to compensate for delays in the coincidence and priority logic matrices.

The HTC is of the Wilkinson discharge type, the usual choice for nuclear spectrometers because of its excellent differential linearity characteristics. The gated constant current source remains on between events and is turned off slightly after opening of the linear gate. This minimizes the effect of noise spikes associated with opening of the linear gate, and improves the low-channel resolution and linearity significantly. The PHA's are able to resolve Channel 1 (5 millivolts) and produce a total differential non-linearity of $\pm$ 1.5% over the top 99% of full scale (5 volts or Channel 1024). The digitizing clock is 500 kHz, providing a 2-millisecond conversion time for full-scale inputs. The three 1024 channel PHA's used in HET require less than 30 milliwatts of power.

The PHA system outputs three gated pulse trains which are counted in binary counters. Additional tag bits are stored with each three-parameter PHA quantity which identifies the event type, priority, sector ID of spacecraft spin and a CII range indicator to further characterize each event.

The LET-I and -II systems shown in Figures 3 and 4 operate very similarly to HET. The linear buffers, discriminators and coincidence matrix use the same circuits as in HET. LET-I PHA data contains digitized values of the DI, DII and E detector pulses, and tag bits provide sector ID, priority and event type information. A two-level priority system is used, and both event types are allotted equal time as highest priority events. The coincidence rates detected by LET-I and -II are also listed in Table 2.

Data Systems

All rate data is counted in "Mars bugs," a custom PMOS LSI chip developed at GSFC. A single chip contains a 24-bit binary counter, a quasi-log compressor to convert the 24-bit binary number to a 5-bit characteristic and a 7-bit mantissa and a 12-bit storage buffer to hold the data for readout. PHA data are also counted and stored in PMOS IC's. The Pioneer and Helios PMOS data systems are quite similar in design. All spacecraft interface, command processing logic, control of the accumulation intervals and formatting of Rate and PHA data into the available telemetry space is accomplished in a spacecraft-unique Interface Data System (IDS) using low-power T^2L circuits. Discreet components were used where necessary to comply with spacecraft interface impedances and levels.

The telemetry formatting was designed to keep the rate data cycle time between 3 and 7 minutes for as many bit rates and formats as possible which were most likely to be used during a nominal mission, or not more than one-half of the science telemetry available to each experiment. PHA data is inverleaved with rate data and can process up to 3 events per second on available bit rates. PHA telemetry is always equally divided between HET and LET. Because of the wide variation in bit rate (2048/sec to 16/sec) on Pioneer, a complete data cycle for all rates becomes as long as ~ 1.7 hours.

The experiment acquires spin-sectored data. A sectored rate synchronizer generates suitable control signals to insure that the sectored rate accumulators are live for an exact integral number of spacecraft revolutions. The number of revolutions is determined by the bit rate in use and varies from 1 rev/readout to 31 rev/readouts (spin rate $\simeq$ 5 RPM), and between 53 rev/readouts to 2231 rev/readouts on Helios (spin rate ~ 60 RPM). Sectors are 45^{o} wide on both spacecraft.

Commandable features include (a) disabling the sector synchronizers in the event of failure and (b) turning on internally-generated test pulses to stimulate the electronics for pre-flight and in-flight checkout.

This hardware is an example of an extremely lightweight, low-power electronic design for severe environmental conditions. The experiment qualified in vibration at 50 g's and was subjected to almost 5×10^5 rads in Jovian radiation belts. It has already been operating in flight for 9 years, and we expect to be able to receive data from Pioneer 10 until the telemetry signal is lost. Weight was a major problem, especially on Pioneer. The experiment weighed 2.2 kg for the sensor systems, the electronics system consisting of the charge-sensitive preamplifiers, shaping amplifiers, thresholds and logic circuitry, priority control system, six 10-bit pulse-height analyzers, an extensive data system and the low-voltage and detector bias dc-dc converters. Power consumption was 2.4 watts. The Pioneer experiment includes more than 8,000 discrete electronic components per system and more than 40,000 transistors--largely in medium- and large-scale integrated circuits.

Experiment performance has been excellent. Figure 5 shows the LET PHA data for the August 1972 event. This is a plot of the average dE/dx value ([DI + DII]/2) vs. the E value with a consistency check applied to the DI and DII values. The chemical elements are readily identified, and isotopic separation, even for the Magnesium line, is possible.

TIME PERIOD COVERED

The data for the planetary encounters has been excluded from these tapes. The following time periods were, therefore, excluded from the interplanetary data for the spacecraft/encounter indicated:

Pioneer 10/Jupiter: 11/26/73, 00:00, to 12/16/73, 00:00

Pioneer 11/Jupiter: 11/26/74, 00:00, to 12/10/74, 00:00

Pioneer 11/Saturn: 08/31/79, 00:00, to 09/05/79, 00:00

This data will be supplied on their own tapes complete with similar documentation concerning their content.

The time periods included on these tapes are as follows:

Pioneer 10: 03/06/72, 00:00, to 01/01/81, 00:00

Pioneer 11: 04/02/73, 00:00, to 01/01/81, 00:00

Table 3 lists the particles and their energy range to which the different rates are sensitive.

DATA FORMAT

Time-history of Pioneer Cosmic-ray Telescope data described above is being submitted on 9-track tapes recorded at 1600 BPI. The tape marked PIOEPF contains Pioneer 10 data and the one marked PIOEPG contains Pioneer 11 data.

Each tape contains one file of data. The file consists of a number of frames. A frame covers a period of one month or less and consists of eight Flux Time-history (FTH) records. Data items contained in the FTH records in each frame are described in Table 3. An FTH record contains a count of the number of data items (NBIN) whose time-history is included in the record, a count of the number of averaging intervals (NINT) included in the record, definitions of data items included and time-history data. Table 4 defines the structure of an FTH record in detail. These tapes were generated on an IBM System 360 computer; thus, a word consists of 32 bits, half-word 1 is the high order 16-bit field of the word and half-word 2 the low order half (bits 16-31, with the left-most or MSB numbered 0). Characters are represented in 8-bit EBCDIC byte, real numbers are represented in the IBM single precision floating point format. Length (in words) of an FTH record is given by

200 + (3 + 2 * NBIN) * NINT	NBIN $\leq$ 5
233 + (3 + 2 * 6) * NINT	NBIN = 6

Thus, FTH records have a maximum length of 1812 words (7248 bytes).

Table 1

Summary of the Characteristics of Each
of the Telescopes and Their Component Detectors
(One of Each Carried on Board Pioneer)

TELESCOPE	HET	LET-I	LET-II
Geometrical Factor (cm^2-ster)	.22	.155	.015
Detectors (thickness × area)	A,B: 2.5mm×3cm^2	DI,DII: 100μ×1cm^2	SI: 50μ×50mm^2
	C's: 2.5mm×8.5cm^2	E,F: 2.5mm×3cm^2	SII: 2.5mm×50mm^2
			SIIA: 2.5mm×50mm^2
			SIII: 2.5mm×200mm^2

Table 2

RATE	COINCIDENCE	PARTICLE/ENERGY[+]
*R1	$(A_2K_1+A_1CI)B\overline{CIII}$	Protons, Z≥2: 20-56 MeV/nuc
		Electrons: 2-8 MeV
*R2	$A_1\overline{A_2}B$ CIII	Protons: >230 MeV
*	$A_1BK_2\overline{CIII}$	Z≥2: 20-56 MeV/nuc
*R3	A_2B CIII	Protons, 56-220 MeV; Alphas, >56 MeV
	$A_2BK_2\overline{CI}$	Alphas: 20-30 MeV/nuc
R4	$A_2BK_2CI\overline{CII}$	Alphas: 30-45 MeV/nuc
	A_1	
R5	$A_2BK_2CICII\overline{CIII}$	Alphas: 45-56 MeV/nuc
	A_2	
R6	$A_1\overline{A_2}BCI$	Electrons: 2-4 MeV
	$A_1\overline{A_2}BCI\overline{CII}$	Electrons: 4-6 MeV
R7	$A_1\overline{A_2}BCICII\overline{CIII}$	Electrons: 6-8 MeV
	$A_2BK_1\overline{CI}$	Protons, Alphas: 20-30 MeV/nuc
R8	$A_2BK_1CI\overline{CII}$	Protons, Alphas: 30-45 MeV/nuc
	$A_2BK_1CICII\overline{CIII}$	Protons, Alphas: 45-65 MeV/nuc
R9	B	
	CI	
	CII	
	CIII	
R10	DI_1	
	.	
	.	
	.	
	DI_8	
*R11	$DIDII\overline{F}$	Protons, Z≥2: 3-21 MeV/nuc
*	$DIDII\Sigma D\overline{F}$	Z≥2: 3-21 MeV/nuc
R12	$DIDIIE_1\overline{F}$	Protons, Z≥2: 6-21 MeV/nuc
	$DIDII\Sigma DE_3\overline{F}$	Z≥2: 6-21 MeV/nuc
R13	$DIDIIE_2\overline{F}$	Protons, Z≥2: 10-21 MeV/nuc
	$DIDII\Sigma DE_4\overline{F}$	Z≥2: 10-21 MeV/nuc

Table 2, Continued:

RATE	COINCIDENCE	PARTICLE/ENERGY+
R14	DI	
	DII	
	E_1	
	F	
	SI	
	SII	
	SIII	
	SIIA	
R15	SI_1 $\overline{SII}$ $\overline{SIIA}$ $\overline{SIII}$	Protons: .15-2.1 MeV
	SI_2 $\overline{SII}$ $\overline{SIIA}$ $\overline{SIII}$	Protons: .72-2.1 MeV
	SI_3 $\overline{SII}$ $\overline{SIIA}$ $\overline{SIII}$	Protons: 1.2-2.1 MeV
	SI_4 $\overline{SII}$ $\overline{SIIA}$ $\overline{SIII}$	Alphas: .6-2.1 MeV/nuc
R16	$SI\ SII_1$ $\overline{SIIA}$ $\overline{SIII}$	Protons: 2.1-21 MeV
	$SI\ SII_2$ $\overline{SIIA}$ $\overline{SIII}$	Protons: 5.7-21 MeV
	$SI\ SII_3$ $\overline{SIIA}$ $\overline{SIII}$	Protons: 15.1-21.2 MeV
	$SI\ SII_4$ $\overline{SIIA}$ $\overline{SIII}$	Alphas: 6-21.2 MeV/nuc
SR1	$A_1\overline{A_2}B\ CI\ \overline{CIII}$	Electrons: 4-8 MeV
	$A_2BK_1\overline{CIII}$	Protons, $Z \geq 2$: 20-56 MeV/nuc
	$DIDII\overline{F}$	Protons, $Z \geq 2$: 3-21 MeV/nuc
	$DIDIIE_1\overline{F}$	Protons, $Z \geq 2$: 6-21 MeV/nuc
SR2	SI_5 $\overline{SII}$ $\overline{SIIA}$ $\overline{SIII}$	Protons: .12-2.1 MeV
	SI_6 $\overline{SII}$ $\overline{SIIA}$ $\overline{SIII}$	Protons: .52-2.1 MeV
	SI_7 $\overline{SII}$ $\overline{SIIA}$ $\overline{SIII}$	Protons: 1.5-2.1 MeV
	SI_8 $\overline{SII}$ $\overline{SIIA}$ $\overline{SIII}$	Protons: 1.5-2.1 MeV
	$\overline{SI}\ SII_5$ $\overline{SIIA}$ $\overline{SIII}$	Electrons: .12-2 MeV
	$\overline{SI}\ SII_6$ $\overline{SIIA}$ $\overline{SIII}$	Electrons: .40-2 MeV
	$\overline{SI}\ SII_7$ $\overline{SIIA}$ $\overline{SIII}$	Electrons: .68-2 MeV
	$\overline{SI}\ SII_8$ $\overline{SIIA}$ $\overline{SIII}$	Electrons: .97-2 MeV

+Design goals, actual parameters for the submitted rates are listed in Table 3.

*Designates PHA conditions.

$K = A+B + 1.8(CI+CII)$

$\Sigma D = DI+DII +1.6E$

Table 3. Data Content of a Frame on PIOEPF and PIOEPG

FTH RECORD # WITHIN A FRAME	DATA ITEM
1	112.0 -400.0 MeV Proton
	30.0 - 56.0 MeV Proton
	3.44- 5.2 MeV Proton
	112.7 -400.0 MeV Alpha
	30.0 - 56.0 MeV Alpha
2	10.0 - 21.0 MeV Alpha
	3.44- 5.2 MeV Alpha
	2.0 - 6.0 MeV Electron
	R1 2-8 MeV electrons, 20-56 MeV protons
	R2A >180 (P-10), >220 (P-11) MeV protons, >8 MeV electrons
3	R2B All $Z \geq 2$ ions with a range < 1.5 cm in Si
	R3A 56-180 (P-10)-220 (P-11) MeV protons plus > 56 MeV alphas
	R9A 0.22 MeV threshold on Det. B
	R9B 1.0 MeV threshold on Det. CI
	R9C 1.1 MeV threshold on Det. CII
4	R9D 0.23 MeV threshold on Det. CIII
	R10A 0.13 MeV threshold on Det. DI
	R10B 0.60-33 MeV protons, > 0.39 MeV alphas
	R10C 0.72-20 MeV protons, > 0.42 MeV alphas
	R10D 0.84-14.2 (P-10), 0.82-15.1 (P-11) MeV protons > 0.46 MeV alphas
5	R10E 1.1-8.1 MeV protons, > 0.53 MeV alphas
	R10F 1.60-5.1 (P-10), 1.56-5.1 (P-11) MeV protons, > 0.63 MeV alphas
	R10G 2.29-3.8 (P-10), 2.13-3.8 (P-11) MeV protons, > 0.75 MeV alphas
	R10H > 0.99 MeV alphas with proton contamination
	R11A 3.2-21 MeV protons and alphas
6	R11B 3.2-21 MeV alphas and heavier ions
	R12A 5.6-21 MeV protons and alphas
	R12B 5.6-21 MeV alphas and heavier ions
	R15A 0.20-2.15 (P-10), 0.20-2.17 (P-11) MeV protons, alpha and ion contamination
	R15B 0.74-2.15 (P-10), 0.72-2.17 (P-11) MeV protons, 0.22-2.05 MeV alphas
7	R15C 1.24-2.15 (P-10), -2.17 (P-11) MeV protons, 0.34-2.05 MeV alphas
	R15D 0.69-2.05 (P-10), 0.66-2.05 (P-11) MeV alphas + ions
	R16A 3.2-20.6 MeV protons, plus some alphas
	R16B 5.7-20.6 MeV protons, plus some alphas
	R16C 14.9-20.6 MeV protons, plus some alphas
8	R16D 6.6-20.6 MeV alphas

Table 4. STRUCTURE OF FLUX TIME-HISTORY RECORD

WORD	HALFWORD	TYPE	DESCRIPTION
1	1	Integer	Number of data items contained in the record (NBIN).
3-35	2	Integer	Number of averaging intervals (NINT) contained in the record.
3-35		character	132-character title identifies satellite and gives the start time of first averaging interval and last averaging interval in the record.
36-68		character	132-character description of first data item.
69-101		character	132-character description of second data item, if NBIN $\geq$ 2. Otherwise, not used.
102-134		character	132-character description of third data item, if NBIN $\geq$ 3. Otherwise, not used.
135-167		character	132-character description of fourth data item, if NBIN $\geq$ 4. Otherwise, not used.
168-200		character	132-character description of fifth data item, if NBIN $\geq$ 5. Otherwise, not used.
		NBIN $\leq$ 5	
201-			NINT Averaging Interval Entries (AIE). The structure of an AIE is shown in Table 4.
		NBIN = 6	
201-233		character	132-character description of sixth data item.
234-			NINT Averaging Interval Entries as defined in Table 5.

Table 5. STRUCTURE OF AVERAGING INTERVAL ENTRY

WORD	HALFWORD	TYPE	DESCRIPTION	
1	1	Integer	2-digit year	
	2	Integer	month of year	
2	1	Integer	day of month	Start time of averaging interval
	2	Integer	hour of day	
3	1	Integer	minute of hour	
	2	Integer	second of minute	
4-(3+2*NBIN)		Real	NBIN FLUX entries. Each FLUX entry is two words long. If the second word of the entry is -1.0, data for this item is not available; otherwise the first word is the value of flux and the second word contains the associated statistical error.	

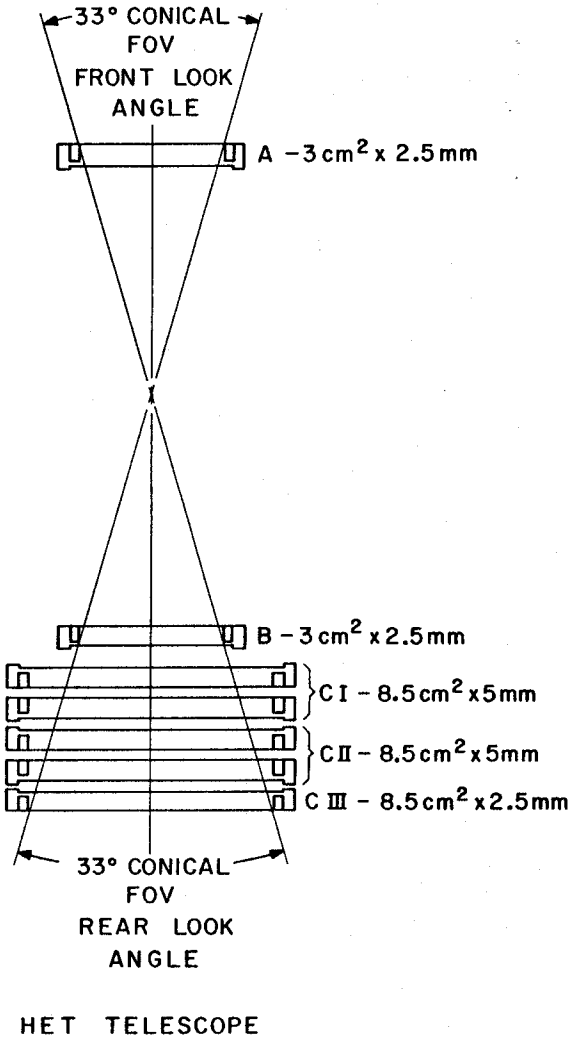

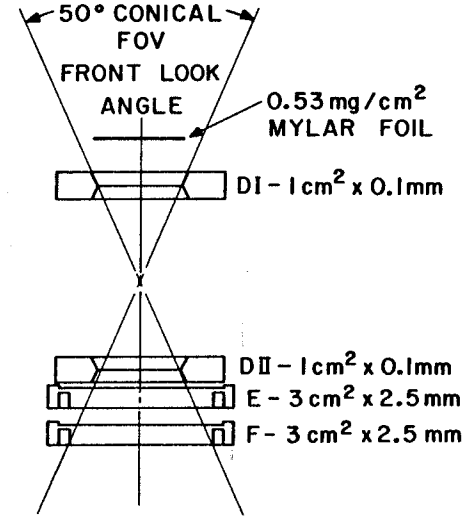

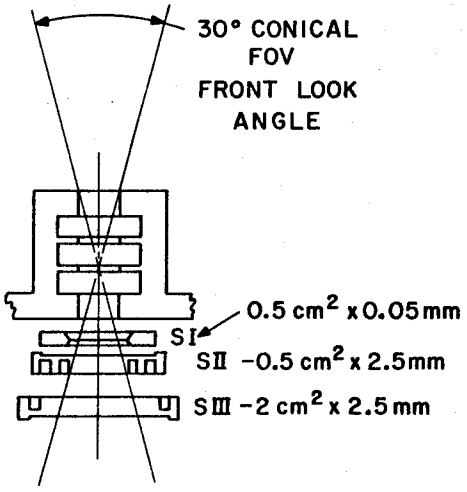

PIONEER F & G DETECTOR COMPLEMENT
COSMIC RAY ENERGY SPECTRA

Figure 1. HET, LET-I and LET-II Telescope Assemblies.

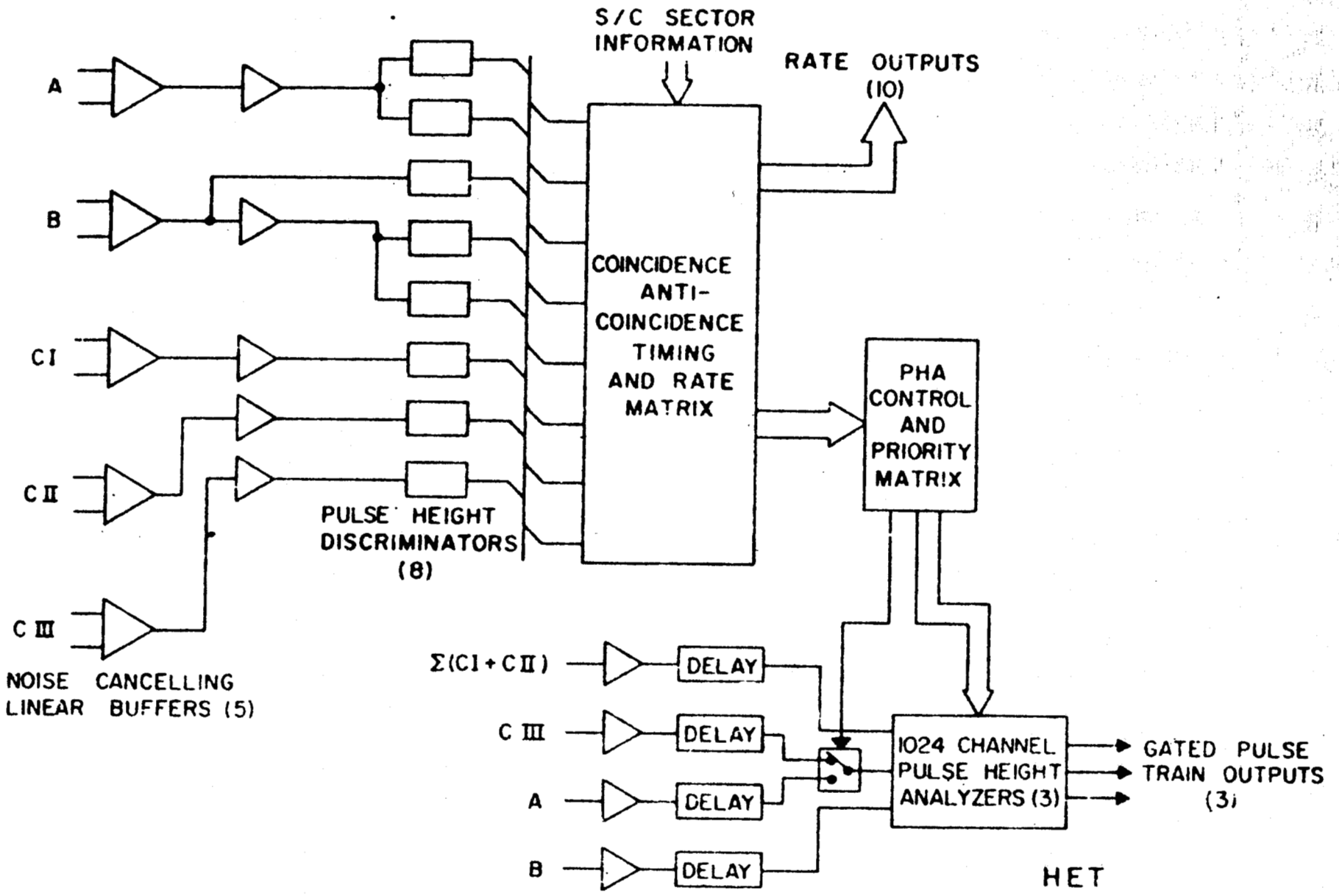

Figure 2. HET Block Diagram.

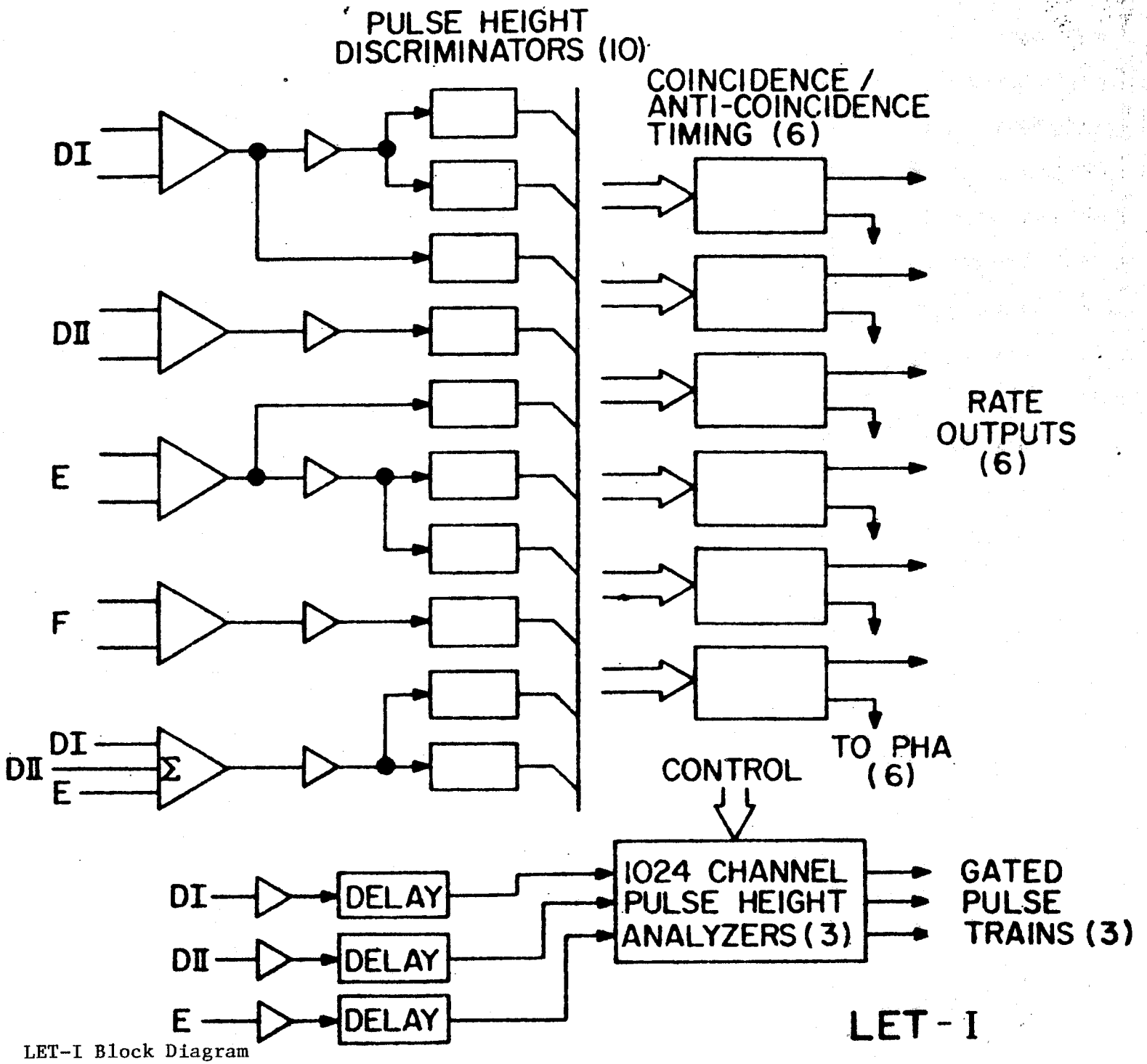

Figure 3. LET-I Block Diagram

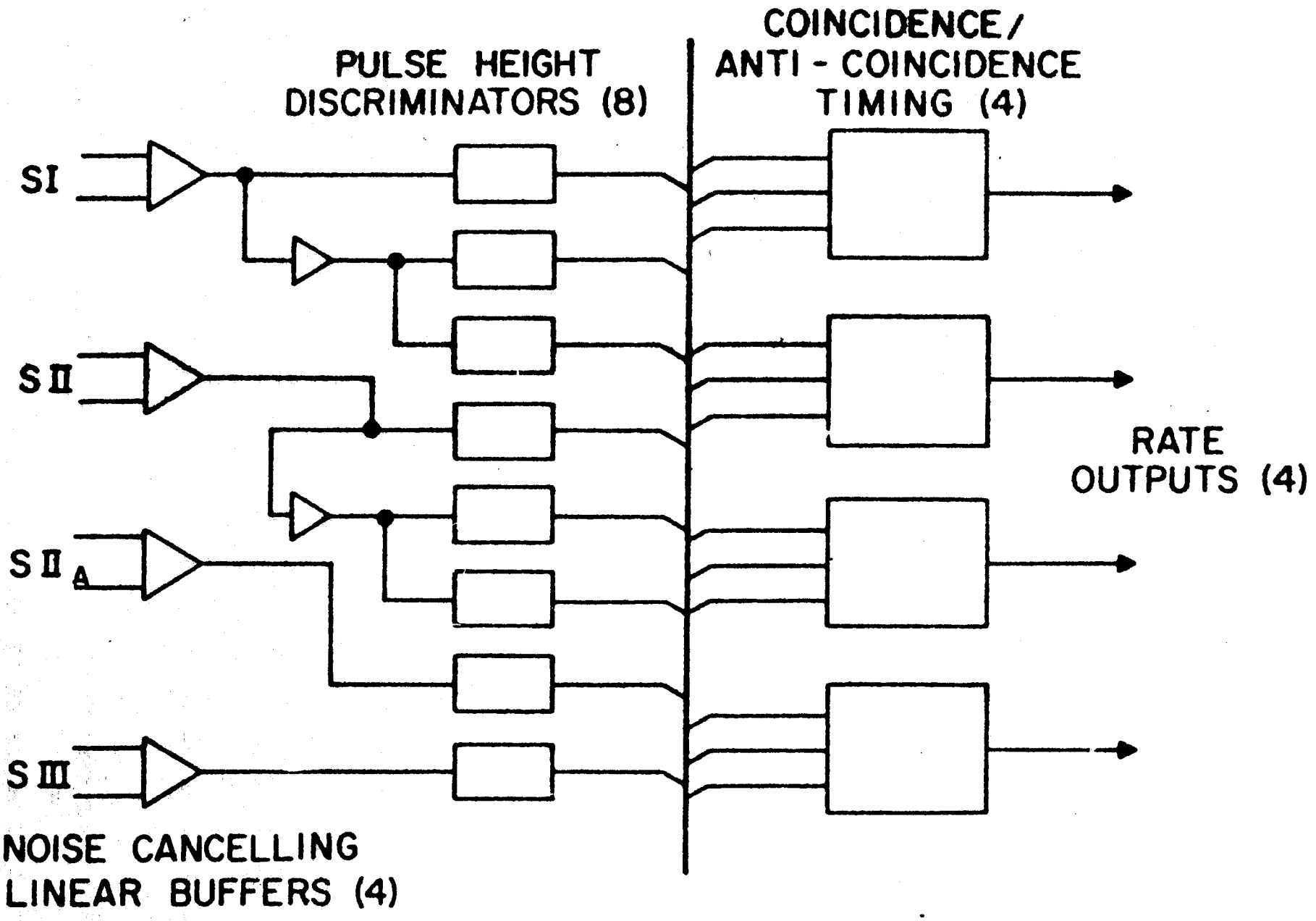

Figure 4. LET-II Block Diagram

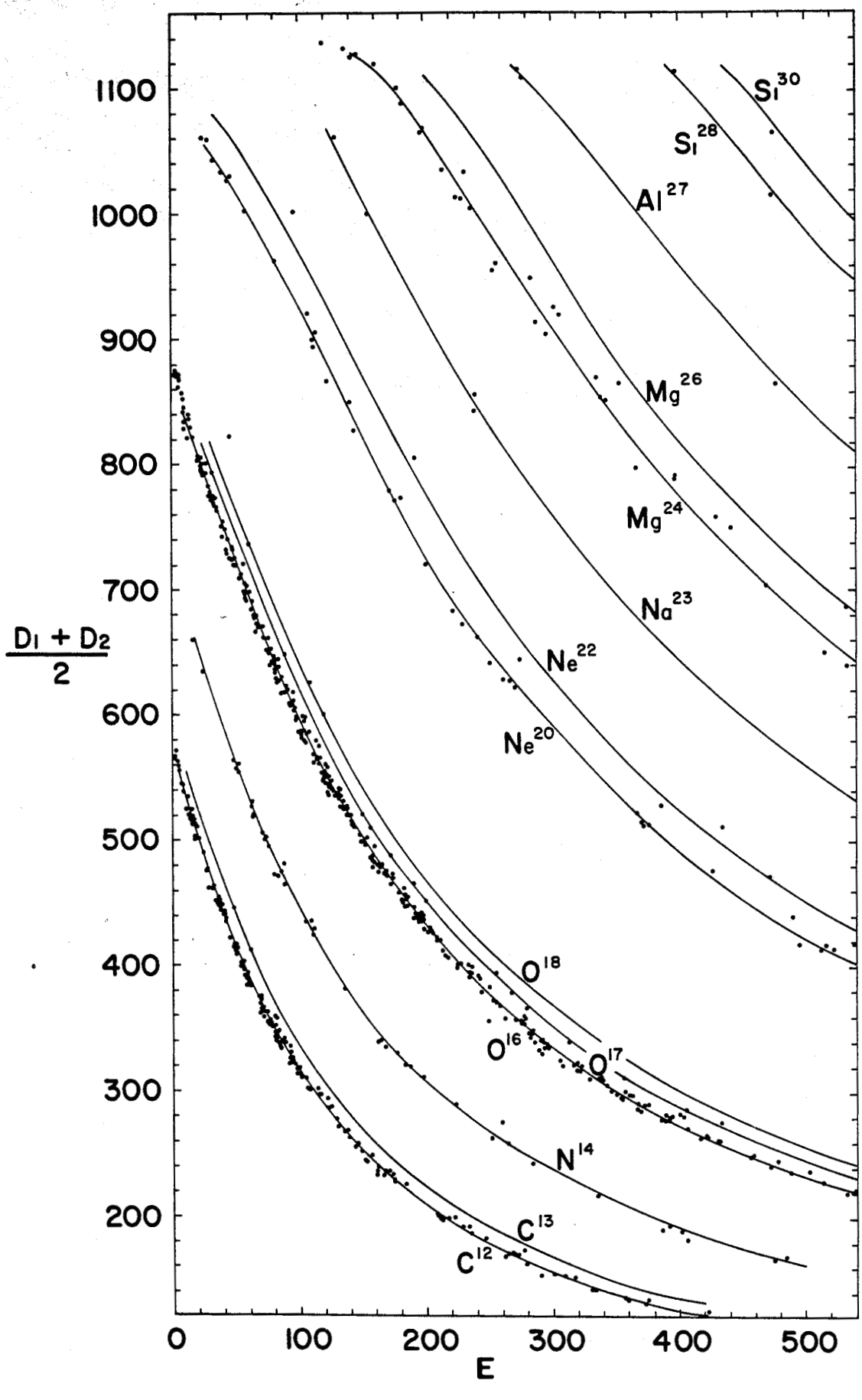

Figure 5.

dE/dx vs. E results from the Pioneer LET-I telescope during the August 1972 solar event. Clear isotopic resolution for elements up to Mg is possible.

A COSMIC RAY DETECTOR SYSTEM FOR THE ANALYSIS OF ENERGY SPECTRA, CHARGE COMPOSITION AND GENERAL FLOW PATTERNS OF SOLAR, GALACTIC AND JOVIAN ENERGETIC PARTICLES DURING THE PIONEER EARTH/JUPITER MISSIONS

BY

FRANK B. MC DONALD

BONNARD J. TEEGARDEN

JAMES H. TRAINOR

NASA/GODDARD SPACE FLIGHT CENTER

AND

EDMOND C. ROELOF

WILLIAM B. WEBBER

UNIVERSITY OF NEW HAMPSHIRE

SEPTEMBER, 1970

I. SCIENTIFIC OBJECTIVES

The proposed Pioneer F and G mission offers a unique opportunity to study the extended regions of the interplanetary medium. The possibility of approaching interstellar electromagnetic conditions must be contemplated and regarded with great interest. These points, coupled with the opportunity to study the Jovian environment, call for a carefully coordinated set of studies in each scientific discipline.

This instrument is designed to exploit to the fullest practical degree the proposed trajectories of Pioneer F and G. The significance of these measurements will be greatly enhanced by concurrent measurements with similar particle telescopes scheduled for flights on satellites of the IMP or similar series in near-earth orbits.

The principal scientific objectives of this experiment are:

1. To measure the flow patterns of energetic solar and galactic particles separately in the interplanetary field. To interpret this measurement, simultaneous determination of the energy spectrum, radial gradient, angular distribution, and streaming parameters is required for each nuclear species and over as wide an energy range as is practicable.

2. To measure the energy spectra, and isotopic composition of galactic and solar cosmic rays from the lowest practical energies up to ~ 800 MeV/nucleon and (by use of objective 1) to unfold the primary flare and interstellar spectrum.

3. To measure the time variations of the differential energy

spectra of electrons, hydrogen and helium nuclei over the corresponding energy intervals. During flare events, to obtain time histories; during quiet times, to relate gross time variations to those near earth thus deducing a spatial gradient for galactic cosmic rays. ✓

4. To study the energy spectra, time variations and spatial gradients associated with recurrent and non-flare associated interplanetary proton and helium streams and to define the related solar or interplanetary acceleration processes.

5. To provide information on the energetic particle distribution surrounding Jupiter. ✓

6. To try to determine the extent of the solar cavity, the energetic particle phenomena occurring at this interface and the cosmic ray density in nearby interstellar space.

The spatial/temporal structure of solar and interplanetary events can only be deduced from continuous monitors at a variety of radial and azimuthal locations. Co-rotating particle streams, interplanetary plasma shocks and Forbush decreases are obvious examples in addition to customary flare events. Quiet-time fluxes measured on the outward journey cannot be interpreted in terms of a galactic gradient unless a sound "base-line" for the solar cycle-dependent time variation of fluxes can be derived from comparable detectors in near-earth orbits. Fortunately such detectors are scheduled for a concurrent period on IMP H and J, and potentially IMP KK'. ✓

The strong collimation of solar particle flow along magnetic field lines during all but the late phases of solar flare events is well established near 1 AU. However, at 5 AU the field may be quite tangled due to the "winding up" of the Archimedean spiral field; it would make an average angle of ~ 80° with the solar radius vector. If the field at this distance is more disordered than at earth, the reverse situation to that at the earth may hold; angular flare particle distributions may aid interpretation of complicated magnetic field measurements. The need for associated magnetic field measurements in interplanetary shocks and Forbush decreases is self-evident. Recent theoretical work (Gleeson, 1969; Roelof, 1969) has shown that the average magnetic field direction governs the flow of quiet-time particles, so simultaneous particle-field observations are required.

II. PHENOMENA TO BE MEASURED

In the field of energetic particles we have tried to design an instrument that will provide the maximum-possible diagnostic power to examine the complex field-particle interactions occurring in the interplanetary environment as well as the Jovian magnetosphere.

To accomplish this we propose a coordinated set of two solid state detector telescopes to study charged particles. The telescopes are designated as:

a. the high energy telescope (H.E.T.),

b. two low energy dE/dx vs. E telescopes (L.E.T. I and L.E.T. II).

Charged particle spectra and angular distributions will be measured over an extended energy interval. These intervals are briefly listed below in Table 1, and are shown graphically in Figure 1.

TABLE 1

Particle Component	Energy Range
Galactic cosmic ray protons	4.5 - 800 MeV
Solar protons	.05 - 800 MeV
Galactic cosmic ray Helium	4.5 - 600 MeV/nucleon
Solar Helium	1.0 - 600 MeV/nucleon
He^3/He^4, D/H	4.5 - 50 MeV/nucleon
Galactic and Solar Electrons	.050- 5.0 MeV
Li, Be, B, C, N, O, F, Ne and their isotopic composition	6 MeV/nuc- 200 MeV/nucleon
Integral flux	> 800 MeV
Energy Ranges for Angular Distribution Studies	
Hydrogen	.05 - 120 MeV
Helium	4.5 - 120 MeV/nucleon
Electrons	.05 - 5 MeV

Geometrical Factors

High Energy Telescope	0.220 cm^2 - ster.
Low Energy Telescope I	0.155 cm^2 - ster.
Low Energy Telescope II	0.015 cm^2 - ster.

III. DETECTOR SYSTEM

We shall now discuss these three telescopes in some detail and how the measurements are coordinated to provide a comprehensive and redundant set of cosmic ray measurements. The redundance of the separate sets of measurements as well as the self-calibration are important features of the system we are proposing. It is a total necessity in view of the prolonged nature of the Pioneer F and G missions and the controversy that currently exists over the interpretation of gradient and anisotropy measurements made in the 0.7 - 1.5 AU interval.

Figure 2 is a picture of the completed experiment with handling fixtures and detector covers attached. The LET-II telescope within its radiation shield is in the center with the LET-I telescope partially visible through the side face. The HET telescope is within the package, directly above the other two telescopes, and looks through the front and side faces shown into the same plane as the LET telescopes. All telescopes look perpendicular to the Pioneer spin axis and thus are always scanning the celestrial sphere.

There are six elements 2.5 mm thickness
15mm

E_i = energy as the particle enters a detector

$$\Delta E_1 = z^2 f(v_1)$$

$$E_2 = E_1 - \Delta E_1$$

$$\Delta E_2 = z^2 f(v_2)$$

$$E_3 = E_2 - \Delta E_2$$

$$\Delta E_3 = z^2 f(v_3)$$

1. given E_1, the entire sequence is clear & easily worked out
2. for low energy particles, $\frac{dE}{dx}$ is a rapidly varying function of v & linear relationships are no longer true.
3. Q. Given how a particular load loses from a given amt of energy after penetrating a given # of absorbers, how can determine energy before it enters the detector?

$$E(x) = E(0) - \int_0^x \frac{dE}{dx} dx$$

$$\cong E(0) - \int f(E(x))\, dx$$

For high energy particles this is small.

$$\frac{dE(x)}{dx} = f(E(x))$$

$$E = m\gamma \qquad \frac{dE}{dv} = m \frac{d\gamma}{dv}$$

$$\gamma = \frac{1}{\sqrt{1-v^2}} \qquad \frac{1}{m}\frac{dE}{dv} = \frac{v}{(\sqrt{1-v^2})^3}$$

$$\frac{d\gamma}{dv} = +\frac{1}{2}(1-v^2)^{-3/2}$$

=

High Energy Telescope:

The high energy telescope is a four element array and is shown schematically in Figure 3. Two of these elements (A and B) are single, lithium-drifted silicon detectors, 300 mm^2 in area and 2.5 mm thick. The third element is a stacked arrangement of four 850 mm^2, 2.5 mm thick lithium drifted silicon detectors (C_1 and C_2), while the fourth element C_3 is a similar detector which identifies events as stopping somewhere in the telescope ABC_1C_2 or as penetrating the entire telescope. For particles which come to rest within the telescope (20 - 50 MeV/nucleon) three measurements are made - energy loss (dE/dx), total energy, and range. The simultaneous measurement of total energy and range provides a very powerful method for rejecting detector background, which is a particularly significant problem in this energy regime. For particles which penetrate completely through the stack of solid state devices, three separate dE/dx measurements are made. This will allow the differential energy spectra to be obtained for helium and hydrogen from 50 - 800 MeV/nucleon. Charge resolution for penetrating particles will be possible up to approximately 200 MeV/nucleon.

Figure 3 also shows a simplified logic drawing for the HET. In addition to the three 10-bit addresses associated with the pulse height analysis of an HET event, we require additional bits as noted to identify the priority mode, identify the data as HET, specify PHA_2, identify the spin sector in which the event occurred, and to

determine if the event penetrated to C_2. The priority mode is the state of a time sharing system based on the four logic conditions shown on Figure 3 which identify stopping particles, stopping heavies (He and above), penetrating heavies, and all penetrating particles. Since these detectors will usually be telemetry-readout limited, the priority system will select these rare particles for analysis on a time shared basis, thus artificially enhancing the fraction of alpha particles and heavies in the data. The many rates which are commutated and counted will allow us to determine the true ratios of these particles in interplanetary space. Certain rates are sectored, e.g., counted into eight different counters corresponding to eight equal sectors (45°) of spin, synchronized to the see-sun direction.

Low Energy Telescope (LET-I):

LET-I is a three element dE/dx vs E telescope plus an anti-coincidence detector. It will cover the energy range from 3 to 22 MeV/nucleon, and in this interval charge resolution will be possible from Z = 1 (hydrogen) to Z = 8 (oxygen). The telescope is designed to measure both the energy spectra and angular distributions over these intervals. This telescope represents a modification to the original LET design to take into account the effects of the Pioneer radioisotope power supply vs the original solar array. Effectively, the very low energy particle information is now taken by LET-II

which is quite small and can be shielded.

The detector configuration is shown in Figure 4. Detectors D_1 and D_2 are identical silicon surface barrier devices each 100 microns thick and 100 mm^2 in area. They serve the dual purposes of defining the geometry of the detector telescope and also providing a redundant double dE/dx measurement. Detector E is a lithium drifted silicon device 2.5 mm in thickness and 300 mm^2 in area. It serves as a total energy measuring element. The F detector, another 2.5 mm thick lithium drifted silicon device, simply acts as an anticoincidence. Events of the type $D_1D_2\overline{E}$ and $D_1D_2E\overline{F}$ will be analyzed. The $D_1D_2\overline{EF}$ events correspond to protons between 3 and 5 MeV whereas the $D_1D_2E\overline{F}$ events include the 5 to 22 MeV range for protons, for instance.

Figure 4 also outlines the pulse height analysis system, conditions and the auxilliary bits required. A priority system similar to HET is incorporated to emphasize rare events, and many different count rates are monitored. Several rates are also sectored by eight to allow us to reconstruct an angular scan.

This detector, like the HET, will be self-calibrating. In addition the telescopes have been designed such that an overlap in the individual energy responses of the detectors does exist. This will then allow cross calibrations between detectors.

Low Energy Telescope (LET-II):

This telescope is designed to study low energy protons and

electrons in the Jovian radiation belts and particles of solar origin in the interplanetary region. A schematic of this detector is shown in Figure 5.

There are three elements:

S_1	50μ	-	50 mm^2 Silicon Surface Barrier
S_2	2.5 mm	-	50 mm^2 Lithium-drifted Silicon
S_3	2.5 mm	-	200 mm^2 Lithium-drifted Silicon

The S_1 thickness was chosen to minimize the electron response without making an unreasonable sacrifice in the detector performance.

The detectors S_1 and S_2 are used individually and in coincidence as total absorption spectrometers. S_3 operating in an anticoincidence mode insures that only stopping particles are analyzed. In addition, S_2 is made with a coaxial detector enclosing the center active region so as to provide anticoincidence to particles coming from the sides. S_1 will stop electrons in the range 50 - 150 KeV and protons in the range 50 KeV - 3 MeV. The S_2 detector will respond to electrons in the energy interval 150 KeV - 1 MeV and the proton interval is 3 MeV - 20 MeV, and in these ranges an unambiguous separation of electrons and protons is possible. Figure 5 also lists the large number of rates and sectored rates that are monitored for this detector. Stopping alphas in the S_1 detector will have a unique response from 1 MeV - 3 MeV/nucleon for solar alpha events.

Considerable precautions have been taken to minimize the effects of radiation damage in all the telescopes. The primary concern is for the trapped radiation belts about Jupiter. There is no reliable

prediction of proton fluxes and low energy electrons (< 1 MeV) in the Jovian magnetosphere. This experiment can tolerate the high energy electrons inferred from radio data, however, the proton and lower energy electron fluxes could be large enough to seriously damage many solid state detectors. The detectors in this experiment are in all cases fully depleted devices having average electric field strengths in the range 150 volts/mm to 200 volts/mm. Additionally, all detectors directly exposed or with minimum shielding are oriented in the telescope so that the rear or aluminum contact will be irradiated primarily.

IV. INSTRUMENTATION

The charge sensitive preamplifiers, shaping amplifiers, the output data system and the power supplies are constructed primarily of small or miniature components soldered to "daughter" boards which are then soldered to a "mother" board which provides the interconnect. The linear gates, threshold discriminators, pulse height analyzers, integral analyzers and priority and control matrices are constructed by soldering dual transistors and diodes in discrete, miniature ceramic or glass packages to hybrid, thick film substrates. The extensive data system is constructed primarily of P channel, enhancement mode MOSFETS using both medium scale integration (MSI) and large scale integration (LSI). Much of the interfacing circuitry is done with T^2 L integrated circuits. There are more than 40,000

transistors in the data system.

This entire experiment including the LET-II radiation shield weighs 6.9 pounds and consumes 2.28 watts at 28 volts.

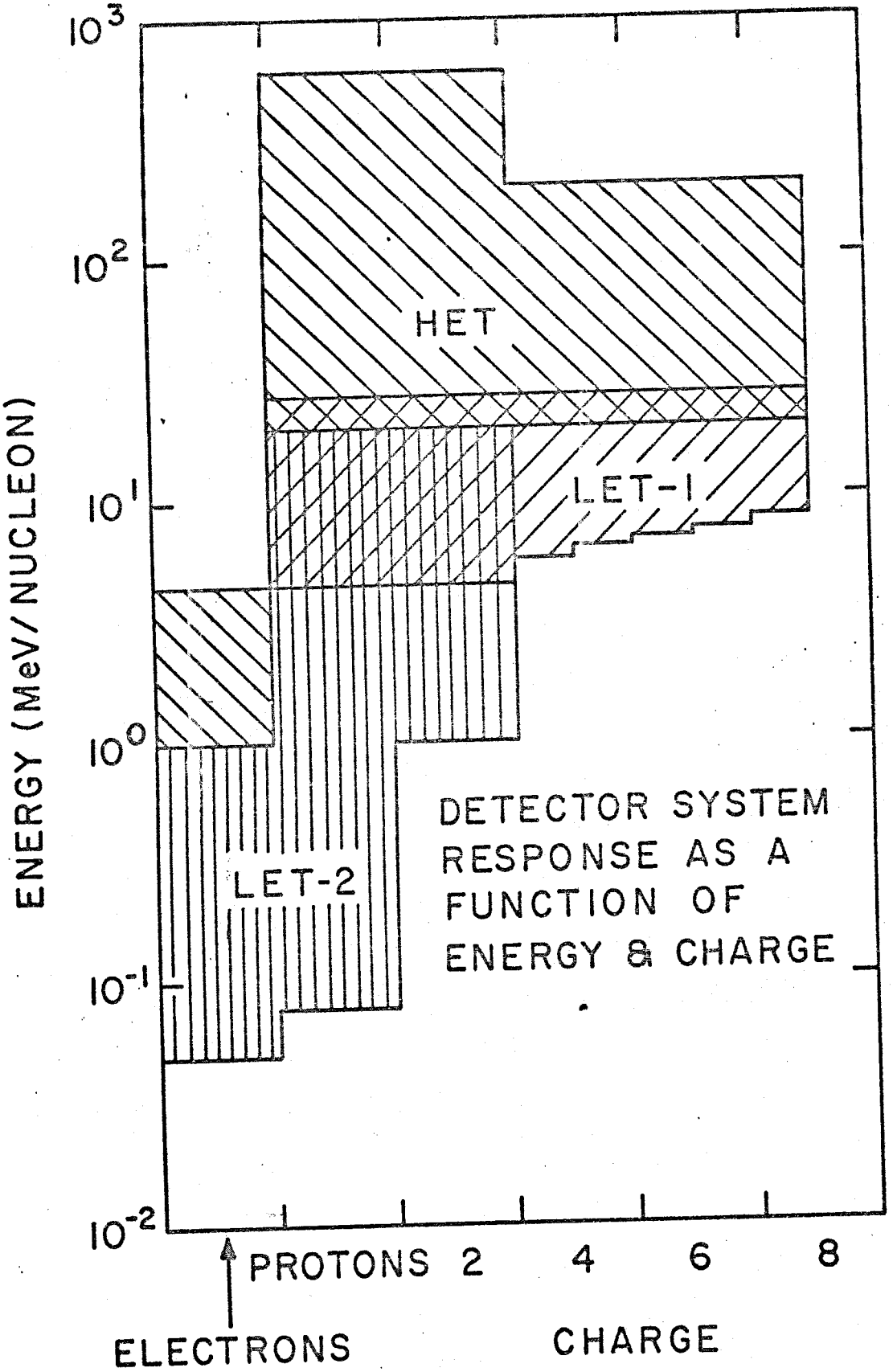
10^3
10^2
10^1
10^0
10^{-1}
10^{-2}
ENERGY (MeV/NUCLEON)
HET
LET-1
LET-2
DETECTOR SYSTEM
RESPONSE AS A
FUNCTION OF
ENERGY & CHARGE
PROTONS 2 4 6 8
ELECTRONS
CHARGE

FIG. 1

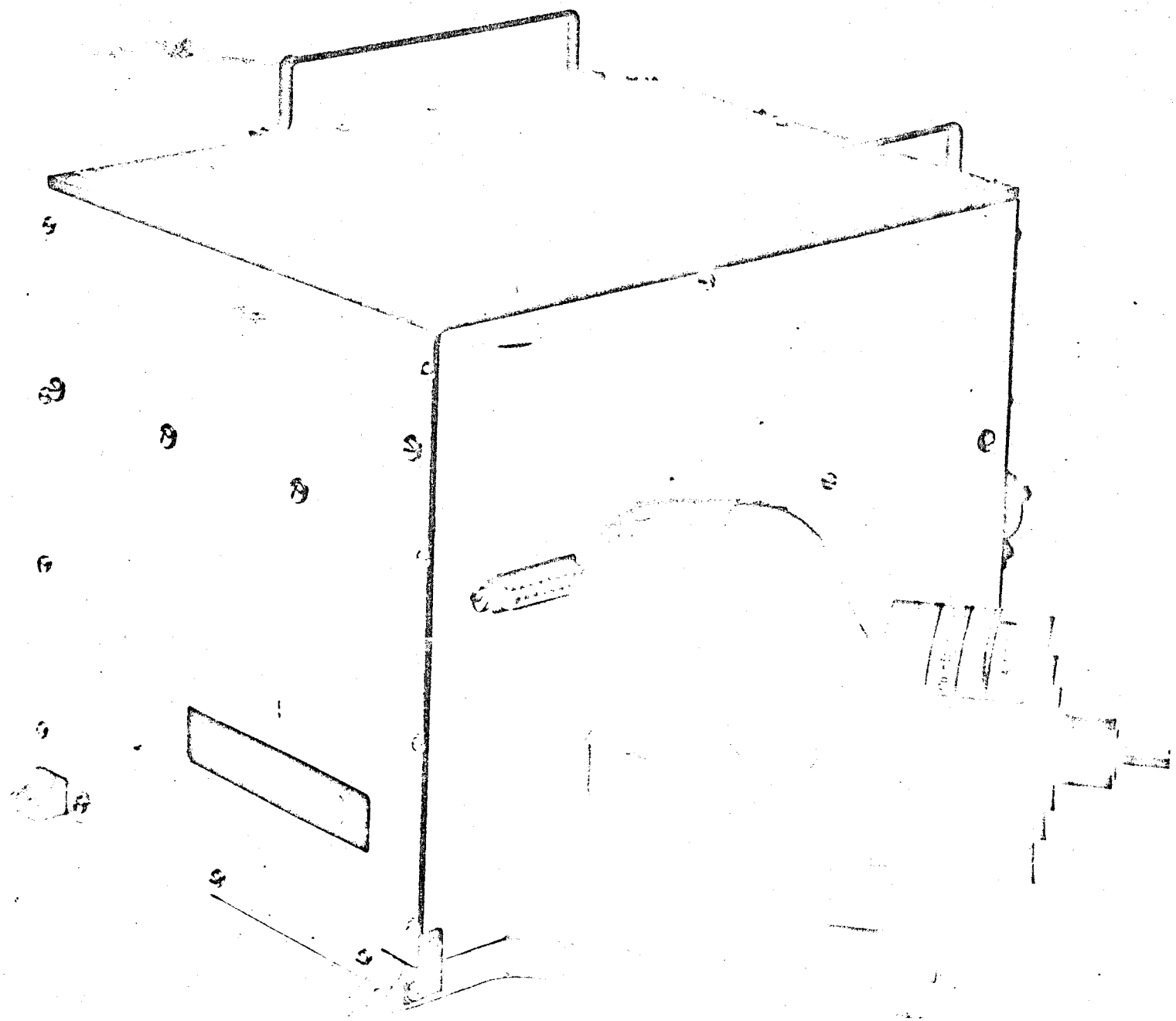

NASA G-71- 1216

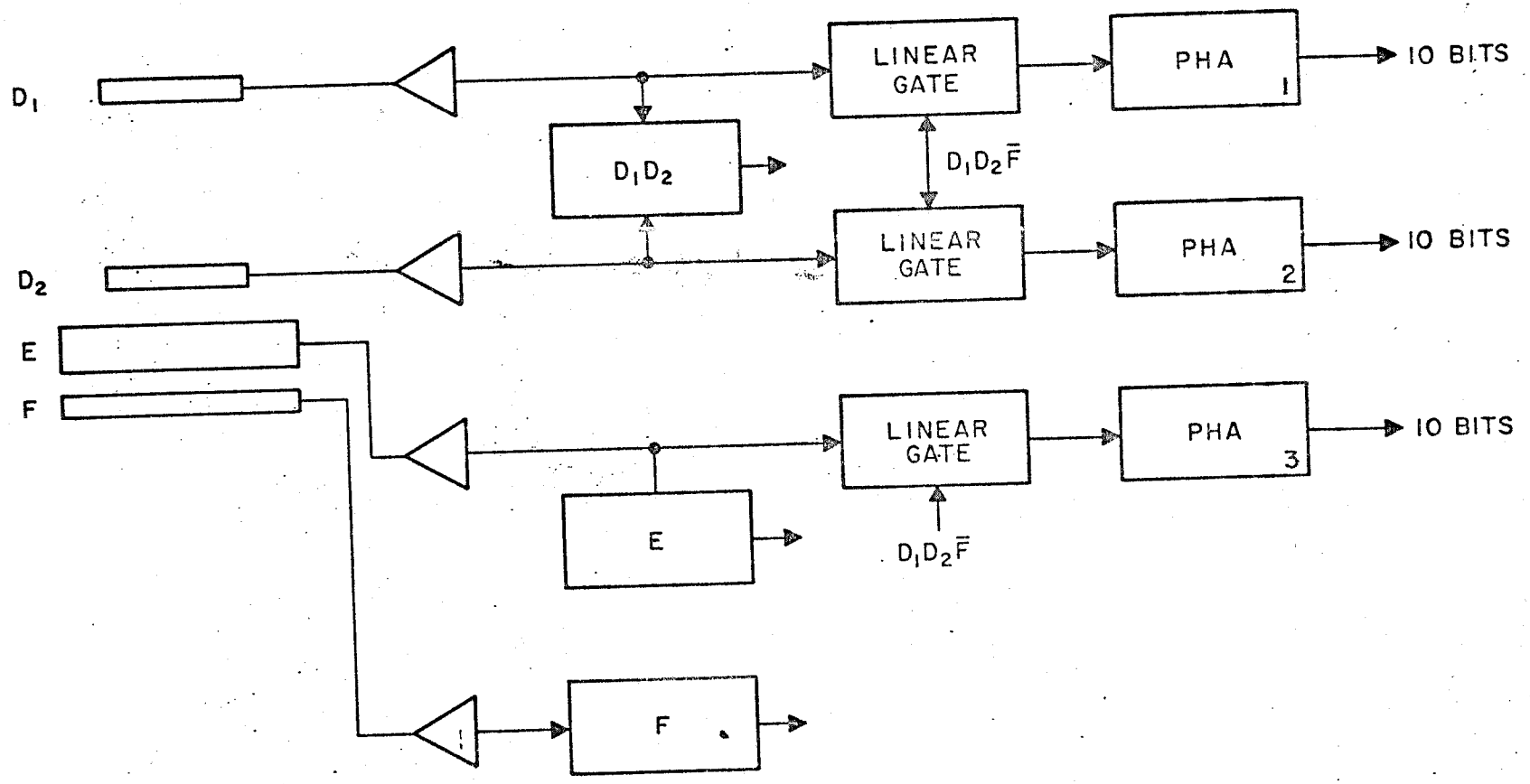

RATES

$D_1D_2(D_1+D_2)E\bar{F}$ (2 LEVELS ON E)

$D_1D_2E\bar{F}$ (2 LEVELS ON E)

D_1 (8 LEVELS)

$\bar{D}_1\bar{D}_2E\bar{F}$

2 BITS REQUIRED TO IDENTIFY PRIORITY MODE.

1 BIT REQUIRED TO IDENTIFY PHA DATA AS LET-I.

3 BITS REQUIRED TO IDENTIFY SECTOR.

FIG. 4

SIMPLIFIED LET-I DETECTOR

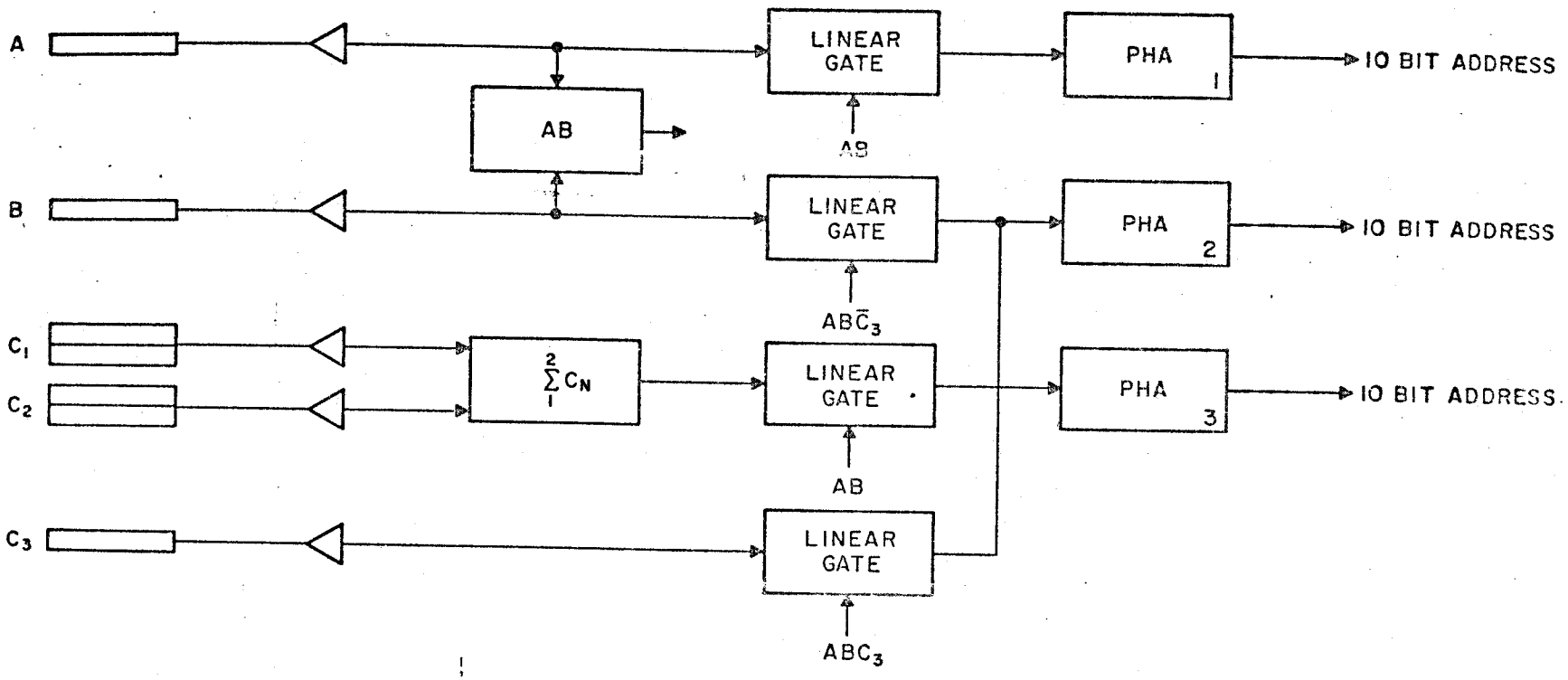

PRIORITY MODES

$AB\bar{C}_3$

$AB\bar{C}_3$ (A > 2 x MIN.)

ABC_3 (A AND C > 2x MIN.)

ABC_3

RATES

A (2 LEVELS)

B, C_1, G_2, C_3

$AB\bar{C}_1\bar{C}_2\bar{C}_3$

$AB C_1\bar{C}_2\bar{C}_3$ } (2 LEVELS ON A)

$AB C_1 C_2\bar{C}_3$

$AB C_1 C_2 C_3$

2 BITS REQUIRED TO IDENTIFY PRIORITY MODE.
1 BIT REQUIRED TO IDENTIFY PHA DATA AS H.E.T.
1 BIT REQUIRED TO DETERMINE IF PHA 2 ADDRESS IS B OR C_3
3 BITS REQUIRED TO IDENTIFY SECTOR.
1 BIT REQUIRED FOR RANGE.

FIG. 3
SIMPLIFIED HIGH ENERGY DETECTOR

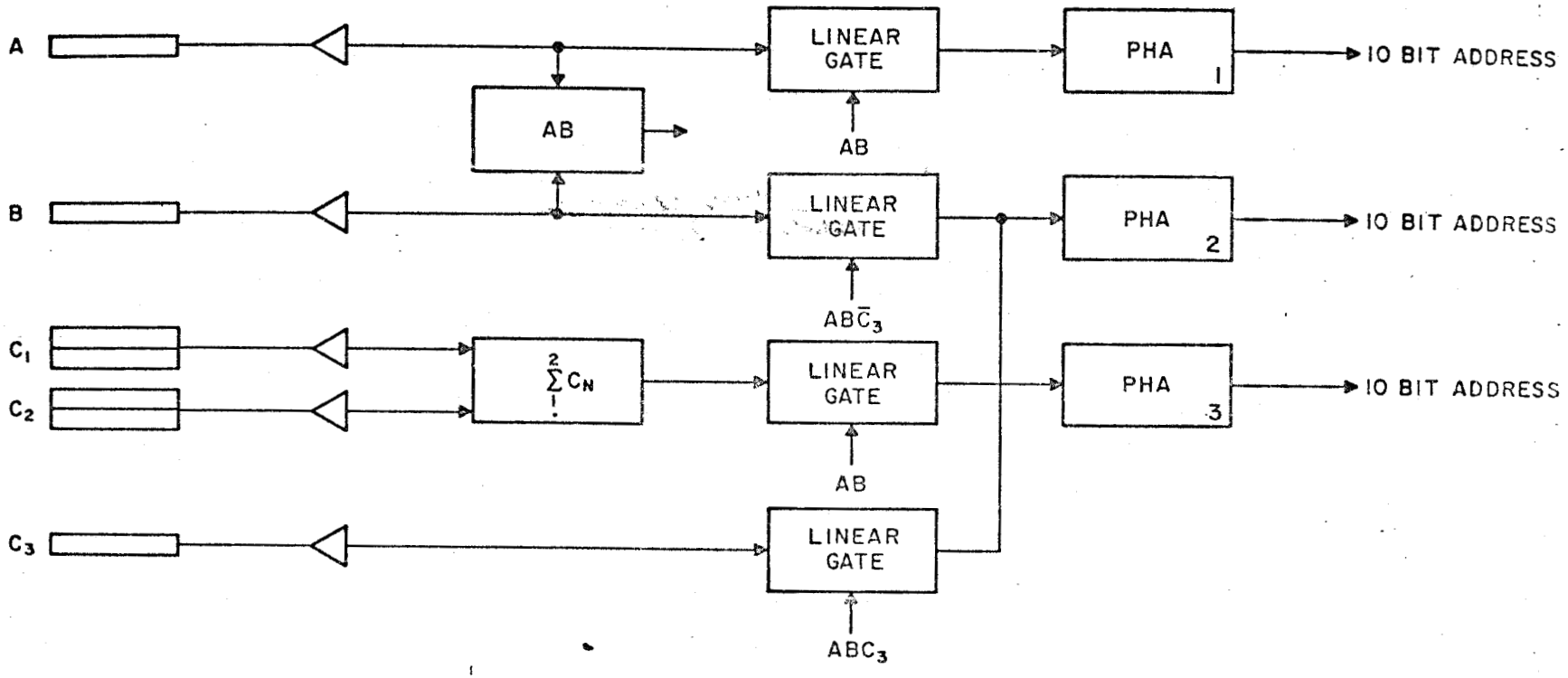

PRIORITY MODES

$AB\bar{C}_3$

$AB\bar{C}_3$ (A > 2 x MIN.)

ABC_3 (A AND C > 2x MIN.)

ABC_3

RATES

A (2 LEVELS)

B, C_1, C_2, C_3

$AB\bar{C}_1\bar{C}_2\bar{C}_3$
$AB C_1\bar{C}_2\bar{C}_3$
$AB C_1C_2\bar{C}_3$
$AB C_1C_2C_3$
(2 LEVELS ON A)

2 BITS REQUIRED TO IDENTIFY PRIORITY MODE.
1 BIT REQUIRED TO IDENTIFY PHA DATA AS H.E.T.
1 BIT REQUIRED TO DETERMINE IF PHA 2 ADDRESS IS B OR C_3
3 BITS REQUIRED TO IDENTIFY SECTOR.
1 BIT REQUIRED FOR RANGE.

FIG. 3
SIMPLIFIED HIGH ENERGY DETECTOR

LOW ENERGY DETECTOR-II

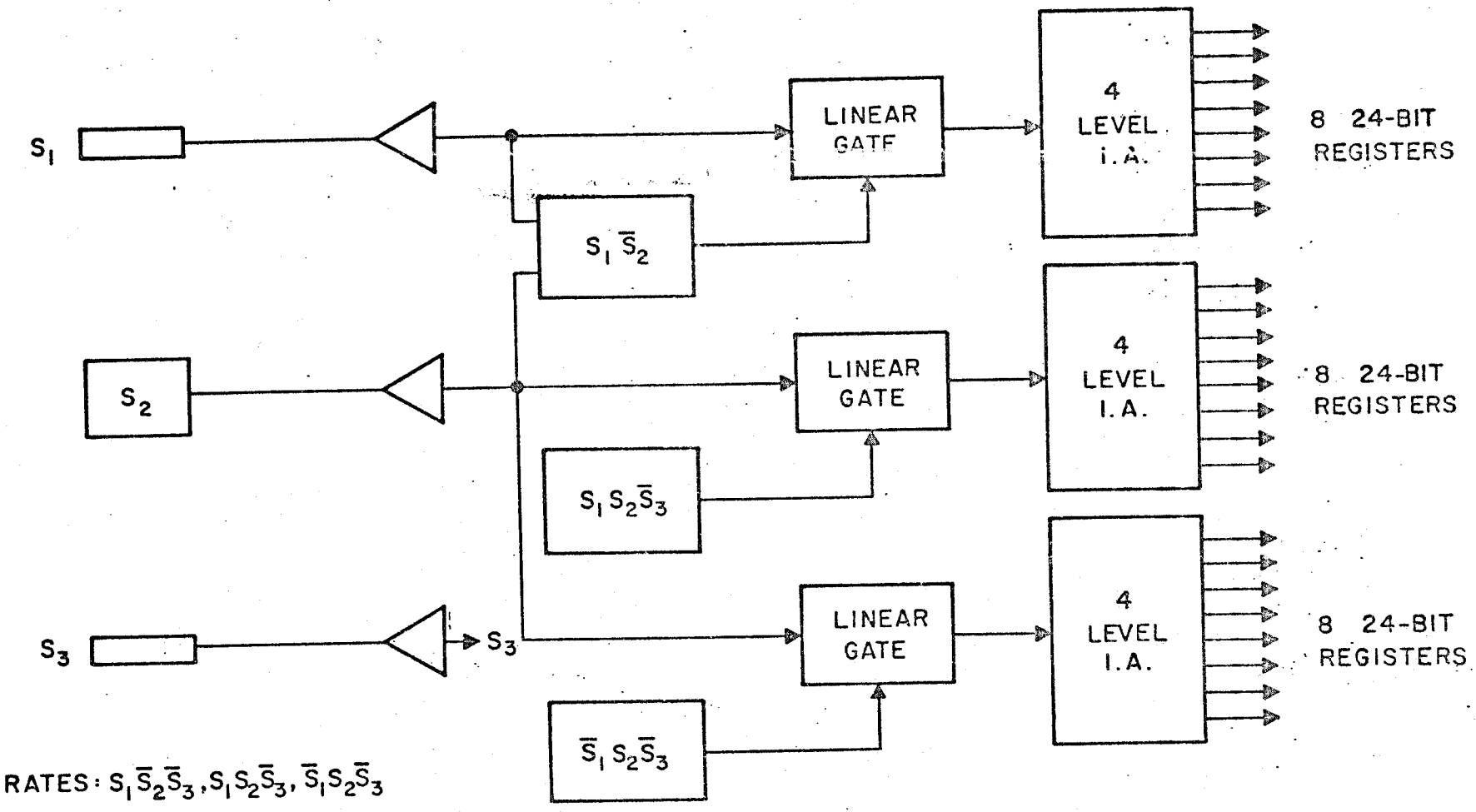

RATES: $S_1\bar{S}_2\bar{S}_3, S_1S_2\bar{S}_3, \bar{S}_1S_2\bar{S}_3$

SECTOR x 8: $S_1\bar{S}_2\bar{S}_3$ LOW ENERGY PROTONS

$\bar{S}_1S_2\bar{S}_3$ ELECTRON SLICE

} 4 ENERGY LEVELS ON EACH ACTIVE TERM

FIG. 5

LOW ENERGY DETECTOR-II

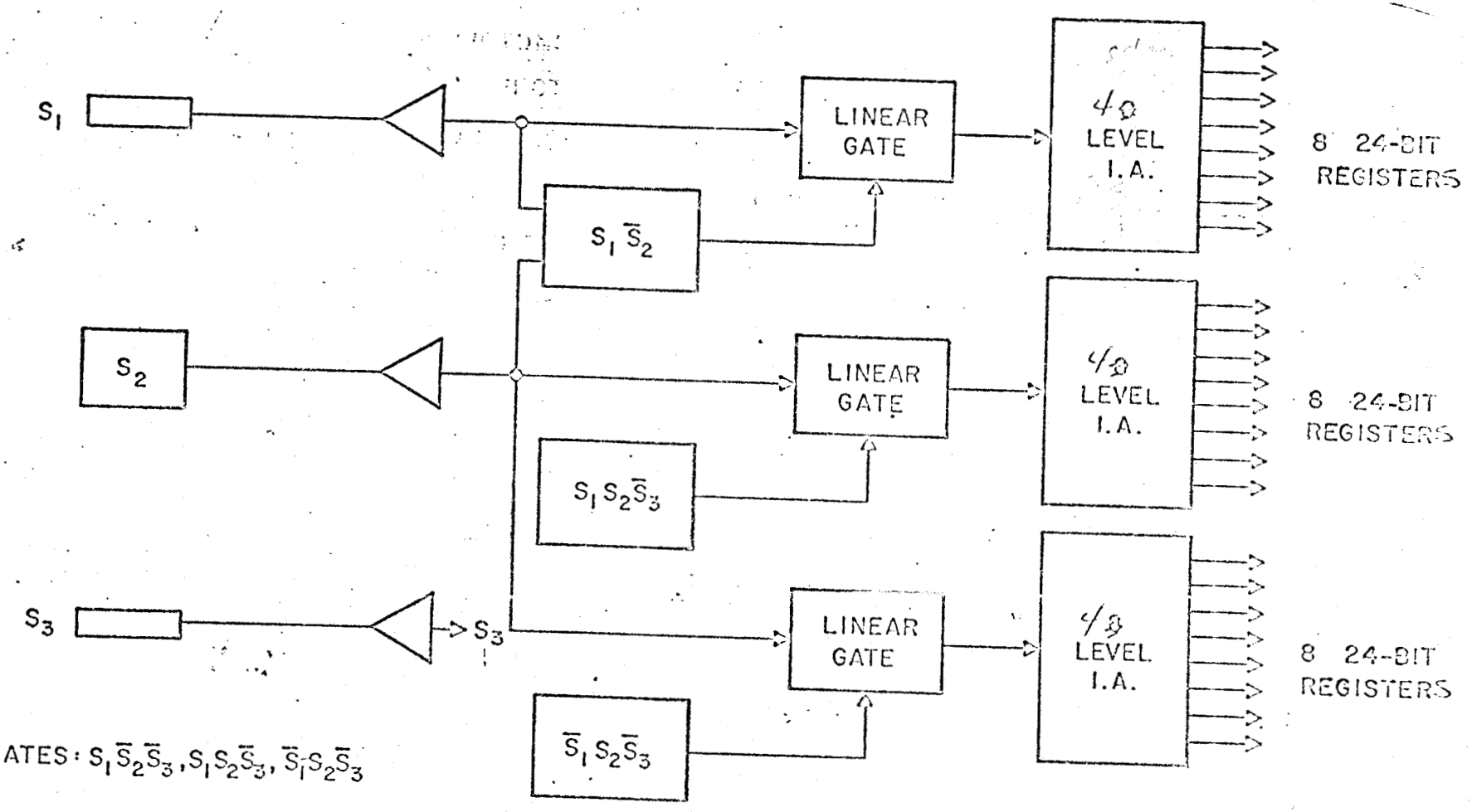

RATES: $S_1\bar{S}_2\bar{S}_3, S_1S_2\bar{S}_3, \bar{S}_1S_2\bar{S}_3$

SECTOR x 8: $S_1\bar{S}_2\bar{S}_3$ LOW ENERGY PROTONS

~~$S_1S_2\bar{S}_3$ HIGHER ENERGY PROTONS~~

$\bar{S}_1S_2\bar{S}_3$ ELECTRON SLICE

~~Figure 1.2-1~~

4 energy levels on each active team.

Fig 5

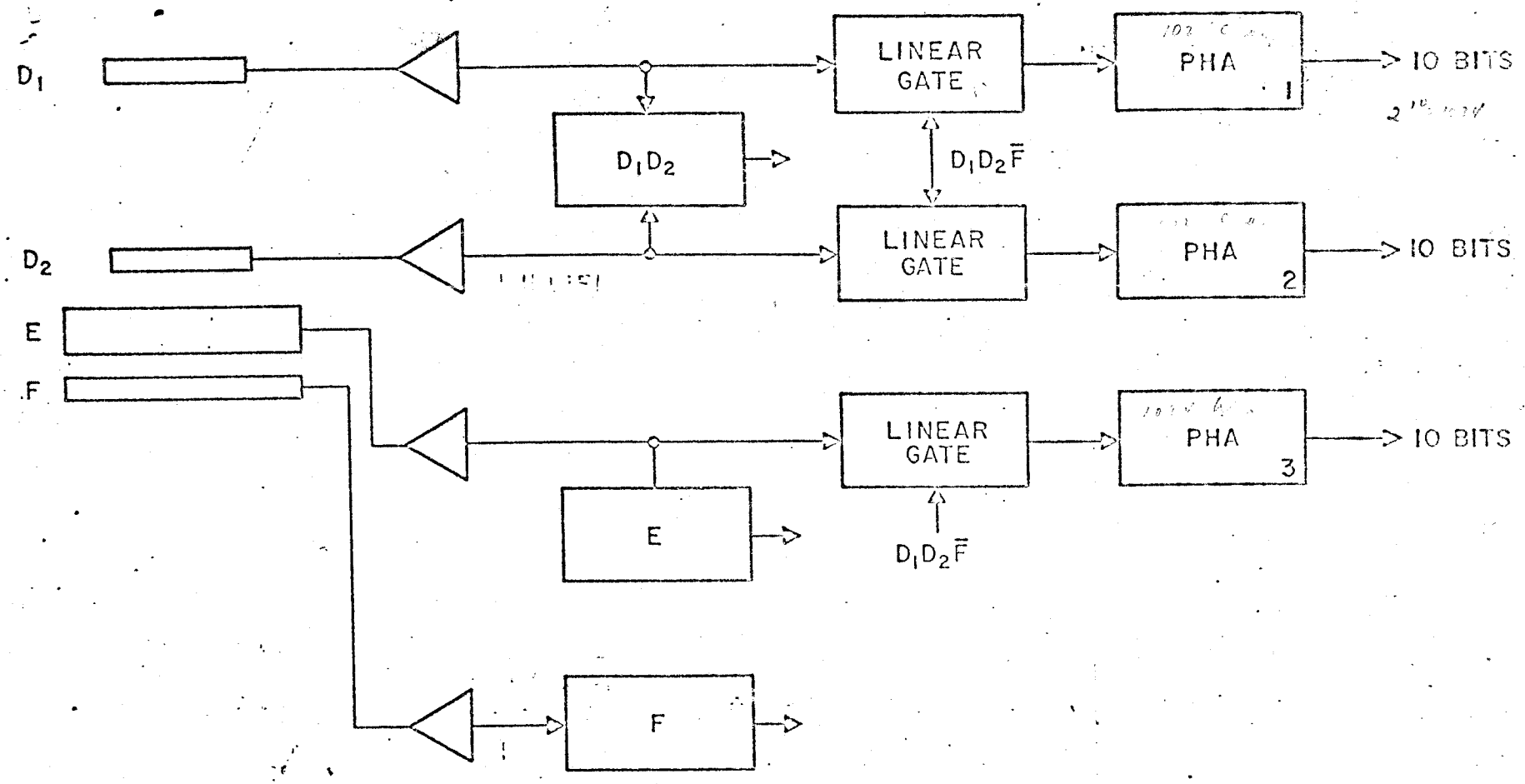

RATES

$D_1D_2(D_1+D_2)E\bar{F}$ ~~$D_1D_2\bar{E}\bar{F}$ (2 LEVELS)~~ (2 levels on E)

$D_1D_2E\bar{F}$ (2 levels on E)

D_1 (8 LEVELS)

$\bar{D}_1\bar{D}_2E\bar{F}$

- 2 BITS REQUIRED TO IDENTIFY PRIORITY MODE.
- 1 BIT REQUIRED TO IDENTIFY PHA DATA AS LET-I.
- 3 BITS REQUIRED TO IDENTIFY SECTOR.

~~FIG. III—2~~

SIMPLIFIED LET-I DETECTOR

Fig 4

A COSMIC RAY DETECTOR SYSTEM FOR THE ANALYSIS OF ENERGY SPECTRA, CHARGE COMPOSITION AND GENERAL FLOW PATTERNS OF SOLAR, GALACTIC AND JOVIAN ENERGETIC PARTICLES DURING THE PIONEER EARTH/JUPITER MISSION

KENNETH G. McCRACKEN
WILLIAM R. WEBBER
FRANK B. McDONALD
EDMOND C. ROELOF
BONNARD J. TEEGARDEN
JAMES H. TRAINOR

REVISED JUNE 1969

A Cosmic Ray Detector System

for the

Analysis of Energy Spectra, Charge Composition and General Flow Patterns

of

Solar, Galactic and Jovian Energetic Particles

during the

Pioneer Earth/Jupiter Mission

by

Kenneth G. McCracken
University of Adelaide

William R. Webber
University of New Hampshire

and

Frank B. McDonald
Edmond C. Roelof
Bonnard J. Teegarden
James H. Trainor
NASA/Goddard Space Flight Center

Revised June 1969

INDEX

I. INTRODUCTION

The proposed Pioneer F and G mission offers a unique opportunity to study the extended regions of the interplanetary medium. Furthermore the possibility of approaching interstellar electromagnetic conditions must be contemplated and regarded with great interest. These points, coupled with the opportunity to study the Jovian environment, call for a carefully coordinated set of studies in each scientific discipline. In the field of energetic particles we have tried to design an instrument that will provide the maximum possible diagnostic power to examine the complex field-particle interactions occurring in the interplanetary environment as well as the Jovian magnetosphere.

To accomplish this we propose a coordinated set of two solid state detector telescopes to study charged particles. The telescopes are designated as:

a. the high energy telescope (H.E.T.),

b. two low energy dE/dx vs. E telescopes (L.E.T. I and L.E.T. II).

Charged particle spectra and angular distributions will be measured over an extended energy interval. These intervals are briefly listed below, and are shown graphically in Figure I-1.

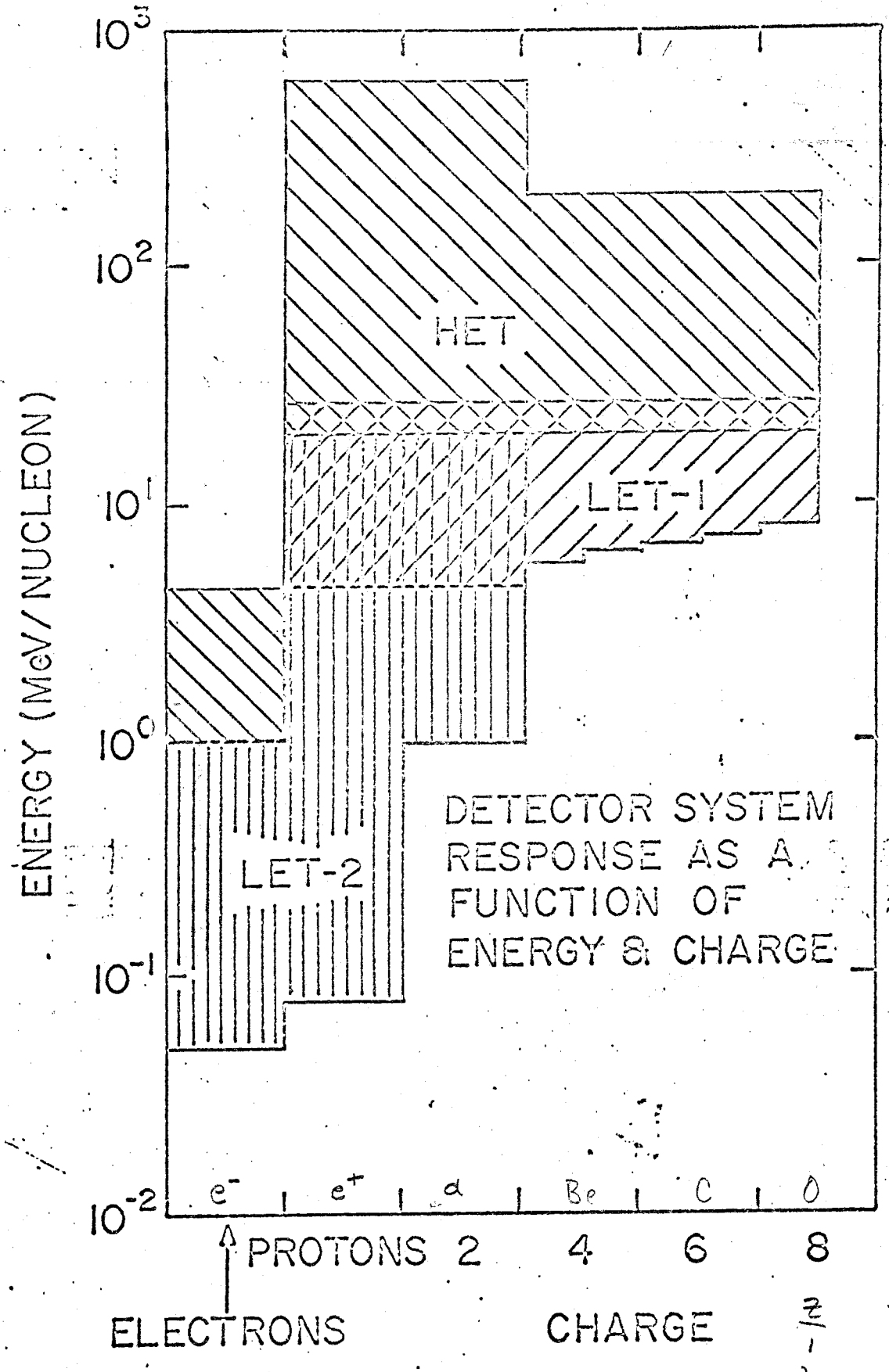
ENERGY (MeV/NUCLEON)
10^3
10^2
10^1
10^0
10^{-1}
10^{-2}
HET
LET-1
LET-2
DETECTOR SYSTEM
RESPONSE AS A
FUNCTION OF
ENERGY & CHARGE
e⁻
e⁺
d
Be
C
O
PROTONS 2 4 6 8
ELECTRONS
CHARGE
Z
1
2
3
4
5
6
7
8
element
H
He
Li
Be
B
C
N
O

FIG. I-1

Particle Component	Energy Range
Galactic cosmic ray protons	4.5 - 800 MeV
Solar protons	.05 - 800 MeV
Galactic cosmic ray Helium	4.5 - 600 MeV/nucleon
Solar Helium	1.0 - 600 MeV/nucleon
He^3/He^4, D/H	4.5 - 50 MeV/nucleon
Galactic and Solar Electrons	.050 - 5.0 MeV
Li, Be, B, C, N, O, F, Ne and their isotopic composition	6 MeV/nuc - 200 MeV/nucleon

Energy Ranges for Angular Distribution Studies

Hydrogen	.05 - 120 MeV
Helium	4.5 - 120 MeV/nucleon
Electrons	.05 - 5 MeV

The above measurements extend the work of the principal investigators on previous Pioneer vehicles as well as numerous studies on IMPs and OGOs. It is anticipated that each investigator will bring to bear his full experience on previous spacecraft in his area of competence. The collaborative effort already undertaken to design these telescope systems and prepare this proposal will be extended to the preparation and testing of the instruments and the analysis of of the data. The operational modes of each of the telescopes are as follows:

High Energy Telescope: The HET consists of a multi-element array of solid state detectors. For particles which come to rest within this stack (20 - 50 MeV/nucleon) three measurements are made - energy loss (dE/dx), total energy, and range. The simultaneous measurement of total energy and range provides a very powerful method for rejecting detector background, which is a particularly significant problem in this energy regime. The telescope is also designed to measure the energy and charge of particles which penetrate completely through the stack of solid state devices. In this mode three separate dE/dx measurements are made. Charge resolution for penetrating particles will be possible up to approximately 200 MeV/nucleon.

Low Energy Telescope I: The LET I is a double dE/dx vs. E. solid state detector. Two thin (100 micron) surface barrier detectors serve to define the geometry and to provide a double dE/dx measurement. A thick (2.5 mm) lithium drift detector provides a total energy measurement. LET I will cover the energy range from 3 to 22 MeV/nucleon. In this interval charge resolution will be possible from Z = 1 to 8. In addition angular distributions for different charge species and energies will be obtained.

Low Energy Telescope II: Two solid state detectors, one thin and one thick, are used individually and in coincidence as total absorption spectrometers. A third detector operating in an anticoincidence mode ensures that only stopping particles are analyzed. The thin detector

will respond to protons between 50 KeV and 3 MeV and electrons between 50 and 150 KeV. The thick detector will be sensitive to protons between 3 and 20 MeV and electrons between 150 KeV and 1 MeV, and in these latter energy intervals an unambiguous separation of protons and electrons will be possible. This telescope is intended to be primarily a monitor of solar particle fluxes.

We have developed these telescope systems specifically for a mission such as Pioneer F and G where a reliable operation over a period of several years is required. In particular the high energy telescope is self-calibrating. We refer the reader to section III for a more detailed description of the instrument.

II. SCIENTIFIC OBJECTIVES

This instrument is designed to exploit to the fullest practical degree the proposed orbit of Pioneer F and G. The significance of these measurements will be greatly enhanced by concurrent measurements with similar particle telescopes scheduled for flights on satellites of the IMP or similar series in near-earth orbits.

The principal scientific objectives of this experiment are:

1. To measure the flow patterns of energetic solar and galactic particles separately in the interplanetary field. To interpret this measurement, simultaneous determination of the energy spectrum, radial gradient, angular distribution, and streaming parameters is required for each nuclear species and over as wide an energy range as is practicable.

2. To measure the energy spectra, and isotopic composition of galactic and solar cosmic rays from the lowest practical energies up to ~800 MeV/nucleon and (by use of objective 1) to unfold the primary flare and interstellar spectrum.

3. To measure the time variations of the differential energy spectra of electrons, hydrogen and helium nuclei over the corresponding energy intervals. During flare events, to obtain time histories; during quiet times, to relate gross time variations to those near earth thus deducing a spatial gradient for galactic cosmic rays.

4. To study the energy spectra, time variations and spatial gradients associated with recurrent and non-flare associated interplanetary proton and helium streams and to define the related solar

or interplanetary acceleration processes.

5. To provide information on the energetic particle distribution surrounding Jupiter.

6. To try and determine the extend of the solar cavity, the energetic particle phenomena occurring at this interface and the cosmic ray density in nearby interstellar space.

We shall now consider these scientific objectives in more detail and examine how they will be achieved by the proposed experiment system.

OBJECTIVE 1:

To measure the flow patterns of energetic solar and galactic particles separately in the interplanetary field.

The telescopes are designed with appropriate directional response to define the quiet time flow pattern of galactic (and probably solar) cosmic rays both in and out of the ecliptic plane.

Quiet-time: At high energies, the galactic particle streaming is expected to be negligible. At medium energies, the detailed angular resolution obtainable by sectoring the high energy telescope will allow comparison of particle flow patterns with the general field structure which collimates them. The directional properties of the low energy telescope will be helpful in sorting out a possible outward streaming quiet-time solar component at very low energies. The

quiet-time flow patterns which the experiment will measure may be more complicated than currently thought (particularly at larger distances from the sun), possibly involving flow out of the ecliptic plane (unmeasured to date) and hence directional measurements pointing off of the ecliptic plane are essential. The net result will be an estimate of the cross circulatory pattern of cosmic rays in the solar system.

The radial gradient measurements will be made by monitoring the differential energy spectra of particle species throughout the flight and carefully correlating them with comparable data simultaneously recorded by similar instruments near Earth. With a firmly established temporal "base-line" which removes solar cycle and flare event effects, a true spatial gradient may be derived. However, a direct estimate of the gradients of the separate species is available from the measurements of the streaming current and the energy spectrum made by the medium and high energy telescopes. Recent theories (Axford and Gleeson, 1967; Gleeson, 1969; Roelof, 1969) show that the gradient is linearly related to the particle streaming current through the diffusion coefficient of the scattering magnetic irregularities and to the solar wind velocity through the energy spectrum (the Compton-Getting effect). Since the spectrum will be measured in detail and the current flow may be derived from the velocity anisotropy measurements of the HET, the gradient may be estimated if the statistical parameters of the magnetic field are available. Thus an independent

estimate of the gradient is available from spectrum, flow and field measurements, as a result of the velocity anisotropy sensitivities of the particle telescopes. The above considerations are particularly important for the separation of the solar and galactic particle population at low energies where a continuous low level flux of solar particles may greatly modify the features of the galactic particle gradient and spectrum.

Flare events: A fundamental problem relating to solar cosmic rays - that of deducing the flare particle spectrum and composition - requires isolation of the effects of interplanetary propagation. Early in flare events, the low and medium energy velocity anisotropies are extremely well correlated with the local direction of the magnetic field at 1 AU. As the orbit nears 5 AU the magnetic field structure may not be as well defined as near earth and flare particle velocity anisotropies could well be the best means of tracing out the connection of field lines back to the sun.

Measurements over a wide range of energies covered by the high, and low energy telescopes will provide tests of models of interplanetary propagation unavailable with only near-earth observations. Time histories recorded by similar detectors near earth and enroute to Jupiter will define the azimuthal spread of flare particles (or the radial variation when the spacecraft are on proximate field lines).

OBJECTIVES 2 & 3:

To measure the hydrogen and helium energy spectra and isotopic composition for galactic and solar cosmic rays in the charge range from the lowest practical energies up to ~800 MeV/nucleon.

To measure the time variations of the differential spectra of electrons and hydrogen and helium over the corresponding energy intervals.

Since the particle telescopes will cover two to three decades in energy for hydrogen and helium nuclei (and also electrons), demodulation of solar induced changes will yield extensive interstellar spectra for these particles. Of course, if the modulation region terminates within the Jovian orbit (as do, for instance, some comet-tail interactions), then the high charge and spectral resolution of the detector system is capable of directly obtaining detailed interstellar spectra.

Modulation theories can be critically examined by comparing the spatial dependence and time variations of spectra of particles with different charge to mass ratios such as protons/electrons, protons/alphas, and the He^3/He^4 with solar wind velocity and magnetic field measurements.

However, current ideas on modulation which describe it in terms of a statistical interaction with a spectrum of magnetic irregularities may be incomplete by not including the effects on energy loss as has been suggested by recent theoretical and experimental work (Webber, 1968; Roelof, 1969). If this is so, the measurement of the energy spectrum over a large range of energies but particularly at low

energies, (including electrons) will be invaluable in separating energy loss processes from simple diffusion processes. This "local" energy loss may mask the ionization energy loss occurring in interstellar space. In the latter, ionization losses (which vary as Z^2) predominate at low energies, while in the former interactions are with the interplanetary electromagnetic field (which current theory predicts vary only as Z). Thus the variation with distance from the sun of the lower end of the energy spectra of different elements may be the only definite test of the magnitude of the local modulation. The question is, of course, a very important one, since the interstellar spectra contain the interstellar propagation history and source spectra of galactic cosmic rays. The derived interstellar charge and isotopic composition and energy spectra will be a stringent test of theories of cosmic ray origin.

OBJECTIVE 4:

To study the energy spectra, time variations and spatial gradients associated with recurrent and non-flare associated interplanetary proton and helium streams, and to define the related solar or interplanetary accleration processes.

The low energy telescope will be particularly useful in monitoring and examining the anisotropies associated with the wide variety of non-flare associated low energy proton, helium and electron events at positions away from earth: These include energetic storm particle events (Bryant et al, 1962; Rao et al, 1967), recurrent and long lived particle streams (Bryant et al, 1965), and active center associated

events (Fan et al, 1968; Anderson, 1969). These provide evidence for continuous acceleration processes on the sun or in interplanetary space which may be similar to small-scale flare acceleration or could be an entirely different process. Only with spacecraft both near earth and in interplanetary space can spatial and temporal variations be separated so that the evoluton of these events can be followed throghout their lifetimes (which may be several solar revolutions).

OBJECTIVE 5:

To provide information on the energetic particle distribution surrounding Jupiter.

The proposed trajectories for Pioneers F and G, the proposed spin axis alignment, and the look angle directions of the detectors are ideal in terms of studying the Jovian radiation belts with this set of detectors. Jupiter offers the unique opportunity in that it has the only other known planetary magnetosphere in our solar system. In a sense it offers the opportunity for a "second point on the curve;" a chance to study the generation, acceleration and loss of particles in a magnetosphere with different boundary conditions from that of the earth. Estimates for the boundary of the Jovian magnetosphere on the Sun side range around 40 Jupiter radii (R_J). It is probably not unreasonable to expect that the Jovian magnetosphere also possesses an extended tail.

We expect that this experiment can provide a variety of rapid proton and electron flux measurements, together with pitch angle distributions and rapid 8 channel spectra in the low and medium energy

regimes deep within the Jovian magnetosphere. Much of this information could not be supplied by a typical trapped radiation detector sized for a 3 R_J pass because of the detector geometrical factor which is several orders of magnitude smaller. The low energy telescope detector system can handle penetrating fluxes approaching 5×10^5 particles/cm^2-sec-ster before pulse pile-up becomes a major correction problem.

OBJECTIVE 6:

To try to determine the extent of the solar cavity, the energetic particle phenomena occurring at this interface and the cosmic ray density in nearby interstellar space.

The termination of the modulation region is a lower bound on the extent of the solar plasma, and a useful one since the extent is presently uncertain within (at least) an order of magnitude. By careful analysis of the energy spectrum flow pattern and gradient throughout the flight, such a termination may be detected if it is < 10 AU from the sun.

CORRELATED MEASUREMENTS:

Correlation with near-earth particle measurements. The spatial/temporal structure of solar and interplanetary events can only be deduced from continuous monitors at a variety of radial and azimuthal locations. Co-rotating particle streams, interplanetary plasma shocks and Forbush decreases are obvious examples in addition to customary flare events. Quiet-time fluxes measured on the outward journey cannot be interpreted in terms of a galactic gradient unless a sound "base-line" for the solar cycle-dependent time variation of fluxes can be derived

from comparable detectors in near-earth orbits. Fortunately such detectors are scheduled for a concurrent period on IMP H, J and K.

Correlation with on-board magnetometer and plasma measurements. The strong collimation of solar particle flow along magnetic field lines during all but the late phases of solar flare events is well established near 1 AU. However, at 5 AU the field may be quite tangled due to the "winding'up" of the Archimedean spiral field; it would make an average angle of $\sim 80^{\circ}$ with the solar radius vector. If the field at this distance is more disordered than at earth, the reverse situation to that at the earth may hold; angular flare particle distributions may aid interpretation of complicated magnetic field measurements. The need for associated magnetic field measurements in interplanetary shocks and Forbush decreases is self-evident. Recent theoretical work (Gleeson, 1969; Roelof, 1969) has shown that the average magnetic field direction governs the flow of quiet-time particles, so simultaneous particle-field observations are required.

III. DETECTOR SYSTEM

A set of 3 solid state detector telescopes is proposed to accomplish the scientific objectives listed above. We shall now discuss these telescopes in some detail and how the measurements are coordinated to provide a comprehensive and redundant set of cosmic ray measurements. The redundance of the separate sets of measurements as well as the self-calibration are important features of the system we are proposing. It is a total necessity in view of the prolonged nature of the Pioneer F and G missions and the controversy that currently exists over the interpretation of gradient and anisotropy measurements made in the 0.7 - 1.5 AU interval.

High Energy Telescope:

The high energy telescope is a three element array (figure III-1). Two of these elements are single lithium drift detectors, 300 mm^2 area and 2.5 mm thick. The third element is a stacked arrangement of five 850 mm^2, 2.5 mm thick lithium drift detectors. This telescope has two basic modes of operation - penetrating and stopping particle modes. For penetrating particles differential energy spectra are obtained for helium and hydrogen from 50 - 800 MeV/nucleon. The stopping particle mode covers the range from 22 - 50 MeV. We will consider each of these modes separately.

High Energy Mode:

The primary mode of operation is triggered by a particle traversing

A, B and the complete C element as identified by ABC_3 coincidence. The quiet time distribution of galactic cosmic rays is such that a well defined minimum ionizing peak is obtained from A, B and C. The position of this peak in both the proton and alpha particle region provides a self-calibration feature which allows for the detection and correction either in the detector or associated electronics.

This detector can measure the quiet time flux of galactic cosmic ray protons inthe region 20 - 800 MeV. The ability to perform such a measurement has been amply demonstrated by the analysis of the August 1961 quiet time data from Explorer XII. Since the relative calibration throughout the flight can be determined within 4%, it is felt that the flux changes greater than 3% can be detected in the 20 - 400 MeV region. In the interval 400 - 800 MeV long term flux changes greater than 5% can be measured. The detector system proposed here has a factor of ~1.8 improvement in resolution over that of the Explorer XII telescope. This should lead to a well defined alpha peak (which we now find alpha detect in our OGO V $(dE/dx)^3$ telescope). This will provide information on the relative flux of alpha particles inthe region 20 - 800 MeV/nucleon.

In the energy range 20 - 120 MeV/nucleon it is possible to identify the direction the particle traverses the telescope. This makes it possible to measure angular distributions over this interval. An accurate intergral flux of both hydrogen and helium above 800 MeV/nucleon is also determined. Differential spectra will be measured between 120 and ~800 MeV/ nucleon.

The look angles for this telescope are defined by figure IV-4. There are two primary constraints set by this position of the experiment which are also discussed in the environment section:

a. There must be a bi-directional look angle. The experiment can tolerate ~.050 g/cm^2 of additional material in the forward direction, and .25 gm/cm^2 in the back direction.

b. The maximum temperature must be less than 40°C. Consideration will be given to providing micrometeorite shielding after consultation with the project.

Stopping Particle Mode:

Stopping particles are identified by the coincidence requirement $AB\overline{C_3}$. This covers H and He from 20 - 50 MeV/nucleon and electrons from 1 - 5 MeV. The A and B detectors define the particle acceptance cone while the stacked array, C, measures both the residual energy and the range.

All elements in the telescope are pulse height analyzed. There are four measurements for each event, 2 dE/dx, residual energy and range, while there are 3 dE/dx measurements for penetrating particles. This provides the ability to use selection techniques to improve resolution and provide discrimination against unwanted spurious events. We believe that this improvement in resolution may be sufficient to allow us to resolve the isotopes of H and He. We, further, believe that this combination of dE/dx, E and range totally eliminates the need for a "guard" counter. On IMP-IV we have flown a three element E vs. dE/dx where the anti-coincidence requirement is relaxed on alternate readouts. With the anticoincidence relaxed adequate resolution is obtained in the

H and He range from 4.5 - 22 MeV/nucleon. With the addition of a well defined aperture, and the particle range we feel confident that the added complexity of a "guard" counter would not offer any improvement in detector resolution.

We have supplemented the pulse height data with a number of different rates. The rate data has two important uses. They should provide a method for determining energy spectra of solar cosmic rays on a very short time scale. They will also provide a means of measuring the anisotropy of these particles on a short time scale by sectoring some of the rates.

The telescope is essentially self-calibrating. For example, the measurement of residual energy and range allows us to accurately determine end-points for various particle species in each element of the range array. The A element can be calibrated in-flight for stopping particles in the usual way.

2. Low Energy Telescopes: (LET I)

The low energy telscope (LET I) is a three element dE/dx vs. E detector sensitive to protons and higher Z particles in the range 3 to 22 MeV/nucleon. The telescope is designed to measure both energy spectra and angular distributions over this energy interval. This represents a modification of the previous LET design to take into account the effects of an isotope power supply.

The detector configuration is shown in figure III-2. Detectors D_1 and D_2 are identical silicon surface barrier devices each 100 microns

thick. They serve the dual purposes of defining the geometry of the detector telescope and also providing a redundant double dE/dx measurement. Detector E is a lithium drifted silicon device 2.5 mm in thickness. It serves as a total energy measuring element. The F detector, a 1 mm thick lithium drifted silicon device, simply acts as an anticoincidence. Events of the type $D_1D_2\overline{E}$ and $D_1D_2E\overline{F}$ will be analyzed. The $D_1D_2\overline{E}F$ events correspond to protons between 3 and 5 MeV whereas the $D_1D_2E\overline{F}$ events include the 5 to 22 MeV range for protons.

An important innovation in this telescope (as in the HET) is the absence of a guard counter. With our well-defined geometry and redundant dE/dx measurements the background intensity should be minimized. In addition the low mass and small geometry for particles entering the E element from the side will further reduce background levels relative to larger, more massive detectors flown in the past. This technique allows us to do away with the weight and power consuming photomultiplier-scintillator systems used in the past.

This low energy telescope will cover the charge range Z = 1 to 8 (excluding electrons). This will require circuitry having a single linear region with a dynamic range of 1000.

State of the art technology will be used with all solid state devices. This laboratory has had a great deal of experience with such detectors used in spaceflight applications. Overall system noise levels (detector + electronics) should be in the neighborhood of 30 KeV for each

detector. The minimum energy losses of interest will be ~400 KeV. This then gives us a worst case resolution better than 10% FWHM. Precautions will be taken to minimize the effects of radiation damage. In all cases fully depleted devices having electric field strengths in excess of 150 V/mm will be used.

We intend to sector several rates from the LET I. Division of the data into 8 equal sectors will be commensurate with our viewing cone half angle of 25°. To obtain an angular scan we require mounting such that the LET look direction is perpendicular to the spin axis of the spacecraft.

A priority system will be incorporated into the electronics to give preferential coverage to the rarer events e.g., alpha particles, heavies. During large solar events the detectors will almost certainly be readout limited. The priority system will select these rare particles for analysis thus artifically enhancing the fraction of alpha particles and heavies in our data. Of course, rate counters will allow us to determine the true ratios of these particles in interplanetary space.

This detector, like the HET, will be self-calibrating. In addition the detectors will be designed such that an overlap in the individual energy responses of the detectors will exist. This will allow cross calibrations between detectors.

3. Low Energy Telescope: (LET II)

This low energy detector system is designed to study very low energy protons and electrons in interplanetary space. Studies in interplanetary

space will be primarily limited to particles of solar origin. Energy spectra and angular distributions are measured. A schematic of the detector is shown in figure III-3.

There are three elements:

S_1	100μ	-	50 mm^2 Silicon Surface Barrier
S_2	2 mm	-	50 mm^2 Lithium-drifted Silicon
S_3	1 mm	-	200 mm^2 Lithium-drifted Silicon

The S_1 thickness was chosen to minimize the electron response without making an unreasonable sacrifice in the detector performance. A total resolution of 15 - 20 KeV will be easily attainable. We have determined in the laboratory that specially constructed detectors of this type are insensitive to sunlight. Using this technique, we can have detectors exposed to sunlight with proton thresholds of 75 KeV. Mechanical collimation is used to limit the detector's field of view to $\pm$ 15° and thus provide a reasonably fine grained measurement of angular distributions.

The top detector S_1 will stop electrons in the range 50 - 150 KeV and protons in the range 50 KeV - 3 MeV. The S_2 detector will respond to electrons in the energy interval 150 KeV - 1 MeV and the proton interval is 3 MeV - 20 MeV. Stopping alphas in the S_1 detector will have a unique response from 1 MeV - 3 MeV/nucleon for solar alpha events.

The proton and electron responses for the very low energy system are summarized in figure III-4. Note that the electron response curves are idealizations and do not include the effects of electron scattering which are significant at these energies. We have calibrated similar detectors in 50 KeV and 2 MeV electron beams.

There are three basic operating modes for this system that are specified by the following logic:

$S_1\bar{S}_2\bar{S}_3$: 50 KeV $< E_e <$ 150 KeV / 8 levels; 50 KeV $< E_p <$ 3 MeV

$\bar{S}_1S_2\bar{S}_3$: 150 KeV $< E_e <$ 1 MeV/ 8 levels

$S_1S_2\bar{S}_3$: 3 MeV $< E_p <$ 20 MeV/ 8 levels

where E_e = electron energy and E_p = proton energy.

The advantages of this system are twofold:

1. The double valued response of the usual one-dimensional detector is eliminated by removing all penetrating particles.

2. Electrons and protons are unambiguously separated over a significant energy range.

Each of the three logic modes is connected to an 8 level integral analyzer. This should provide ample energy resolution for spectral measurements.

It is proposed that two levels for each logic mode be sectored. This might be as follows:

$S_1\bar{S}_2\bar{S}_3$: 50 KeV $< E_p <$ 3 MeV; 500 KeV $< E_p <$ 3 MeV

$\bar{S}_1S_2\bar{S}_3$: 150 KeV $< E_e <$ 1 MeV; 500 KeV $< E_e <$ 1 MeV

$S_1S_2\bar{S}_3$: 3 MeV $< E_p <$ 20 MeV; 10 MeV $< E_p <$ 20 MeV

We have allocated the weight and power for the sector accumulators in the weight and power budgets.

A detector of the S_1 type has been integrated into the IMP-G spacecraft by the Goddard Space Flight Center group. A system of the

type $S_1\bar{S}_3$ has already been developed with all logic elements designed for IMP-"eye". This includes both 8 level analyzers and sectoring. We are merely adding S_2 to an already developed detector.

The proposed mounting schemes are shown in Figure IV-4. The viewing angles are obtained should allow the determination of complete pitch angle distributions from 1 - 5 AU.

IV. INSTRUMENTATION

A. Introduction:

The instrumentation described here uses existing, proven, low power circuitry with some available improvements in semiconductors and, in general, more efficient and lighter packaging. Our flight experience with similar equipment in the past several years is consistent with the required lifetimes for these missions. We will approach the description of the instrumentation by describing the operation of each of the telescopes first, followed by a description of the individual circuits, the data system, parts, the mechanical system, thermal requirements, environmental problems, the spacecraft interfaces, quality assurance provisions, and the weight and power analyses.

B. Low Energy Telescope II:

Figure IV-1 is a simplified block diagram of the detection system and shows the logical conditions. The charge signal from each detector is integrated and converted to a voltage pulse, then shaped and amplified; discriminators fire if their thresholds are exceeded, providing the inputs to the various logic circuits; and if the conditions are met, the proper linear gate is opened, and the signal is analyzed into one of 8 channels by the integral analyzer.

A 24 bit register accumulates the data for each channel of each analyzer. Additionally, two more registers are used to monitor the rates $S_1 \bar{S}_2 \bar{S}_3$, $S_1 S_2 \bar{S}_3$ and $\bar{S}_1 S_2 \bar{S}_3$, and 8 more are shared in accumulating sectored (x8) information for $S_1 \bar{S}_2 \bar{S}_3$, $S_1 S_2 \bar{S}_3$ and $\bar{S}_1 S_2 \bar{S}_3$.

LET-I: (Figure IV-2)

As with the LET-II, charge pulses from each of the solid state detectors are converted into voltage pulses by low noise charge sensitive preamplifiers. The outputs of threshold circuits for the D_1, D_2 and F elements are fed into logic circuitry which produces a pulse when the $D_1 D_2 \overline{F}$ condition is met. This pulse is in turn used to open the D_1, D_2 and E linear gates. Each of the analog D_1, D_2 and E pulses are then fed into three 1000 channel pulse height analyzers. Ten bits will be required for each PHA and two bits for priority level identification, plus an additional bit to identify this group as data from LET-I. This is necessary since we share the differential pulse height analyzers between LET-I and the HET. One 8-level integral analyzer is shared between D_1 and $\overline{D}_1$ $\overline{D}_2$ E $\overline{F}$. Sixteen accumulators are shared between the various rates and sectored rates.

C. High Energy Telescope:

Figure IV-3 is a simplified block diagram of this system, and the logic is shown. Again each detector has its own charge sensitive preamplifier, shaping amplifier and threshold discriminators. Detectors A, B, and C_1 - C_3 each have two threshold discriminators selecting protons, and He and above, respectively.

To discuss the logical arrangement, consider a particle entering through A, B. Pulse height analyzers 1 and 3 analyze the A and $\sum_{1}^{2} C_N$ pulses respectively, while PHA 2 analyzes B or C_3, depending on whether one has a penetrating event (C_3) or not. In addition to the three 10 bit addresses associated with an HET event, we require 2 bits

to identify the priority mode; 1 bit to identify the data as HET; 1 bit to determine if the PHA 2 address is B or C_3; 1 bit to determine if C_2 was penetrated (range); and 3 bits to identify the spin sector in which the event occurred. The time-shared priority modes listed on Figure IV-3 refer to stopping particles ($AB\overline{C_3}$), stopping heavies ($AB\overline{C_3}$, thresholds for He and above), penetrating heavies ABC_3 (A and C_3 > 2x minimum), and all penetrating particles (ABC_3). The many rates listed will be internally commutated into registers.

Note that while PHA 1, 2 and 3 are shown both on Figure IV-2 and Figure IV-3, there are in fact only three differential pulse height analyzers within the experiment and they are block shared between the HET and LET-I.

D. Electronics:

1. Charge Sensitive Preamplifiers: The charge signals from each solid state detector are integrated and converted to voltage pulses in these amplifiers which are similar to the units used successfully on IMP's F and G and OGO-F. While the existing noise performance easily exceeds the requirements of any of the detectors, modifications have been made in some units to accommodate the very wide range over which linear response is required.

2. Shaping Amplifiers and Linear Mixers: The voltage signals from the preamplifiers are shaped by actively differentiating, integrating and differentiating at equal time constants while being amplified as necessary. The time constants will probably be chosen to be ~ 0.8 μsecs, allowing for the charge collection time for some of the thicker detectors

while still giving adequate signal-to-noise and high count rate capability. The High Energy Datector also requires a linear mixer to sum C_1 and C_2 linearly for pulse height analysis.

3. Discriminators and Logic Circuitry: Very stable, tunnel diode discriminators are used as threshold devices to set up the required logic conditions amongst the various detectors. We have used these circuits extensively in the IMP and OGO series. The coincidence/ anticoincidence logic which follows is quite conventional.

4. Pulse Height Analyzers: Fast integral pulse height analyzers are required for LET-I and LET-II. The 3 differential pulse height analyzers required are our standard units using a 2MHZ ADC. Conversion will be to 10 bits. The pulse height analyzer consists of a linear gate, buffer amplifier, delay circuitry and the A to D converter.

5. Data System: This experiment uses an extensive digital data system to acquire the mass of spectral and flux information required. Nonetheless, the system is low weight and low power. The basic building-block used throughout the system is an 8-bit counter with companion 8-bit shift register, transfer gates and control logic. One of these is used to accept each ADC output directly and together with the gain change bit, makes up a 9-bit pulse height word. Three of the basic blocks are connected together to form a 24-bit counter for the rate channels, and the interconnect of the shift register allows for logarithmic compression to 10 or 12 bits. The inclusion of a shift register for each counter register allows us to take data based on timing or sectoring information and store it in the shift register to

await telemetry. The same MOS technology proposed here has been proven by > 300 million device hours in space on IMP's D, E, F and G with only 2 possible device failures. Analysis has shown that it is improbably that the failure was in the MOS device in these cases. They are extremely reliable devices. The circuit layout and interconnect are exactly those which have been used on IMP-I. A larger chip containing the circuits of three present chips is currently undergoing qualification testing for use on IMP H and J and the Planetary Explorers. If the qualification continues successfully, we would plan to use the larger devices to simplify the interconnect and give us more weight margin.

6. Power Supplies: The experiment will require approximately six low voltages to supply the electronics systems and five higher voltage biases for the solid state detectors. These will range from ~ 25 volts to ~ 600 volts with a capability of up to 5 μ amp per detector.

7. Sectoring System: Since Pioneers F & G will supply sectoring pulses, we will use the see-Sun/Star pulse and the x8 pulses to generate electronically 8 equal sectors in the rotation of the spacecraft, organized around the detectors see-Sun/Star.

8. Solid State Detectors: All devices included in this proposal are commercially available devices which are procured to our rigid specifications. They are then tested and analyzed in our special laboratories. Our experience with these devices over the past 4 years in OGO and IMP experiments has been excellent. Other experimenters have had greater than 5 years successful flight history on a large group of these devices (Williams et al., 1963 38C). The extensive testing of these devices in severe radiation environments by a group at the Goddard

Space Flight Center (Love, Trainor and Williams) and the National Bureau of Standards (Coleman), has resulted in much new knowledge on how to best use these devices (Coleman, Love, Trainor and Williams, 1968a; 1968b). This work is continuing, as is the collaboration with Dr. Joseph Coleman of NBS. When purchased from a reliable company to a stringent specification and when carefully tested and analyzed; we have shown that these devices are excellent and reliable particle detectors for space research.

E. Mechanical Systems:

Our proposed mounting for the experiment detector systems is shown schematically in Figure IV-4. LET-I and II are unidirectional and look out perpendicular to the spin axis as shown. If there were a need to tilt them towards the spin axis in the away-from-earth sense, in order to avoid a possible solar array or boom, this can be done.

On the other hand, the HET is bi-directional in its response, and can tolerate only ~ 0.050 gm/cm^2 of material forward of detector A, and ~ 0.25 gm/cm^2 in the back direction. Actually we intend to use a multiple thin titanium foil approach, as has proven successful on IMP and OGO. As shown in Figure IV-4(B), the detector assembly must be in some sort of bubble or enclosure outside the main body in order to get the clear look angles. Additionally, if we were mounted on face 1 (Figure IV(A)) and a boom was also extended away from this face, then we would have to cant the detectors look cone to the right or left to avoid the obstruction.

The specifics of the mechanical mounting (for the detector assemblies) are quite unclear in our minds at this time, since spacecraft drawings are not available. Conversations with the engineering representatives of the Pioneer project office have led us to assume that our detectors will be mounted to our honeycomb baseplate which extends from the main body of the spacecraft. The entire assembly will be enclosed by a bubble or a box of some sort. We have included the weight of the honeycomb baseplate within our weight analysis.

We estimate the electronics systems will require ~ 300 cu. in. with a large number of form factors available. The actual form taken can be determined in order to efficiently use the available space. In view of the large number of wires carrying low noise signals from the detector assembly, it is clear that it is necessary for the main electronics assembly to be quite close to the detector assembly.

Thermal Requirements

The absolute maximum temperature must be less than 40°C to insure long life for the solid state detectors. The Pioneer F & G compartment specification of -20° to +90°F is acceptable, but we would prefer a -10° to +20°C region if a choice is available. The performance of our detectors and electronics are such that changes due to temperature over these ranges are not observable in the data.

G. Environmental Problems:

In addition to possible problems with micrometeoroids which we have already discussed, the possible problems of radiation damage concerned with the Jovian encounter must be evaluated. Since this is

intimately involved with the trajectory, we can begin by saying that we feel the trajectories outlined for Pioneer F and Pioneer G in P-200 are excellent choices. Additionally, the high energy electron belt predictions by Eggen are probably conservative. However, the proton predictions Eggen which are repeated in P-200 are derived in a much different fashion and are subject to huge uncertainties. In short, we have no confidence that the protons will be limited to a belt as suggested in Section 4.2.2 of P-200 but expect to find them throughout the region where the electrons are shown as well. At this time we know of no one who has been able to predict the details of such a proton belt. Additionally, while Eggen's proton model deals with protons from 100 KeV to 4 MeV, we are much more concerned with the protons from $\sim$ 4 MeV to $\sim$ 100 MeV, for instance.

The two most sensitive devices within this experiment to radiation damage are the detectors themselves and the MOS transistors in the data system. Integration of the electron fluxes shown in Figure 4.2.2 of P-200 leads to an integrated worst case flux greater than $\sim$ 5 MeV of $\lesssim 10^{11}/cm^2$. This can be compared with an acceptable fluence of $\sim 10^{14}/cm^2$ of penetrating electrons before damage effects become noticeable at all for our solid state detectors. Since we have no energetic proton flux predictions, we can only calculate what is required to do damage to our detectors. Detailed radiation damage testing on solid state detectors has been carried out at the Goddard Space Flight Center over the past two years and is continuing in conjunction with the National Bureau of Standards. This work has

led to two recent, comprehensive papers (Coleman, Love, Trainor and Williams, 1968a; 1968b). For protons less than ~ 1 MeV, we can easily tolerate an integrated flux or fluence of 10^{17} protons/cm^2 in the way in which we operate the detectors. For protons with energies greater than 4 or 5 MeV, our detectors could tolerate a fluence of at least 10^{13} protons/cm^2 before any noticeable effects occurred. The Eggen proton model predictions would be several orders of magnitude below these limits for a Pioneer F or G trajectory, but as previously noted, we have no faith in that model. Thus, while it seems that we have a comfortable margin, the fluxes there will be known only when someone sends an instrument there.

The case for the MOS transistors is somewhat more complicated. They are better shielded than the solid state detectors, so that probably only protons with energies greater than ~ 30 MeV or electrons with energies greater than 3 MeV will penetrate. Much of the solid angle will be shielded even from more energetic particles. With this in mind, we estimate that the electron damage effects will dominate, just as in the case of a system orbiting in the Earth's radiation belts. Detailed work done at the Goddard Space Flight Center on the radiation damage effects of penetrating electrons on these MOSFETS has shown that they can tolerate $\gtrsim 10^{12}$ electrons/cm^2 of several MeV before gate threshold effects begin to affect circuit performance. Flight experiments on IMP D, E and especially F have shown that the degradation effects measured in space for a given fluence have been smaller than those measured in the laboratory for the same fluence (Wolfgang,

1968). This may be due to rate of irradiation effects on the ground or possibly annealing. In any event, it again seems that we have a comfortable margin, probably much greater than an order of magnitude.

Of more concern to us at this time is the problem of "maverick" semiconductor devices ragardless of their type. Since we will be going into a radiation regime more severe than we normally have to contend with, the problem may be severe. By the word "maverick" we refer to those semiconductor components who individually are orders of magnitude more sensitive to the radiation damage effects of a given fluence than the mormal device of that type. The data available to use (New Moons Program for the use of RTG's in space) suggests that this is particularly a problem with bipolar transistors and junction diodes. Our approach here has been to design an electronics system that has many parallel paths leading to data output to the spacecraft, so that a particular device failure leads to a minimum loss of information from the experiment. Alternatively, if desired by the project, we could use semiconductors which have been screened by radiation exposure and test in order to discover such "mavericks."

H. Electromagnetic Interference:

Our past experience leads us to be confident that this experiment will not be a source of electromagnetic interference. Similarly, we are able to build this experiment so that we are virtually immune to such interference. As an example, one of us has a solid state detector experiment with thresholds set at 30 KeV and seeing no interference on OGO-F, one of the dirtiest spacecraft from the point of view of electromagnetic interference.

I. Commands:

In addition to the normal power command, we anticipate the use of two other commands in controlling various modes of the experiment. We are assuming that the sharing of telemetry with Filluis et al., will not require a command by this experiment.

J. Telemetry Assignments:

Our implementation of this experiment leads to a desirable experiment data word of 12 bits. The data scheme worked out at the April 1969 Working Group Meeting was to assign a 12-bit block/frame to this experiment alone and to assign an additional, sequential, 27-bit block to this experiment when the Univ. Cal. trapped radiation experiment is not on. It is anticipated that the Univ. Cal. experiment will be on short time each day when possible, and on all the time at encounter.

We require that the 12-bit block precede the 27-bit block, and that we be furnished an "anticipate pulse" beginning one or two words before our 12-bit word gate. This anticipate pulse tells the experiment to stop data computations/transfers and freeze the data in the output registers in anticipation of readout. Similarly, we prefer the 27-bit block to come to us as a 12-bit gate word plus a 12-bit gate word plus a 3-bit gate word.

Internal to the experiment, we will commutate the various pha addresses and the many rates into a synchronized sequence of 12-bit words which are read out as one word per frame or three words per frame depending on whether the Univ. Cal. experiment is on or off respectively.

For housekeeping and status measurements, we require 4 analog subcom words, 1 digital subcom and one bi-level indicator.

K. Weight Analysis:

Our assignment of 4.3 pounds still appears to be adequate, but with some uncertainty in view of the many unknowns of the mechanical mounting schemes. Additionally, as pointed out in our original proposal, our developed, proven circuitry uses many parts which are not on the Pioneer Parts List, and changes in many of these parts will significantly affect the weight. Most of the data system is to be built using MSI/LSI MOS. Most of the linear circuitry will be built using thick film substrates. Efficient packaging of these thick film circuits requires the use of low profile, dual transistors in TO-89 ceramic packages, for instance. A very detailed parts list, parts qualification and weight analysis is in preparation.

L. Power Requirements:

Based on a 28 volt, 1% power source to drive the converters, we calculate the required power from that 28 volt bus as 2.2 watts.

M. Project Engineer:

As defined in Document P-200 of the Ames Research Center, the Project Engineer for this experiment is Donald Stilwell, Code 611, Goddard Space Flight Center.

N. Quality Engineer:

Mr. Harry Doyle, Code 312, Quality Engineering Branch, GSFC, has been assigned temporarily to oversee the quality engineering aspects of the experiment. The work of he and his associates to date has

consisted of a thorough review of the extensive Pioneer quality specifications. Permanent assignment of a Goddard Q. E. engineer to this experiment will have to await center manpower reviews which should be complete in early August, 1969. If Code 312 is not able to supply the engineer, then we will contract for the support.

V. DATA POLICY:

In Section I under "Correlative Studies" we indicated the importance of knowing the magnetic field magnitude and direction. In addition the solar plasma density and velocity would be important. We would propose making portions of our data available on a short time scale or perhaps on the original data tape. In return we would like to obtain similar averaged quantities from the plasma and magnetic field experiments.

VI. Effects of RTG

We understand that there is a definite possibility that a radioisotope power supply (RTG) will be used as the spacecraft power source on Pioneers F &G. To determine whether radiation from the RTG would impair the operation of our detectors we exposed some sample detectors similar to those we will use in flight to the radiation from a SNAP-27 generator at TRW Systems. The devices used were a 25 mm^2 area, 50 micron thick silicon surface barrier detector and a 500 mm^2 area, 3 mm thick lithium drift detector. Pulse height spectra were taken at various distances from the RTG. Integral count rate for these devices at a distance of 10 ft. (the most probable distance in the spacecraft) are shown in Figs. VI-1 & VI-2. The effects we expect on each of our detectors are outlined as follows:

1. HET: The data in Fig. VI-1 from the lithium drift device is relevant for the HET. From this data we expect that no effect will be seen in the coincidence mode of operation of the telescope (50-500 Mev/nucleon). The background intensity from the RTG is much too small to produce any accidental coincidences. We expect, however, that single rates in all elements of the telescope will be affected. Our lowest threshold in these devices will be $\sim$ 100 kev. From Fig. VI-1 the count rate above this threshold from the RTG will be $\sim$ 60 cts/sec. A factor of four reduction in this intensity may be possible by proper orientation

of the RTG giving a rate of ~ 15 cts/sec. One of the functions of the single rates is a monitor of detector performance. The increased detector background from the RTG will probably eliminate this as a useful function. In addition the sensitivity of this rates to small solar events will be reduced.

2. LET-I: The effects of the RTG on the LET-I will in general be similar to those on the HET. The coincidence mode (3-20 Mev/sec) will not be affected, but the usefullness of the singles rates will be significantly reduced.

3. LET-II: The data in Fig. II-2 (corrected for differences in detector area and thickness and RTG orientation) predict ~ 1 ct/sec for a 50 kev S_1 detector threshold. The detector sensitivity to protons in the .05 - 3 Mev interval ($S_1 \bar{S}_2 \bar{S}_3$) will then be reduced. The most serious problem occurs for electron measurements in the S_2 detector. RTG background will probably be of the order of 5 cts/sec. This will certainly eliminate the possibility of galactic electron measurements in the .15 - 1 Mev interval and also reduce the sensitivity to solar electrons.

In summary, we expect no difficulties with protons and heavier particle measurements in the 3-500 Mev/nucleon interval. In the 50 kev to 3 Mev region detector sensitivity to both protons and electrons will be seriously reduced. We would estimate that the total usefulness of the experiment would be reduced by about 25%. For this

reason we would strongly prefer a solar cell rather than RTG spacecraft power source.

At present we find it difficult to assess the effects of shielding. There are a large number of unknowns, e.g. orientation of the RTG, positioning of our experiment in the spacecraft, orientation of our experiment with respect to the RTG, and spectral changes due to passage through shielding. We note that a weight estimate of 1.38 lb of lead for shielding our experiment has been made by TRW. This estimate apparently was only sufficient for shielding the LET-II with no allowance made for the LET-I and HET. Even with the more comprehensive test data obtained by us we feel that it is still impossible to make an accurate shielding weight estimate. These questions can probably only be resolved with a much more elaborate testing program including a more accurate simulation of the experimental environment in the spacecraft.

REFERENCES

Anderson, K. A., Solar Physics (in press).

Axford, W. I. and L. J. Gleeson, Ap. J., 149, L115, 1967.

Bryant, D. A., T. L. Cline, U. D. Desai and F. B. McDonald, J. Geophys. Res., 67, 4983 (1962).

Bryant, D. A., T. L. Cline, U. D. Desai and F. B. McDonald, Ap. J., 141, 478 (1965).

Coleman, J. A., D. P. Love, J. H. Trainor and D. J. Williams, IEEE Trans. Nuc. Sci., NS-15, No. 1, Feb. (1968a).

Coleman, J. A., D. P. Love, J. H. Trainor and D. J. Williams, IEEE Trans. Nuc. Sci., NS-15, No. 3, June (1968b).

Fan, C. Y., M. Pick, R. Pyle, J. A. Simpson and D. R. Smith, J. Geophys. Res., 73, 1555 (1968).

Gleeson, L. J., in preparation (1969).

Rao, U. R., K. G. McCracken and R. P. Bukata, J. Geophys. Res., 72, 4325 (1967).

Roelof, E. C., in preparation (1969a).

Roelof, E. C., in preparation (1969b).

Webber, W. R., Can. J. Physics (Proc. Calgary Cosmic Ray Conf.), 1968.

Woldgang, J. L., Jr., Results from the Radiation Damage Effects on MOSFETS Experiment on Explorer XXXIV (IMP-F), Internal Report of the Goddard Space Flight Center, 1968.

VERY LOW ENERGY DETECTOR-II

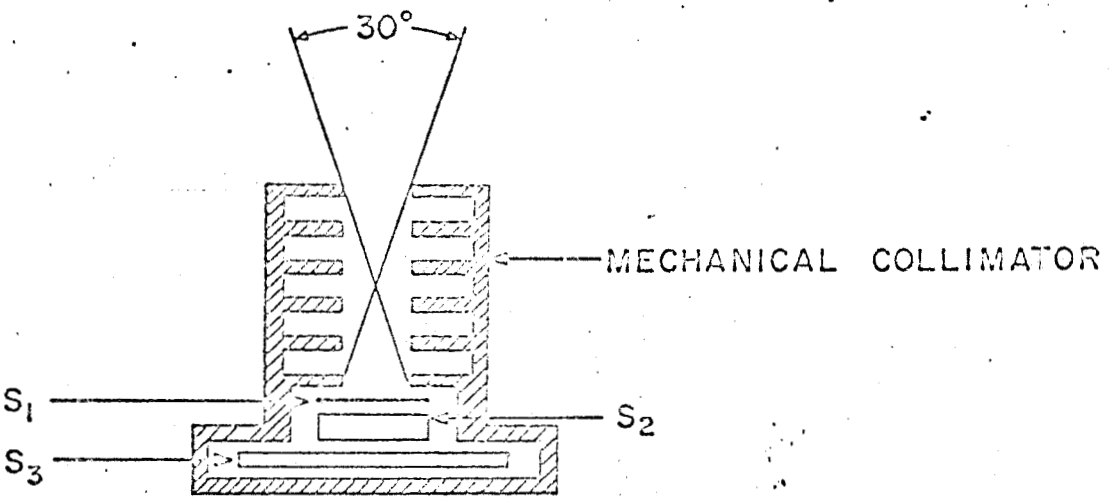

ENERGY RANGES		
	PROTONS	ELECTRONS
$S_1\bar{S}_2\bar{S}_3$	.075-3 MeV	50-150 keV
$S_1S_2\bar{S}_3$	3-20 MeV	———
$\bar{S}_1S_2\bar{S}_3$	———	150-500 keV

DETECTOR	AREA (mm^2)	THICKNESS(mm)	TYPE
S_1	50	.05	SURFACE BARRIER
S_2	50	2	LITHIUM DRIFT
S_3	300	1	LITHIUM DRIFT

Figure III - 3

ENERGY RESPONSE: LOW ENERGY DETECTOR - III

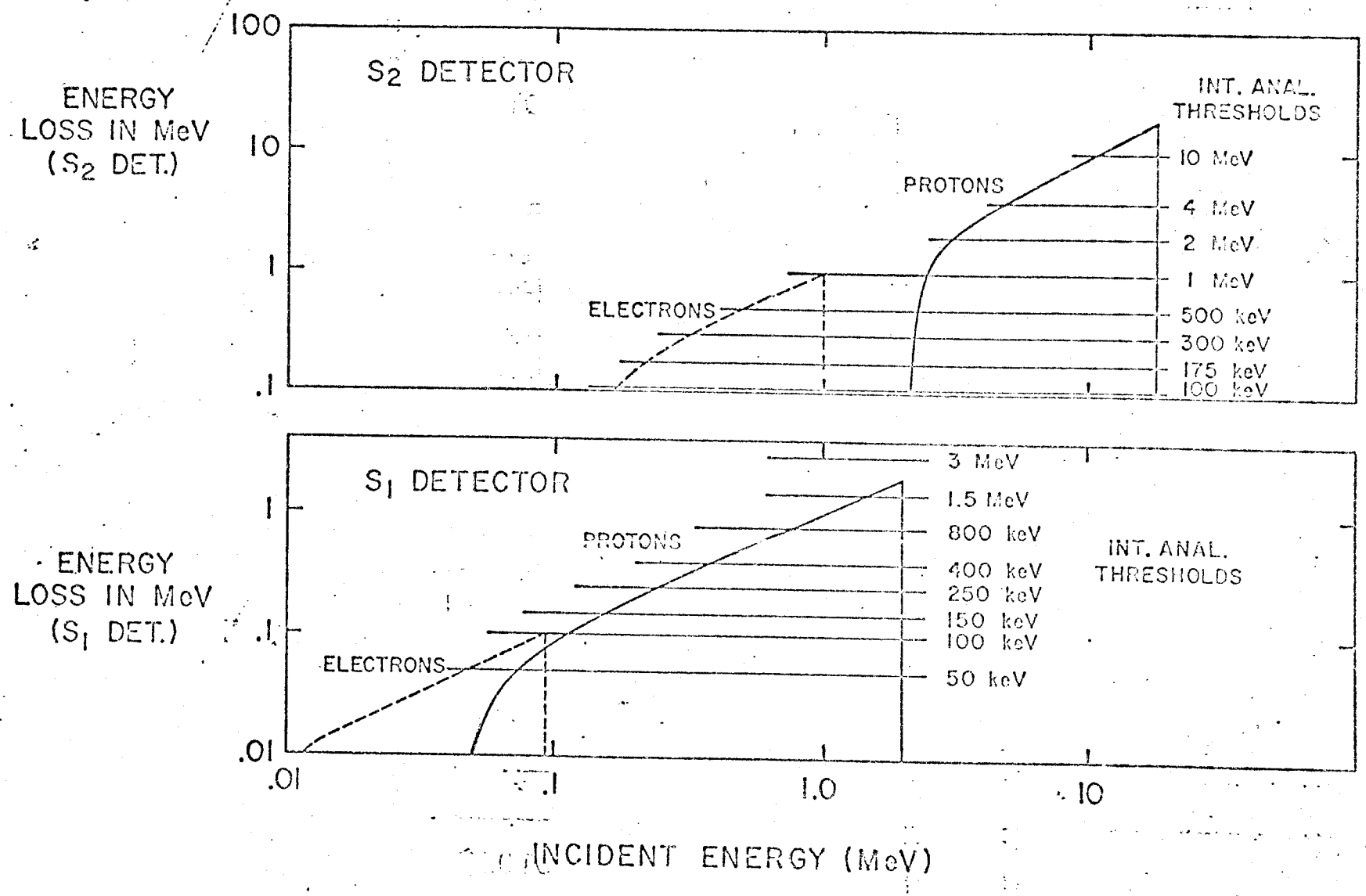

FIG. III - 4

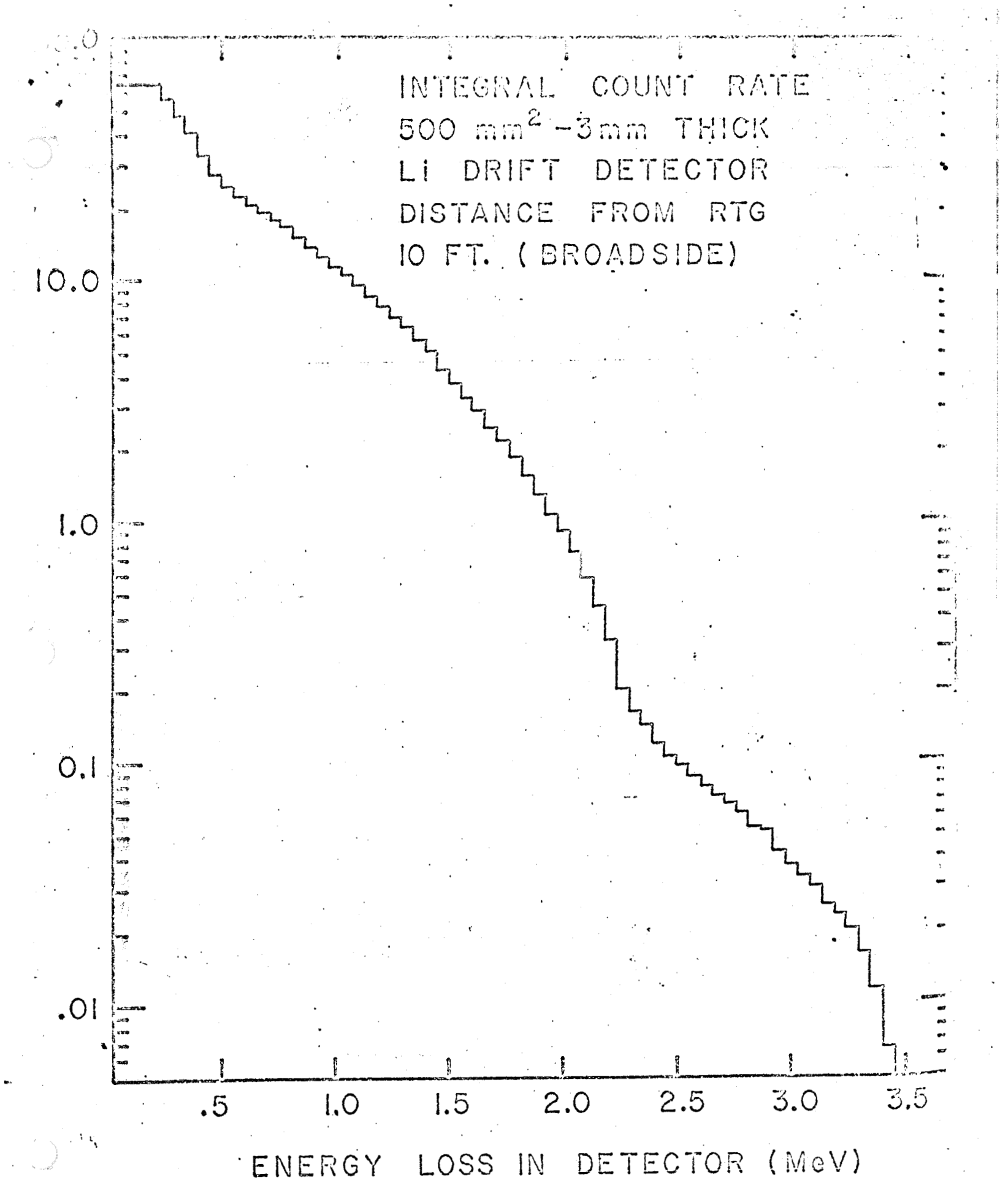
INTEGRAL COUNT RATE
500 mm² - 3mm THICK
Li DRIFT DETECTOR
DISTANCE FROM RTG
10 FT. (BROADSIDE)
10.0
1.0
0.1
.01
.5
1.0
1.5
2.0
2.5
3.0
3.5
ENERGY LOSS IN DETECTOR (MeV)

FIG. VI-1

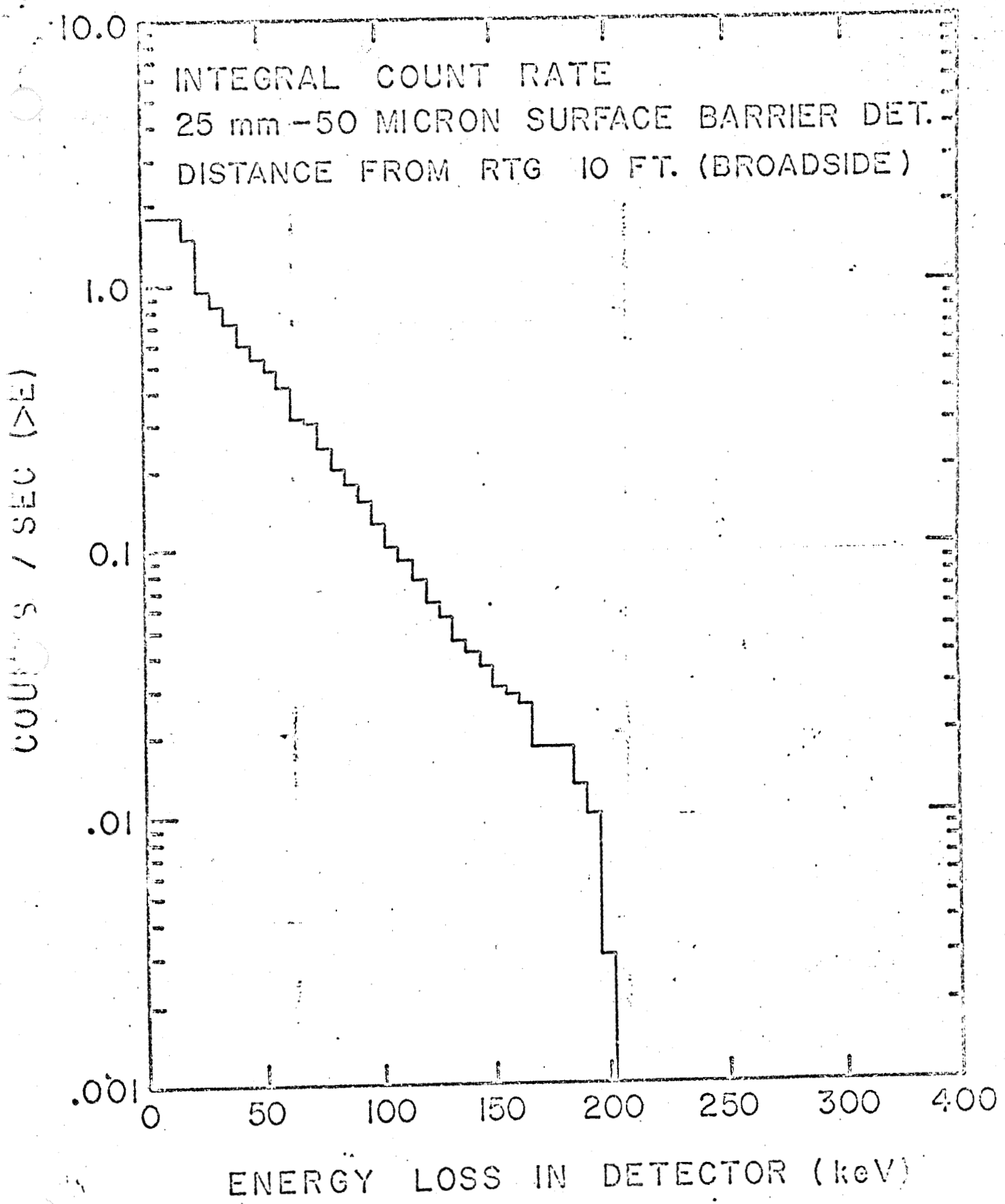
INTEGRAL COUNT RATE
25 mm - 50 MICRON SURFACE BARRIER DET.
DISTANCE FROM RTG 10 FT. (BROADSIDE)
10.0
1.0
0.1
.01
.001
COUNTS / SEC (>E)
0
50
100
150
200
250
300
400
ENERGY LOSS IN DETECTOR (keV)

FIG. VI-2

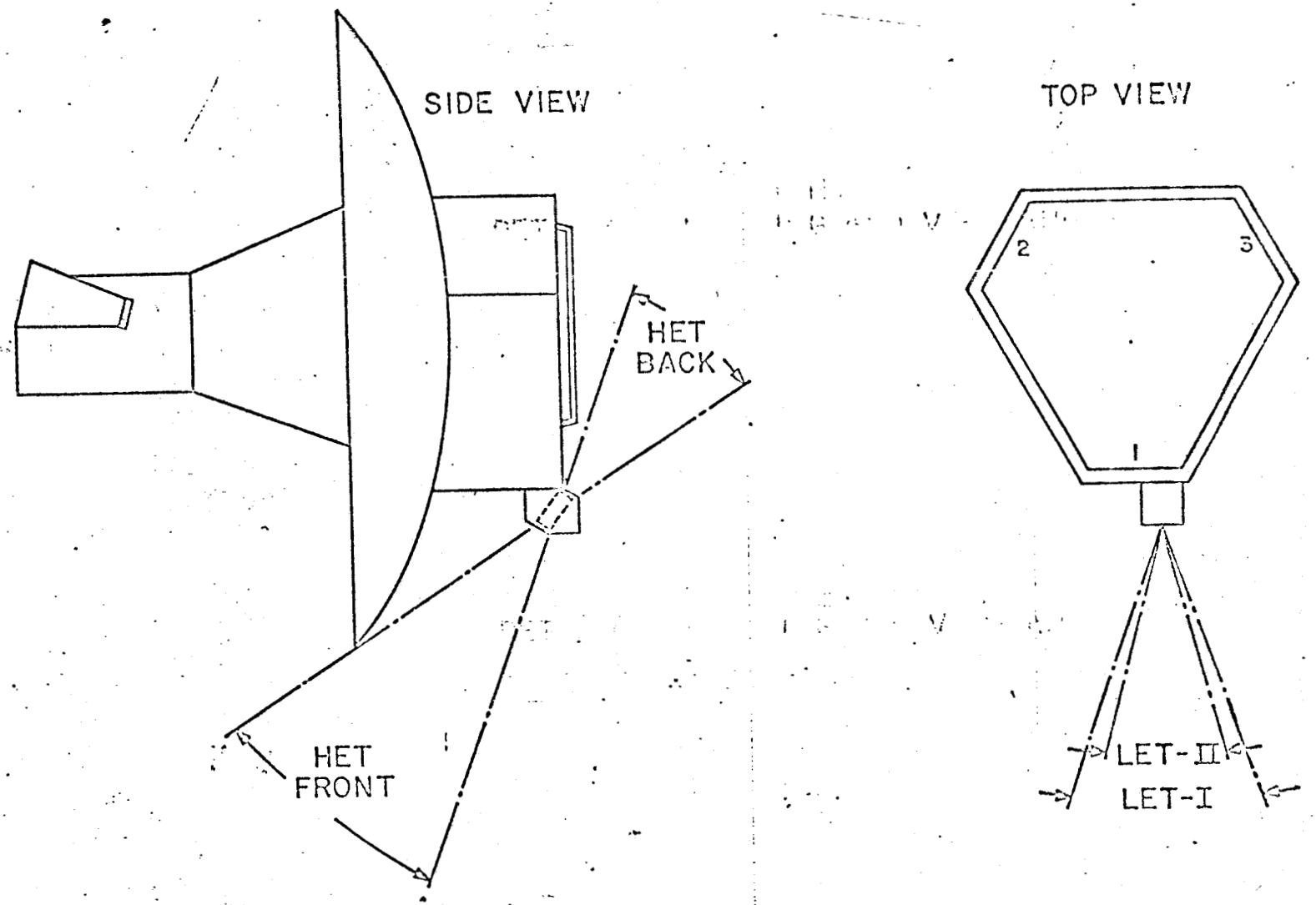

FIG. IV-4
DETECTOR MOUNTING AND VIEW ANGLES